Chapter 5

Selected Sources in the Large Magellanic Cloud

5.1 Introduction

The description of the MOST and ATCA observations of the Small Magellanic Cloud presented in Chapter 4 provided insight into the apparent variation of source morphology with angular resolution and observing frequency. The results showed the difficulty in making accurate source classifications based on a small number of imperfectly measured morphological parameters. The issues involved in classifying sources using spectral indices estimated from data taken from a number of different instruments having vastly differing sensitivity to emission at different angular scales was also discussed. Great care must be taken when using the spectral index as the primary quantitative metric by which to classify a source.

Whilst the reliable classification of sources remains a difficult and challenging problem it is clear that a more systematic method could be developed to classify the LMC sources. To meet this challenge, a "decision-tree" methodology has been developed which extends the knowledge gained from the analysis of the SMC data.

In this chapter, the new classification methodology is discussed, the MOST and ATCA observations of sources in the Large Magellanic Cloud are presented in the form of a mini-catalogue and the actual classifications are explained. A number of sources worthy of further study are presented.

5.2 A Systematic Method of Classifying Sources

Figure 5.1 shows the "decision tree" used to classify the sources discussed in this chapter. This was based on our study of the SMC, a preliminary analysis of the MOST and ATCA LMC radio data presented here and from data in published catalogues. The underlying premise is that the data from the Molonglo Reference Catalogue (MRC; Large et al. 1991) and MC4 catalogue (Clarke, Little & Mills 1976), both at 408 MHz, and the MOST 843 MHz observations have:

1. sampled the full angular extent of the source, and

2. have been measured with relatively high accuracy owing to the absence of baselevel problems in the interferometer data.

Thus, an extrapolation of the spectral index determined from these two values gives a first-order estimate of the expected flux density at 5 GHz. This can then be compared with the actual flux densities in published catalogues (i.e. the Parkes observations) and those reported here from the analysis of the ATCA data, as well as the images obtained with the ATCA at higher angular resolution.

The "decision tree" flow-chart applied to the LMC data presented here is used as follows:

- Inspect the MOST 843 MHz and ATCA 4790 MHz images for characteristic features common to both (e.g. if the source appears elongated at a particular position angle in the MOST image, is there co-aligned structure in the same direction in the ATCA image), general source structure and the environment surrounding the region of interest.

- Compute an *indicative* spectral index emphasizing the catalogued 408 MHz data and the MOST 843 MHz data as both these instruments should have sampled almost all of the flux density from the source and do not suffer baselevel uncertainty. A 5 GHz flux density can be predicted from the extrapolated spectrum and used as the basis of a comparison with the published Parkes data and the ATCA 4790 MHz data.

- Sources for which there are published ATCA continuum flux densities at 1419 MHz (Dickey et al. 1994) and at 1380 and 2378 MHz (Marx, Dickey & Mebold 1997) can be compared to the flux density value predicted from the extrapolated spectrum.

- If it appears that the data from the ATCA and Parkes is consistent with the spectral index determined from the lower frequency measurements, include these data in the determination of the best-fit spectral index. Plot the data and the least squares fit to the selected values. This leads to four scenarios:

  - **Both the ATCA and Parkes 5 GHz data are consistent with prediction:** This suggests that both Parkes and the ATCA has fully sampled the radio emission over necessary angular scales and, further, that the source is compact. If it has sufficient flux density a PTI detection at 2290 MHz may be observed and H I absorption may be seen in the direction of this source. In this case the spectral fit (which would have included most if not all of the data points) can safely be used to aid in the classification of the source.
  - **The ATCA 5 GHz data is consistent with the prediction but the Parkes 5 GHz data is NOT consistent with the prediction:** The

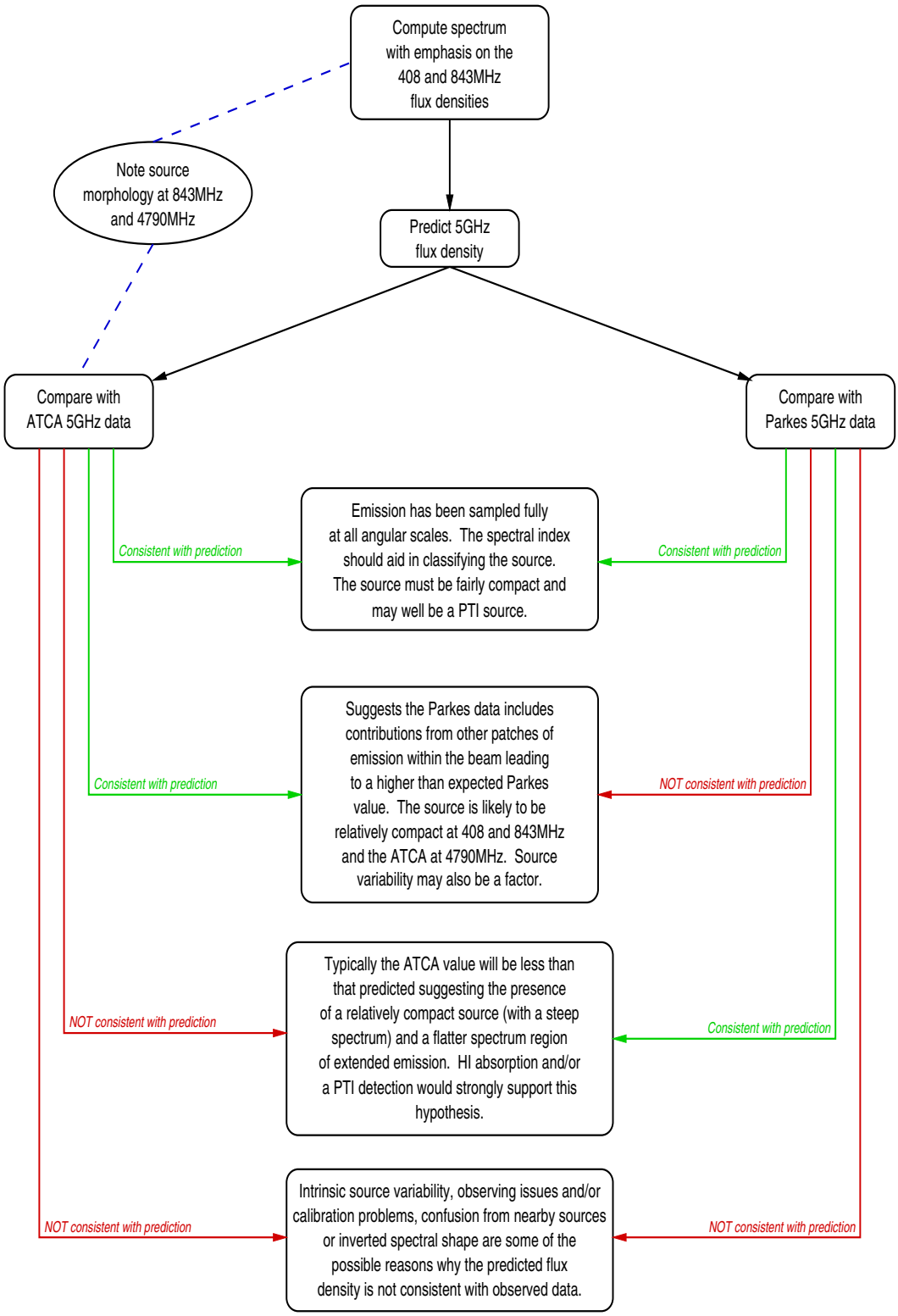

Figure 5.1: The "Decision Tree"used to aid in the classification of sources in the Large Magellanic Cloud. See text for further details.

most common case is that the Parkes 4.75 and 4.85 GHz value(s) are greater than that predicted. This may be due to confusion from other sources in the Parkes beam (which is significantly larger at 5 GHz than that of the other instruments discussed in this study), leading to a higher than expected flux density. On occasions, baselevel errors may lead to smaller Parkes values. Intrinsic source variability needs to also be considered, particularly if the source appears compact at the ATCA. Thus the spectral index (excluding the Parkes values) can be used to help in the classification of this (compact) source.

- **The ATCA 5 GHz data is NOT consistent with the prediction but the Parkes 5 GHz data is consistent with the prediction:** The spectrum determined from the 408, 843 MHz and Parkes 5 GHz values (and possibility at other Parkes frequencies) fits the observed data well. Typically in this case, the ATCA 4790 MHz value will be smaller than expected. One explanation is that there are at least two distinct components: (1) a region of extended (flat-spectrum) emission (possibly located in the LMC) fully sampled at 408, 843 MHz and with the Parkes radio telescope but resolved out with the ATCA and (2) a compact component which is sampled by the ATCA and the other instruments. The extended diffuse emission may be visible on the MOST image. The detection of the compact component with the PTI at 2290 MHz would support this hypothesis as would the detection of H I absorption seen in the direction of the source at the velocity of the LMC. The spectral index for this case will likely give a reasonable estimate of the spectrum of the extended component.
- **Both the ATCA 5 GHz data and the Parkes 5 GHz data are NOT consistent with the prediction:** It is difficult to be certain as to why this is the case. Some possibilities include confusion from nearby sources leading to a greater flux density than expected, intrinsic source variability, an irregular or inverted radio spectrum and calibration or other unknown instrumental factors. In some cases a power-law spectrum cannot be fitted to the data. Sources in this category will often invite further study at other frequencies and angular resolutions to better determine their nature.

- For a source which is extended, and typically this will correspond to the third case given above, the question arises as to whether the ATCA would have completely sampled the flux for the extended component. The largest well-imaged structure in the case of the ATCA 4790 MHz observations presented in this study (given the array configuration and observing strategy used) is around 30 arcsec (The Australia Telescope Compact Array Users' Guide 1999). This suggests that, where there is diffuse extended emission visible in the MOST image, the ATCA will fail to detect much of this extended emission, leading to a lower than expected integrated flux density at 4790 MHz.

- For the case where a source appears to have two distinct and close components

having a similar flux density, the criteria developed by Magliocchetti et al. (1998) can be used to determine if the two components are either subcomponents of the same source or a pair of independent sources. In a flux-density selected sample from a relatively low angular resolution instrument (like the MOST) accidental double-lobed sources will be preferentially selected, thus it is not surprising to find that many sources are double lobed when imaged with the ATCA at 5 GHz.

Using the data from the VLA FIRST survey at 1.4 GHz Magliocchetti et al. (1998) found that a plot of the sum of the fluxes of the components of each apparent double source versus the separation of the two components resulted in two distinct regions. From an inspection of the FIRST images, it was determined that the region on the left of their Figure 2 corresponds to subcomponents of the same source. In addition, for each identified double-lobed source, they plotted the flux of the components against each other (see Figure 3 in Magliocchetti et al. 1998). As would be expected for true double radio sources, the two fluxes are highly correlated and this led to the further criterion that components are considered to be physically associated if the fluxes of each component differ by a factor of less than 4.

The above logic provides an initial method to determine if the spectral shape and source morphology can be used to aid in source classification. Data from other frequencies may also be employed to aid in the classification of the source. Readily available data include, Hα images (e.g. the DEM catalogue of Davies, Elliott & Meaburn 1976), X-ray observations (e.g. the data and analysis from the *Einstein* and *ROSAT* missions) and infra-red observations (e.g. the IRAS catalogue).

5.3 A Catalogue of Selected LMC Sources

Details of the ATCA observations of the LMC are given in Table 3.2. A total of 41 sources in the LMC were observed with the MOST and ATCA. For each source (which are presented in order of increasing right ascension) the MOST 843 MHz and ATCA 4790 MHz total intensity images are presented along with the radio spectrum determined from the available radio data between 408 MHz and 8550 MHz. A power-law fit to the selected data is also shown. The slope of this fit is the spectral index, used to aid in the classification of the source.

The following plot symbols are used throughout to denote the data from different instruments:

- MRC and/or MC4 408 MHz: ■,
- MOST 843 MHz: ×,
- ATCA 1380, 1419, 2378 and 4790 MHz: ●, and
- Parkes 1.40, 2.30, 2.45, 4.75, 4.85 and 8.55 GHz: ⊙.

It is important to stress that the scale of the published MOST and ATCA images are significantly different and this must be taken into account when comparing the source structure at the two frequencies. Source positions and flux densities from both the MOST and ATCA observations are given in Table 5.1. The spectral index determined from the data presented here, PTI results and source classification are given in Table 5.2. Both tables are located towards the end of this chapter.

This page intentionally left blank to maintain formatting.

0440–665 (Figures 5.2 and 5.3) The MOST image shows a compact source with a peak flux density of 870 mJy/beam and an integrated flux density of 889 mJy. The source has not been resolved with the MOST. The ATCA image shows two compact sources, separated by around 5 arcsec, with a combined flux density of both objects being 152 mJy with a peak flux density of 82 mJy/beam at 4790 MHz. This object is located on the north-western edge of the LMC and is located away from the areas with thermal emission and known SNRs.

The MRC lists a flux density of 1.52 Jy at 408 MHz. The Parkes source B0440–6630 was detected at all observed frequencies, apart from the observations at 8.55 GHz, with flux densities of 177 mJy and 173 mJy at 4.75 and 4.85 GHz respectively. These values are greater that that determined from the ATCA observations reported here. This object was detected in the study undertaken by Dickey et al. (1994) who used a number of discrete compact continuum sources to undertake a 21 cm absorption study of the cool atomic gas in the LMC. H I absorption is seen towards this source. This source was not detected with the PTI at 2.3 GHz. No X-ray or infrared emission was detected from this area.

A spectral index of $\alpha = -(0.87 \pm 0.07)$ was determined from 8 data points with only the ATCA 4790 MHz value being excluded from the calculation. It is unclear why the ATCA 1419 MHz value agrees well with the expected value while the 4790 MHz value is significantly lower that that predicted from the spectrum. A possible reason is that there is some emission at an angular scale greater than about 30 arcsec which is the upper limit for structures that would be well imaged at 4790 MHz. Structures up to 100 arcsec in extent would be well-imaged by the ATCA at 1419 MHz. However, it would be expected that any source extension would be seen in the MOST image, and this does not appear to be the case.

Given the location of the object in relation to the LMC, the compact double-lobed morphology and the 21 cm absorption observed with that ATCA, this source can be classified as a double background extragalactic source.

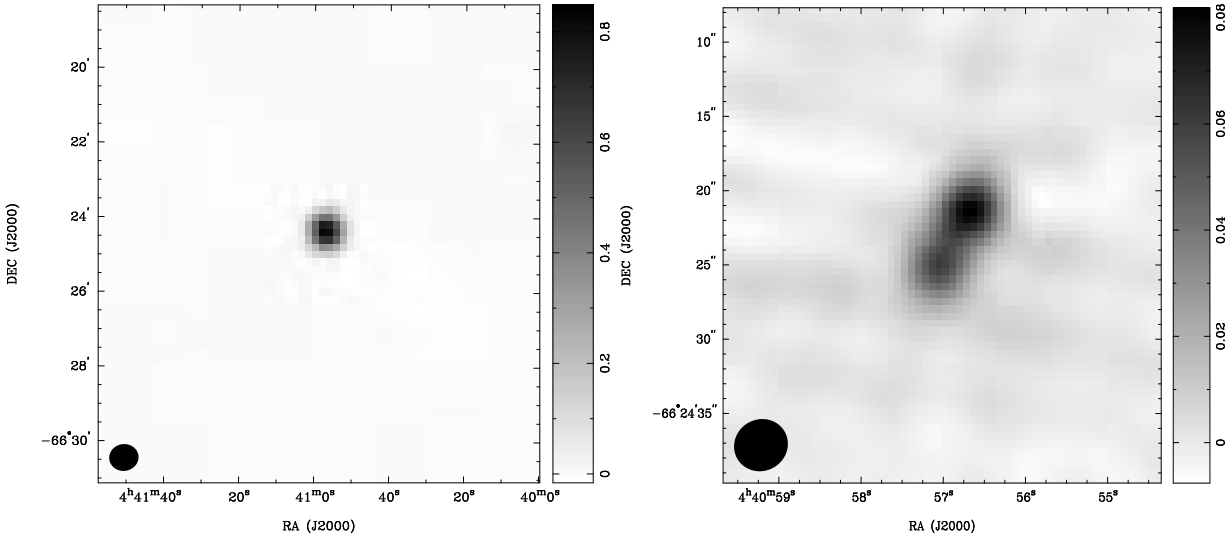

Figure 5.2: The MOST 843 MHz (left) and ATCA 4790 MHz (right) total intensity images of 0440–665 in the Large Magellanic Cloud. The intensity units are in Jy/beam. The wedge to the right of each image gives an indication of the transfer function. The HPBW is shown in the lower-left corner.

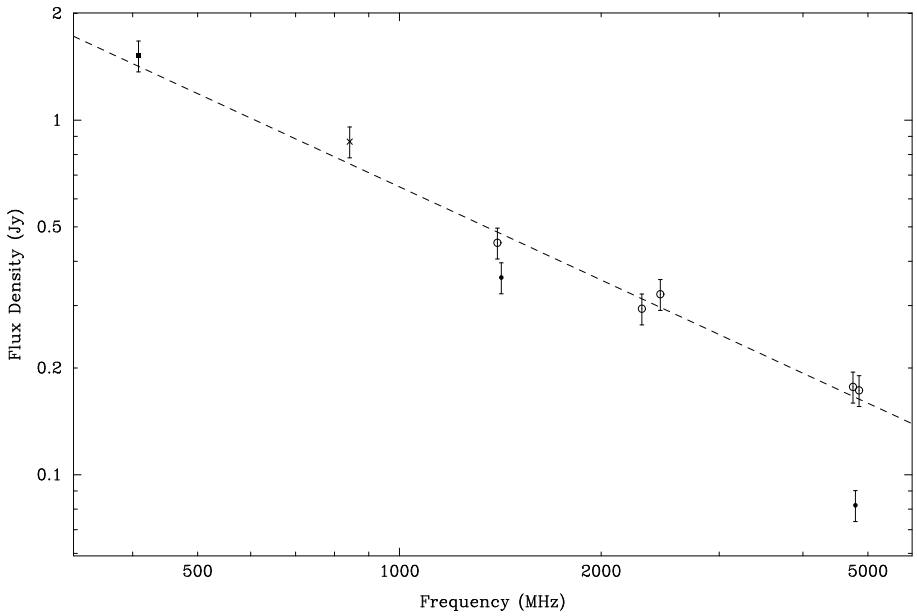

Figure 5.3: The radio spectrum of 0440–665 in the Large Magellanic Cloud.

0449–709 (Figures 5.4 and 5.5) The MOST image shows a compact source with an integrated flux density of 632 mJy; some slight extension is visible in the north-south direction. The ATCA 4790 MHz image shows two regions of diffuse emission, aligned at a similar orientation to the slight extension seen in the 843 MHz MOST image. The integrated flux density was determined by interactively selecting a region around each area of emission giving flux densities of 66 and 71 mJy for each area.

The MRC 408 MHz flux density for this object is 980 mJy. The Parkes source B0449–7057 has catalogued flux densities at 2.30 GHz and in the 5 and 8 GHz bands. The two observations at 4.75 and 4.85 GHz have widely differing flux densities of 151 and 210 mJy respectively. The angular resolution of the Parkes observations is probably not sufficient to distinguish between this source and a stronger Parkes source B0450–7055 located nearby. Confusion with this source may explain why there is no low frequency data given in the Parkes surveys. This apparently has prevented classification of this source by Filipovic and coworkers.

A spectral index of $\alpha = -(0.73 \pm 0.10)$ has been determined by using the full dataset apart from the 8.55 GHz flux density as this seems significantly lower than that predicted, possibly owing to uncertainties in the measurement as the source is relatively weak.

Based on the radio spectrum determined here and source morphology at 843 and 4790 MHz, it is most likely to be a double-lobed radio galaxy background to the LMC. The separation of the two components implies this source is close to the limit for multi-component sources according to the analysis by Magliocchetti et al. (1998) of the VLA FIRST survey data.

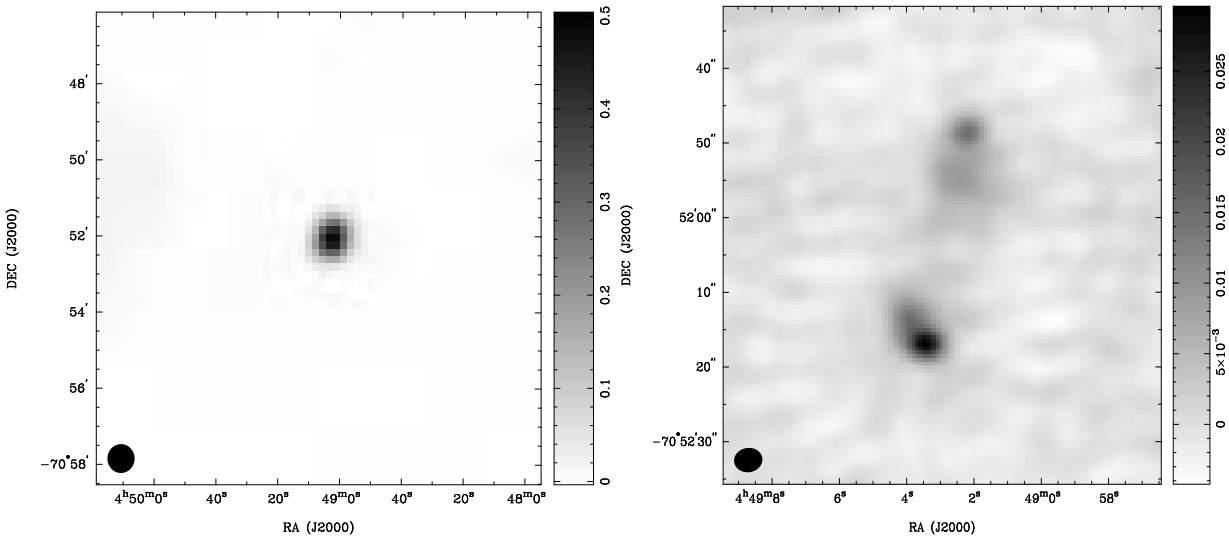

Figure 5.4: The MOST 843 MHz (left) and ATCA 4790 MHz (right) total intensity images of 0449–709 in the Large Magellanic Cloud. The intensity units are in Jy/beam.

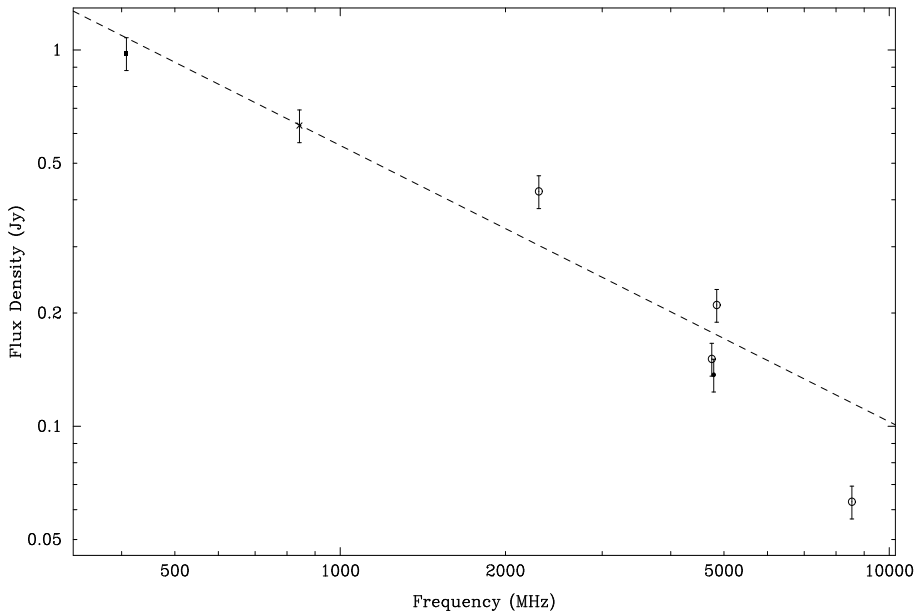

Figure 5.5: The radio spectrum of 0449–709 in the Large Magellanic Cloud.

0451–696 (Figures 5.6 and 5.7) The MOST and ATCA images of 0451–696 are shown in Figure 5.6 and the associated radio spectrum is show in Figure 5.7. The MOST image shows a slightly extended but relatively compact source (deconvolved dimensions of 59.5×43.7 arcsec) with a peak flux density of 274 mJy/beam and integrated flux density of 363 mJy. The ATCA image shows a cluster of two or three distinct but rather weak compact sources, with the peak flux density of the strongest source being 7.6 mJy/beam. These sources all lie well within a diameter of 40 arcsec and thus would not be individually resolved by the MOST although the extension visible in the MOST source is in the same direction as the cluster of sources shown in the ATCA image. An inspection of the MOST image suggests that this object is located in a fairly isolated area with little noticeable diffuse emission nearby.

This object was not detected in the Parkes multi-frequency surveys undertaken by Filipovic and coworkers. This is somewhat surprising, particularly at the lower frequencies of 1.40, 2.30 and 2.45 GHz, where a flux density of around 100 mJy would be expected from the radio spectrum. The 408 MHz MRC flux density is 770 mJy. There is no known X-ray emission from this object.

The spectral index determined from the three data points is $\alpha = -(1.46 \pm 0.13)$ which is steeper than that determined from just the 408 and 843 MHz data points which give a spectral index of around $\alpha \sim -1.0$. This may suggest the presence of flatter spectrum extended emission (which the ATCA data has essentially resolved out) and a steeper spectrum compact component. Given the small number of data points it is difficult to be confident about this conclusion.

The discrete sources may or may not be subcomponents of the same object. The three sources like within about 35 arcsec of each other and have flux density ratios of approximately 2:3:5. Based on morphology and spectrum it is probable that this is an extragalactic background source. Further observations at a range of frequencies and angular resolutions would be needed to determine the nature of this source.

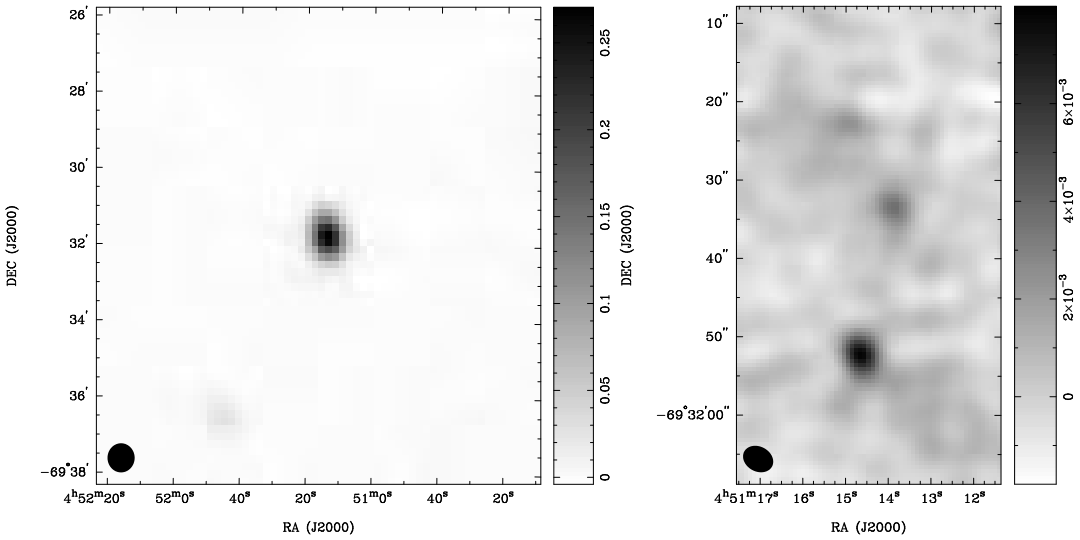

Figure 5.6: The MOST 843 MHz (left) and ATCA 4790 MHz (right) total intensity images of 0451–696 in the Large Magellanic Cloud. The intensity units are in Jy/beam.

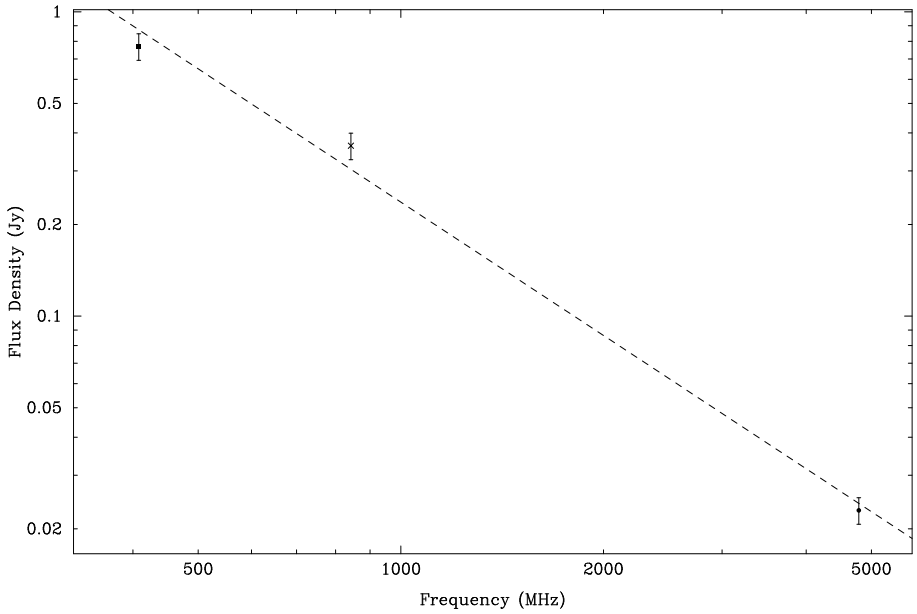

Figure 5.7: The radio spectrum of 0451–696 in the Large Magellanic Cloud.

0454–649 (Figures 5.8 and 5.9) The MOST image shows a compact central source with a peak flux density of 643 mJy/beam and a slightly weaker but compact apparent counterpart. The source could comprise either two distinct sources or possibly a single object with two components. The flux density of both sources combined is 1.402 Jy. The centroids of the two components are separated by about 90 arcsec. The separation and the large combined flux density of the two components makes it difficult to apply the criterion of Magliocchetti et al. (1998) to determine if the components are part of one source. The ATCA image shows a single compact source, located at a position coincident with the stronger of the two sources imaged with the MOST, with a peak flux density of 28 mJy/beam and integrated flux density of 35 mJy. There may be some diffuse emission to the south-west.

At 408 MHz, the MRC lists a flux density of 2.43 Jy. The Parkes source B0454–6454 was detected at a number of frequencies and it is marked as extended at 2.30 GHz. The Parkes flux density of 4.75 GHz is 448 mJy compared to an ATCA determined flux density of less that 30 mJy at a similar frequency. No X-ray or infrared emission has been detected from this region.

Excluding only the ATCA value from the calculation of the spectral index, gives a value of $\alpha = -(0.63 \pm 0.06)$. Thus it appears that the ATCA has only imaged a compact component, resolving out any extended emission thus leading to a lower than predicted ATCA flux density. The compact component is likely to be an extragalactic background source.

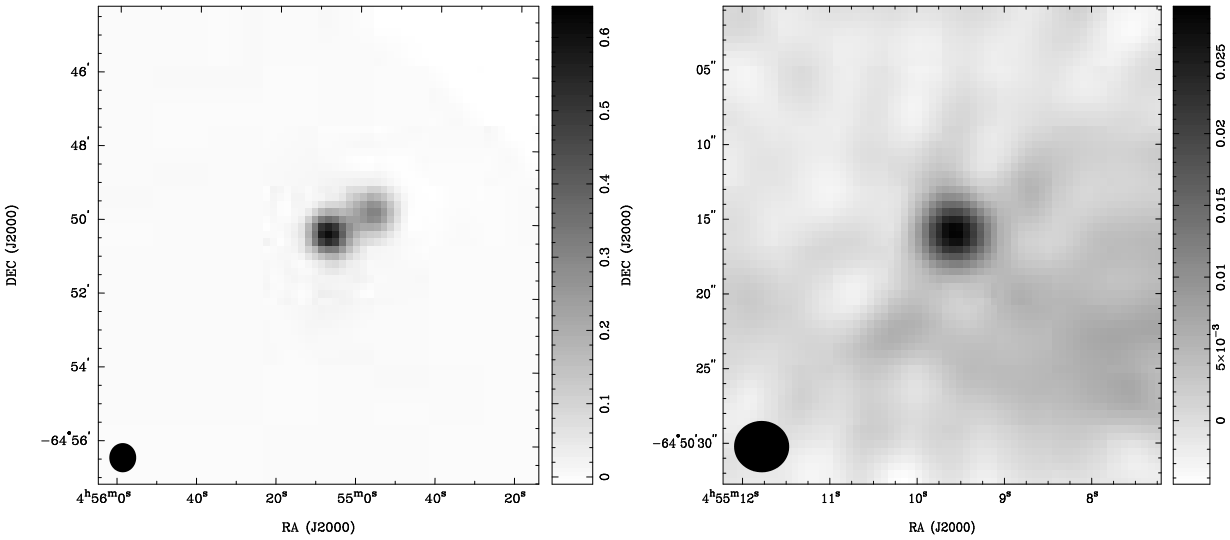

Figure 5.8: The MOST 843 MHz (left) and ATCA 4790 MHz (right) total intensity images of 0454–649 in the Large Magellanic Cloud. The intensity units are in Jy/beam.

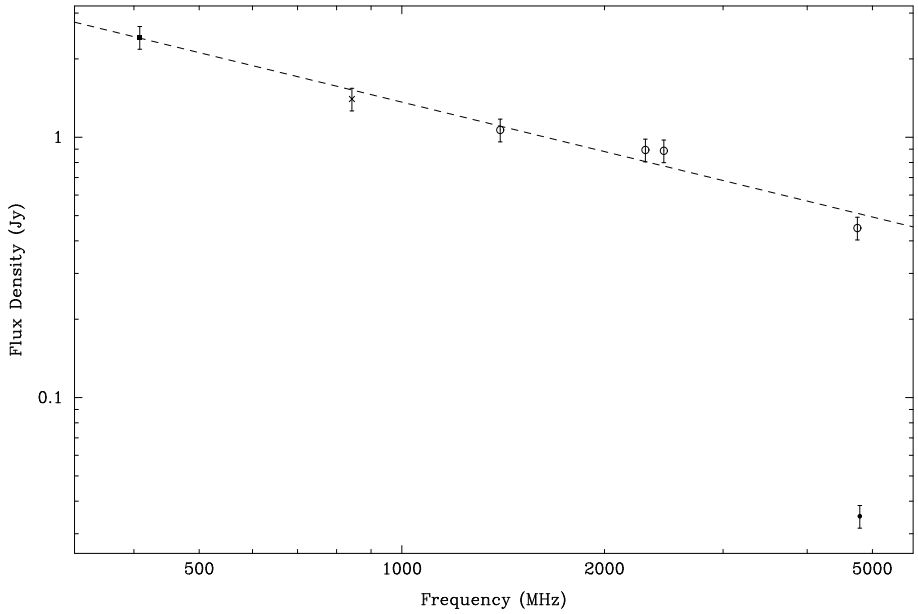

Figure 5.9: The radio spectrum of 0454–649 in the Large Magellanic Cloud.

0456–703 (Figures 5.10 and 5.11) The MOST image shows an isolated, compact source with peak flux density of 187 mJy/beam and an integrated flux density of 201 mJy. The ATCA image shows a compact source (deconvolved dimensions of 4.04×3.09 arcsec) with a peak flux density of 66 mJy/beam and an integrated flux density of 76 mJy. Some faint diffuse emission in the general area of the source is visible on the MOST image.

This source is listed in the MC4 catalogue at 408 MHz with a flux density of 240 mJy and was detected at all frequencies in the Parkes radio surveys, apart from the observations at 1.40 GHz. It is not clear why this source was not detected at this frequency. Dickey et al. (1994) list a continuum flux density of 101 mJy at 1419 MHz and two distinct absorption components were seen in the direction of this source. PTI observations at 2.3 GHz detect fringes at the ATCA 4790 MHz position suggesting the presence of a compact "core" component. In a comparison with IRAS data, Filipovic et al. (1998c), identify the Parkes radio source with an infrared counterpart, LI–LMC221, which has a 60 μm flux density of 2.5 Jy. No X-ray emission was detected from this region.

A spectral index of $\alpha = -(0.32 \pm 0.10)$ was determined from the fit to all 8 data points which is in good agreement with the spectral index determined from the Parkes data of $\alpha = -(0.32 \pm 0.05)$ by Filipovic and coworkers. If the two ATCA values are excluded from the fit, there is negligible difference in the slope but it is clear that both ATCA values are below that predicted from the other data. This suggests the presence of diffuse emission, and it should be noted that the DEM Hα images of this region show some diffuse nebulosity, along with a compact core component.

The observations reported here are consistent with the previous classification that this object is a flat-spectrum background source.

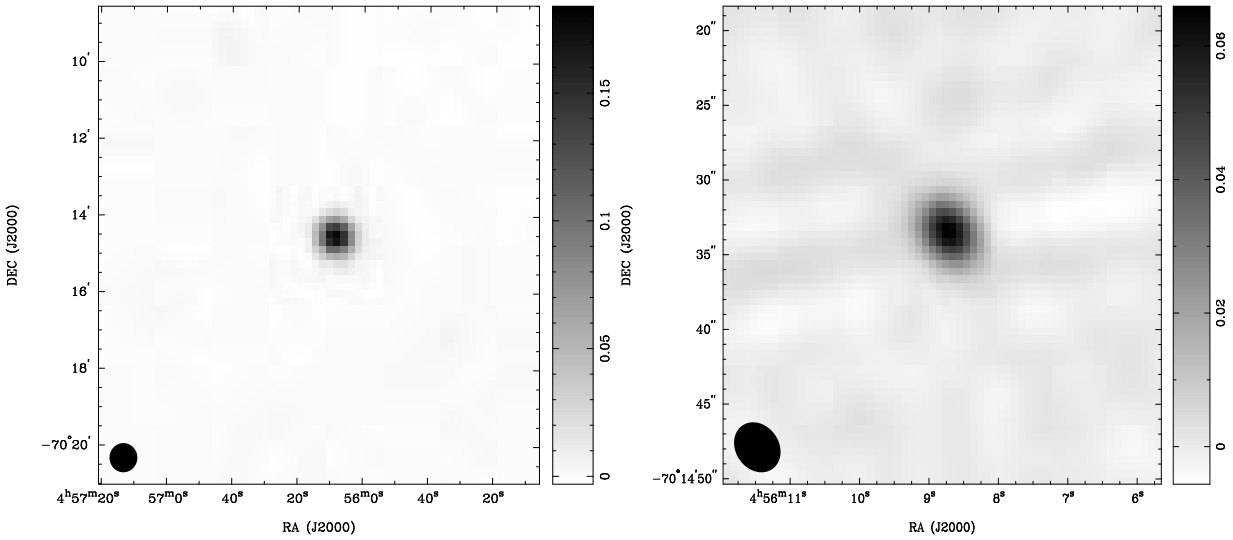

Figure 5.10: The MOST 843 MHz (left) and ATCA 4790 MHz (right) total intensity images of 0456–703 in the Large Magellanic Cloud. The intensity units are in Jy/beam.

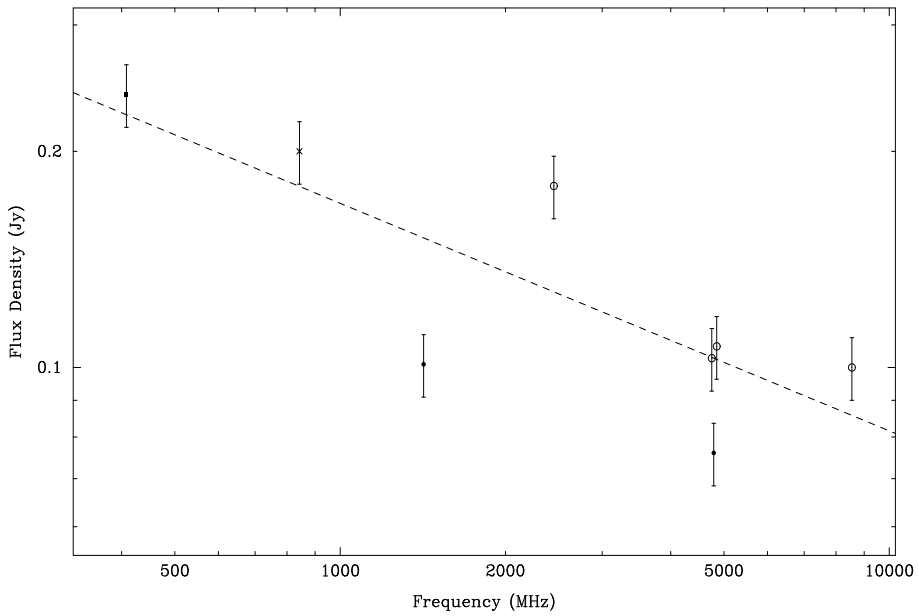

Figure 5.11: The radio spectrum of 0456–703 in the Large Magellanic Cloud.

0458–720 (Figures 5.12 and 5.13) The MOST image shows an extended, double-lobed source with the stronger of the two components having a peak flux density of 124 mJy/beam at 843 MHz. The two sources combined have an integrated flux density of 546 mJy. The ATCA image shows a faint, compact source (deconvolved dimensions of 4.92×3.77 arcsec) with a peak flux density of 7 mJy/beam lying close to the centroid of the brighter of the MOST sources.

Filipovic et al. (1998b) classified 0458–720 as a probable but not certain background source. The source was detected at all frequencies observed at Parkes apart from the 8 GHz band. This non-detection is probably due to the source flux density being below the detection level at this frequency. They determined a spectral index of $\alpha = -(0.60 \pm 0.02)$. There is no detected X-ray or infrared emission from this region.

As listed in the MRC, this source has a 408 MHz flux density of 710 mJy. The ATCA integrated flux density at 4790 MHz is 10.1 mJy compared with a value of 190 mJy obtained with the Parkes radio telescope at a comparable frequency. For the ATCA observations reported here, the angular extent of the largest object that can be well imaged is approximately 30 arcsec whereas the angular extent of the object is around 3 arcmin as determined from the MOST image. Thus the ATCA has resolved out much of the extended emission leading to a significantly lower flux density than predicted. This value should thus be excluded from any spectral index determination. Taking the MRC, MOST and Parkes data gives a spectral index of $\alpha = -(0.56 \pm 0.03)$ which compares well with that determined by Filipovic and coworkers. Weak fringes were detected with the PTI at 2.3 GHz, probably corresponding to the more compact component imaged with the ATCA.

It is not clear from these observations that this source can be confidently classified as a background source. The spectral index is comparable to that of shell-type supernova remnants although no X-ray emission has been detected. Further observations are needed to permit a more certain classification of this source.

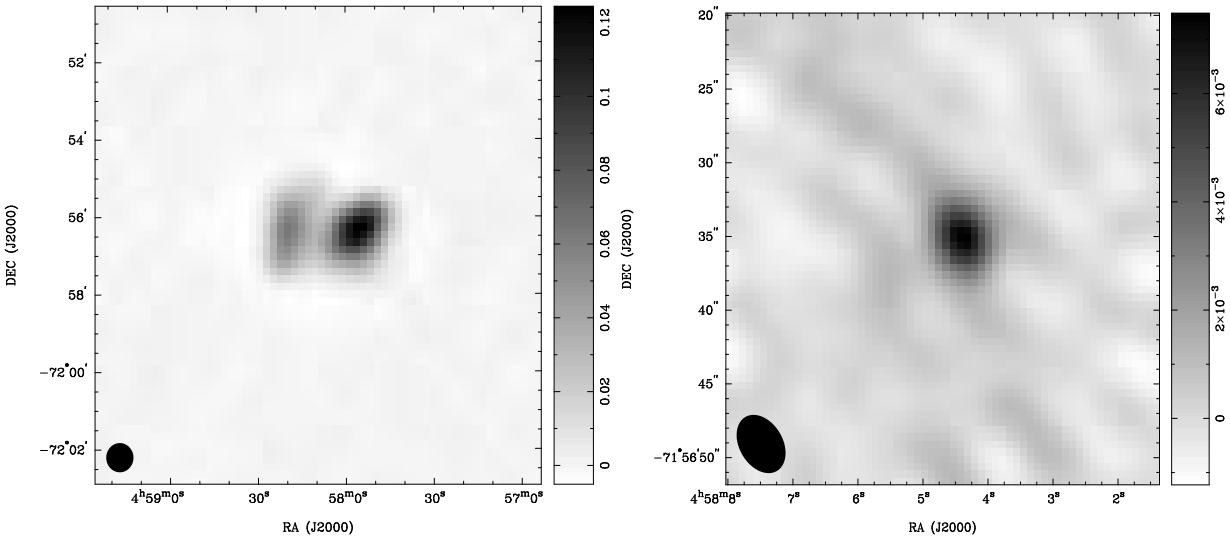

Figure 5.12: The MOST 843 MHz (left) and ATCA 4790 MHz (right) total intensity images of 0458–720 in the Large Magellanic Cloud. The intensity units are in Jy/beam.

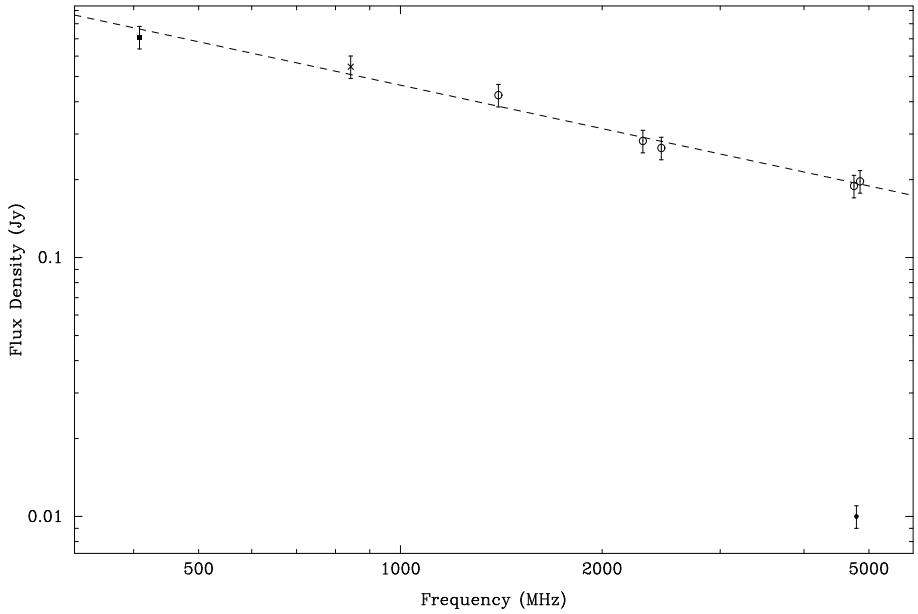

Figure 5.13: The radio spectrum of 0458–720 in the Large Magellanic Cloud.

0502–696 (Figures 5.14 and 5.15) The MOST image shows a compact source with a peak flux density of 1.26 Jy/beam and integrated flux density of 1.389 Jy. The deconvolved source dimensions are only a few arcseconds larger than those of the synthesized beam. The ATCA 4790 MHz image shows an extended region of emission with a stronger component to the east of the subimage with some clumpy emission visible to the south-east. The peak flux density is 14 mJy/beam at 4790 MHz. Because of the complex morphology shown in the ATCA image, automated tasks do not reliably determine source position and flux density. A region containing most of the flux was interactively selected giving an integrated flux density of 109 mJy. This object has a flux density of 2.76 Jy at 408 MHz.

The source B0502–6935 was detected at all observed frequencies in the Parkes surveys and has flux densities of 139 mJy and 136 mJy at 4.75 GHz and 4.85 GHz respectively. These values agree with the value determined from the ATCA observations. Using all the available data, a spectral index of $\alpha = -(1.27 \pm -0.07)$ has been determined. Filipovic et al. (1998c) calculate a spectral index of $\alpha = -(1.24 \pm 0.06)$ which agrees with the value determined here. A known H II region, DEM 54, which is classified as "faint" has good positional agreement with the MOST and ATCA positions and also with infrared source LI–LMC340 which has a 60μm flux density of 2.1 Jy. It seems probable that the infrared emission is from the faint H II region rather than from the radio sources as the radio spectrum is relatively steep and is not characteristic of the flatter spectrum typically seen from H II regions.

This object was previously classified as a background source, and the present work indicates this is probably correct. However, the presence of optical and far infra-red emission from a superimposed H II region in the LMC suggests that there may be some contribution from a thermal source to the radio spectrum

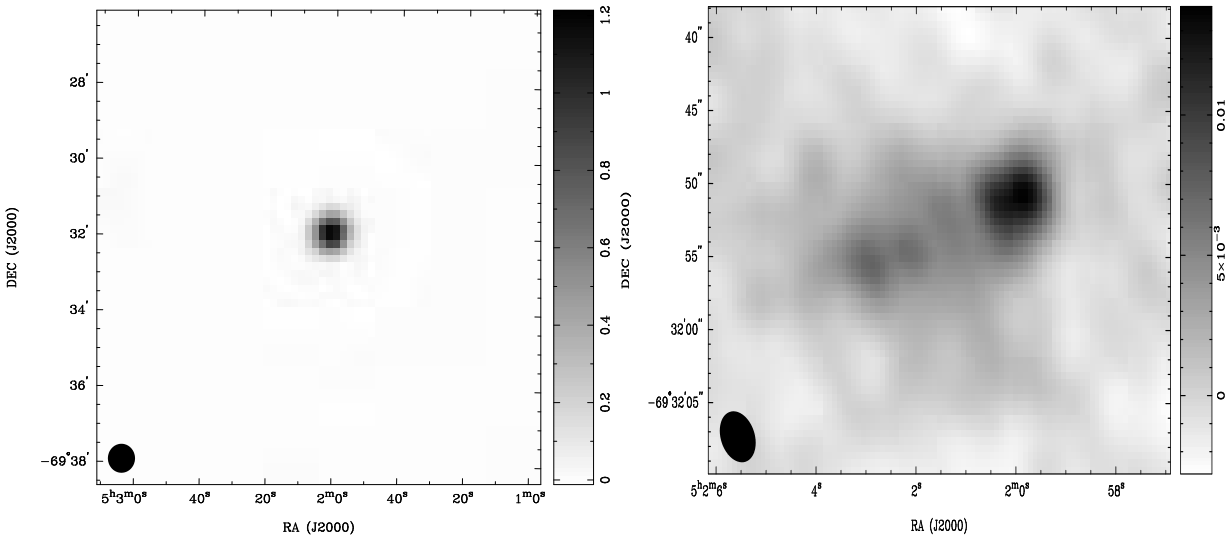

Figure 5.14: The MOST 843 MHz (left) and ATCA 4790 MHz (right) total intensity images of 0502–696 in the Large Magellanic Cloud. The intensity units are in Jy/beam.

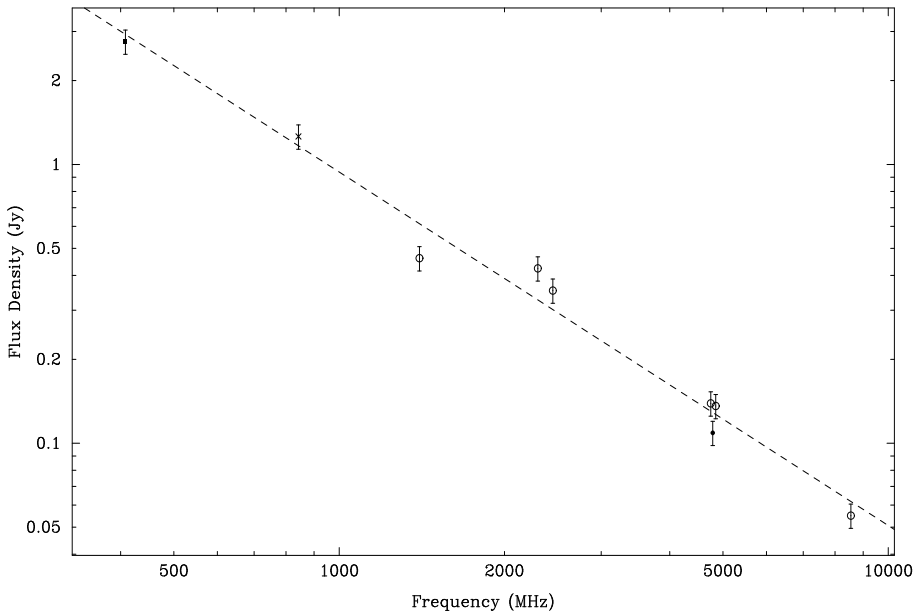

Figure 5.15: The radio spectrum of 0502–696 in the Large Magellanic Cloud.

0503–680 (Figures 5.16 and 5.17) The MOST image shows an isolated point source with peak and integrated flux densities of 312 mJy/beam and 325 mJy respectively. The ATCA image reveals two sources, separated by about 8 arcsec with the dominant source having an integrated flux density of 28 mJy and the weaker source having a flux density of 17 mJy.

The MC4 catalogue lists this source having a flux density of 440 mJy. The Parkes source B0503–6803 has reasonable positional agreement with the ATCA position of the peak of the stronger of the two sources. It should be noted however that there is a relatively large variation in the Parkes positions; the worst case is a difference of over 1.5 arcmin in declination. In general the Parkes source positions typically improve as the angular resolution increases with observing frequency. The flux densities at 4.75 and 4.85 GHz are 82 and 96 mJy respectively which are somewhat higher than the sum of the two ATCA 4790 MHz flux densities. The Parkes source is located near the H II region, N19 (Henize 1956).

A spectral index of $\alpha = -(0.66 \pm 0.05)$ has been determined using the full data set apart from the ATCA 4790 MHz value which is clearly weaker that that predicted from the other data. Given that the components have a flux density ratio of less that two, the analysis of Magliocchetti et al. (1998) suggests that these two sources may be related. Based on morphology and spectral index, it appears that the two objects imaged with the ATCA are a single extragalactic background source.

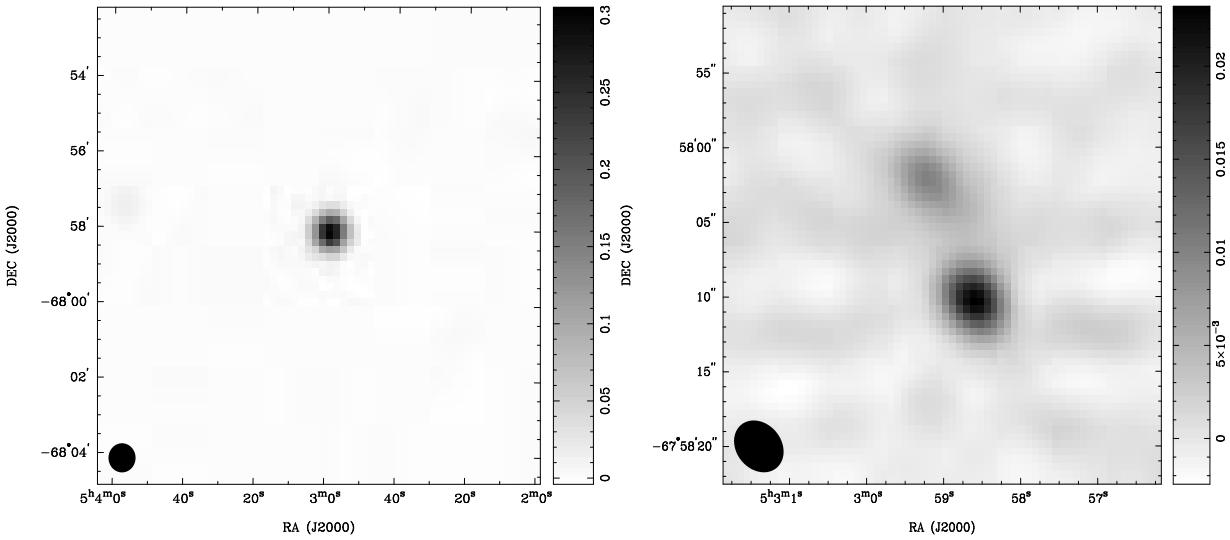

Figure 5.16: The MOST 843 MHz (left) and ATCA 4790 MHz (right) total intensity images of 0503–680 in the Large Magellanic Cloud. The intensity units are in Jy/beam.

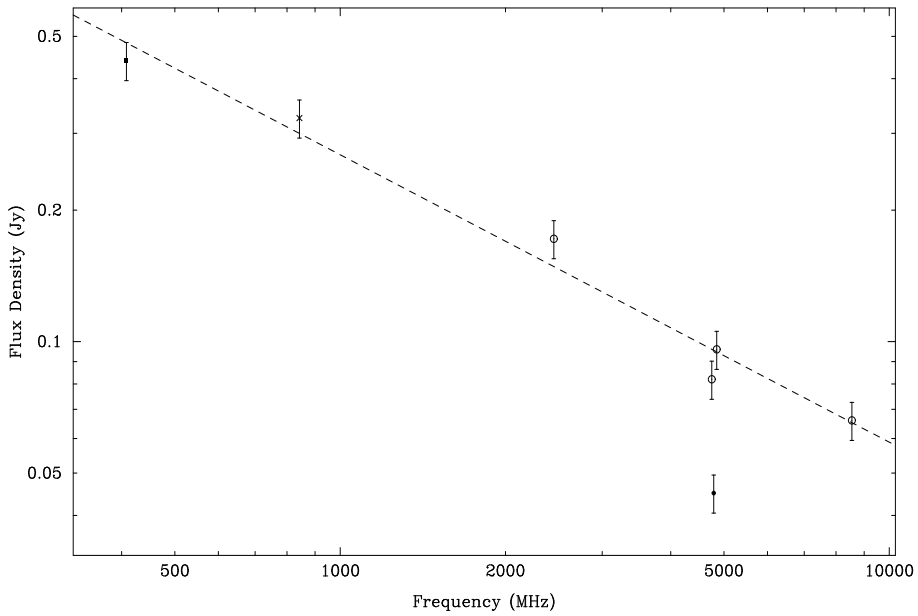

Figure 5.17: The radio spectrum of 0503–680 in the Large Magellanic Cloud.

0504–668 (Figures 5.18 and 5.19) The MOST image shows a compact source with a peak flux density of 333 mJy/beam and integrated flux density of 370 mJy. The fitted source dimensions are approximately 49×45 arcsec suggesting that the source may be slightly extended. The ATCA 4790 MHz image contains two slightly extended sources with the stronger having a peak flux density of 17 mJy/beam and the weaker a peak flux density of around 9 mJy/beam; the integrated flux density of each component is 20 and 14 mJy respectively.

This source is listed in the MC4 catalogue with a flux density of 630 mJy. B0505–6648 was detected in the Parkes surveys only at 2.45, 4.75 and 4.85 GHz. The Parkes flux densities are 61 and 54 mJy at 4.75 and 4.85 GHz respectively. It is somewhat surprising that it was not catalogued at 1.40 GHz although this may be due to the fact that confusion has made accurate position and flux determination difficult. There is no detected X-ray or infrared emission from this object.

The Parkes 2.45 GHz and ATCA 4790 MHz value were excluded from the determination of the spectral index of $\alpha = -(1.10 \pm 0.15)$. The Parkes 2.45 GHz source has a significantly greater flux density than would be expected from the other data, but probably includes contributions from other sources as it is marked as extended in the Parkes catalogue.

The two compact objects are possibly sub-components of the same extragalactic background source.

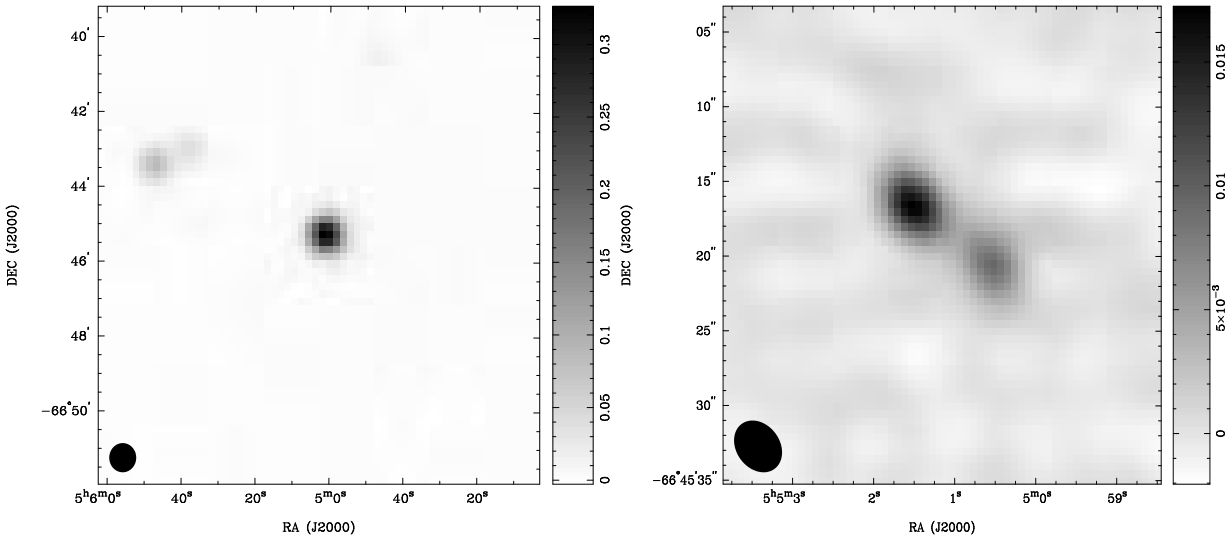

Figure 5.18: The MOST 843 MHz (left) and ATCA 4790 MHz (right) total intensity images of 0504–668 in the Large Magellanic Cloud. The intensity units are in Jy/beam.

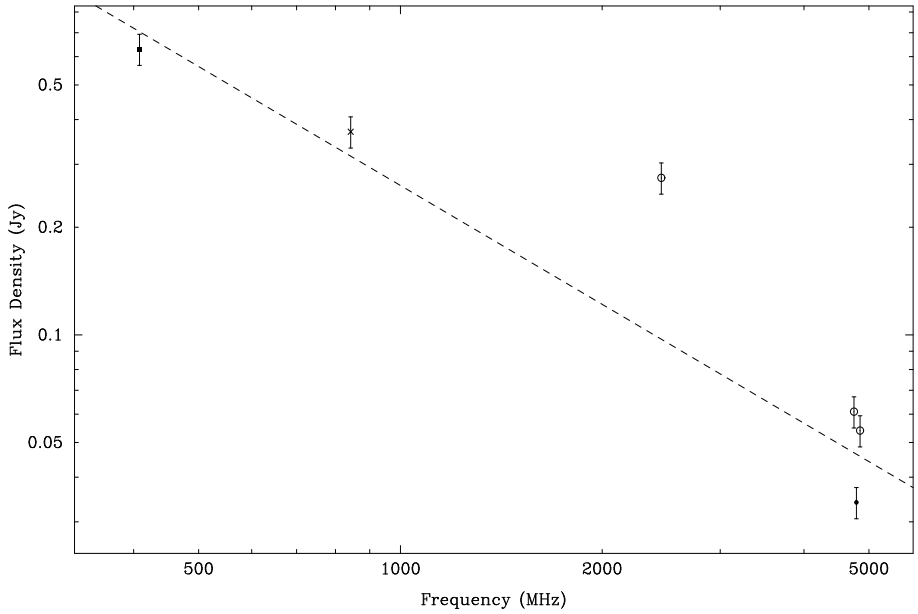

Figure 5.19: The radio spectrum of 0504–668 in the Large Magellanic Cloud.

0505–681 (Figures 5.20 and 5.21) The MOST image shows some faint diffuse emission in the centre of the image and a compact source to the east of the field. The targeted region is the faint diffuse patch of emission in the centre of the subimage which has peak flux density of 37 mJy/beam and an integrated flux density of 129 mJy obtained by interactively selecting the region of interest. The ATCA image appears to be of poor quality which is primarily due to the emission being very weak; the peak flux density is only 1.5 mJy. The integrated flux density is around 2.6 mJy for the source in the centre of the field. There appears to be some diffuse emission to the north-west but this may simply be noise and/or background "ripple".

The Parkes source B0505–6807 has good positional agreement with the ATCA position and it is flagged as being extended in the Parkes beam at the higher frequencies. The catalogued flux densities at 2.45, 4.75, 4.85 and 8.55 GHz are similar and around 300 mJy, suggesting a flat spectrum source. Filipovic et al. (1998c) identify the Parkes source with the known H II region DEM 66 (also known as N23A in the Henize catalogue) which according to DEM has dimensions of 6×5 arcmin and is a bright shell with a core component and filaments. There is an infrared source, LI–LMC405, suggesting that there may be thermal emission associated with the H II region. There is also a known SNR in N23 with source position within an arcminute of the ATCA position and well within the cluster of positions associated with the Parkes source. An X-ray source was detected in both the *Einstein* and *ROSAT* surveys but its position is coincident with the SNR in N23 rather than with the ATCA object. This source was not listed in either the MRC or MC4 catalogue at 408 MHz.

Excluding the MOST 843 MHz and ATCA 4790 MHz flux densities a spectral index of $\alpha = -(0.31 \pm 0.19)$ was calculated, which supports the Parkes identification of this source as an H II region. The ATCA will only well-image emission to a maximum angular extent of around 30 arcsec and the MOST image reveals significant emission at angular scales up to at least 4 arcmin. It is therefore not surprising the ATCA is value is significantly less than predicted from the spectrum. The MOST has sufficient angular resolution to discriminate between this region and other areas of emission in the field, whereas the Parkes radio telescope, particularly at the lower frequencies, would include emission from other sources within the beam. This may explain why the 843 MHz is significantly lower than expected.

It appears that this extended area of emission is an H II region. The compact source imaged with the ATCA may be a brighter knot within the region itself.

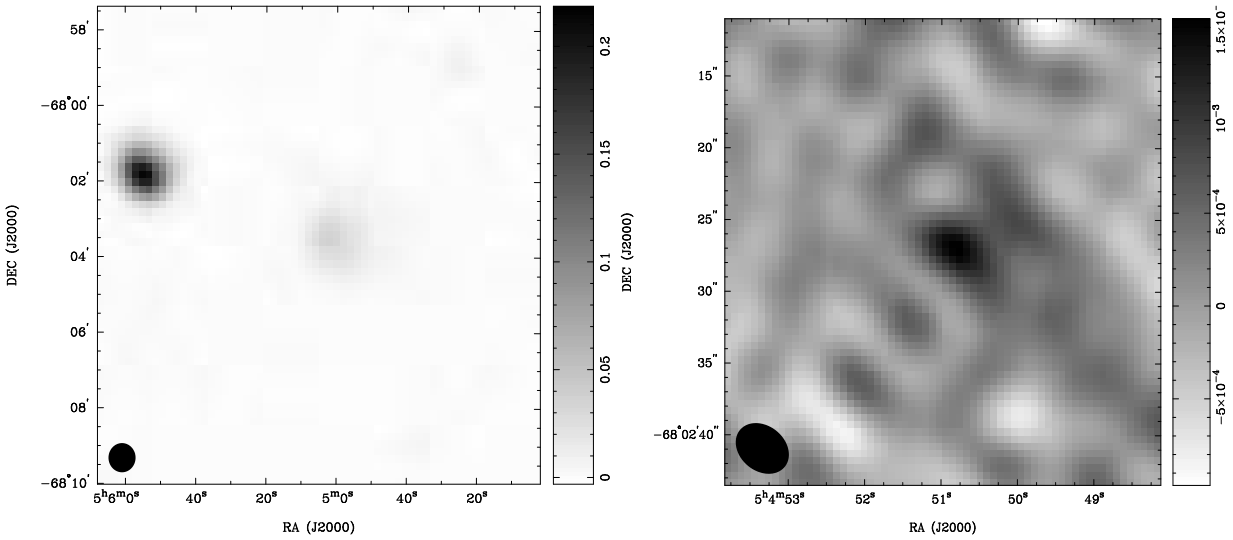

Figure 5.20: The MOST 843 MHz (left) and ATCA 4790 MHz (right) total intensity images of 0505–681 in the Large Magellanic Cloud. The intensity units are in Jy/beam.

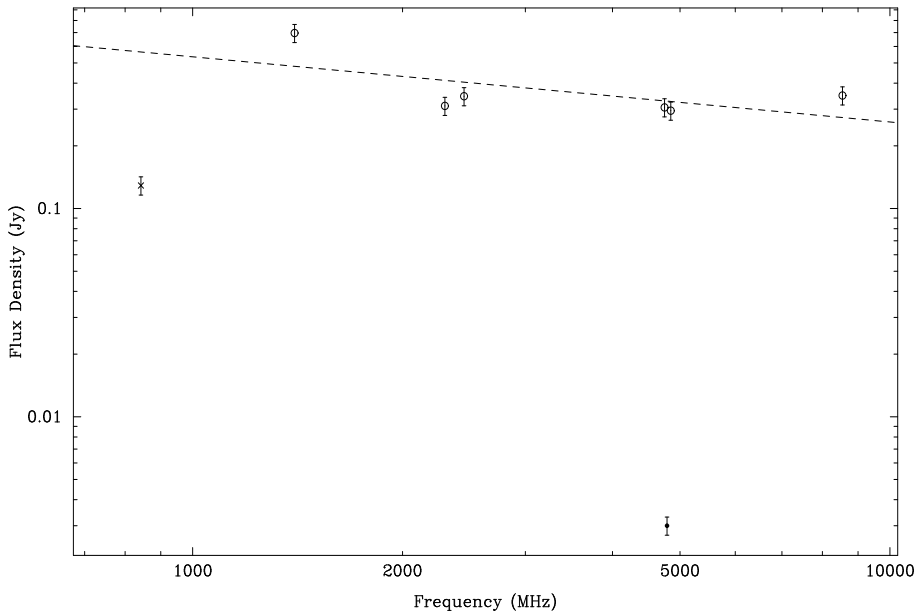

Figure 5.21: The radio spectrum of 0505–681 in the Large Magellanic Cloud.

0510–689 (Figures 5.22 and 5.22) The MOST image shows a compact source with some surrounding diffuse emission and an extension leading away to the south. The 843 MHz peak flux density is 276 mJy/beam with an integrated flux density over the region of 969 mJy. The higher angular resolution ATCA image shows two compact sources with integrated flux densities of 19 and 32 mJy, determined by interactively integrating over the two slightly extended sources.

A flux density of 790 mJy is listed in the MRC at 408 MHz. This is lower than the integrated flux density at 843 MHz although the MC4 catalogue lists a flux density of 1.01 Jy for the same source at the same frequency and flags it as extended. Filipovic and coworkers have detected Parkes source B0510–6857 at all observed frequencies except 1.40 GHz, with flux densities > 1 Jy at all frequencies. This is characteristic of the relatively flat radio spectrum expected at centimetre wavelengths for thermal emission which is commonly associated with H II regions. Filipovic and coworkers identify this Parkes source as being associated with the H II region DEM 86 (Henize: N105A) which consists of a very bright core and outer filaments with dimensions 6×7 arcmin. In addition, Filipovic et al. (1998c) identify the known infrared source LI–LMC534 with B0510–6857. No X-ray emission was detected in the *Einstein* survey although a source was detected in the *ROSAT* PSPC survey of Haberl & Pietsch (1999) around 1.5 arcmin away from the ATCA determined position and is probably unrelated.

Using only the Parkes data, a spectral index of $\alpha = -(0.01 \pm 0.02)$ was determined. Taking the *peak* flux density at 843 MHz and the combined integrated flux density at 4790 MHz gives a spectral index of ~ -1.0, characteristic of an extragalactic background source.

The diffuse emission observed with the MOST is most likely associated with the H II region. The spectrum of the compact components suggests that these may be steep spectrum background sources that happen to be superimposed on the emission from the H II region rather than bright spots within the region itself.

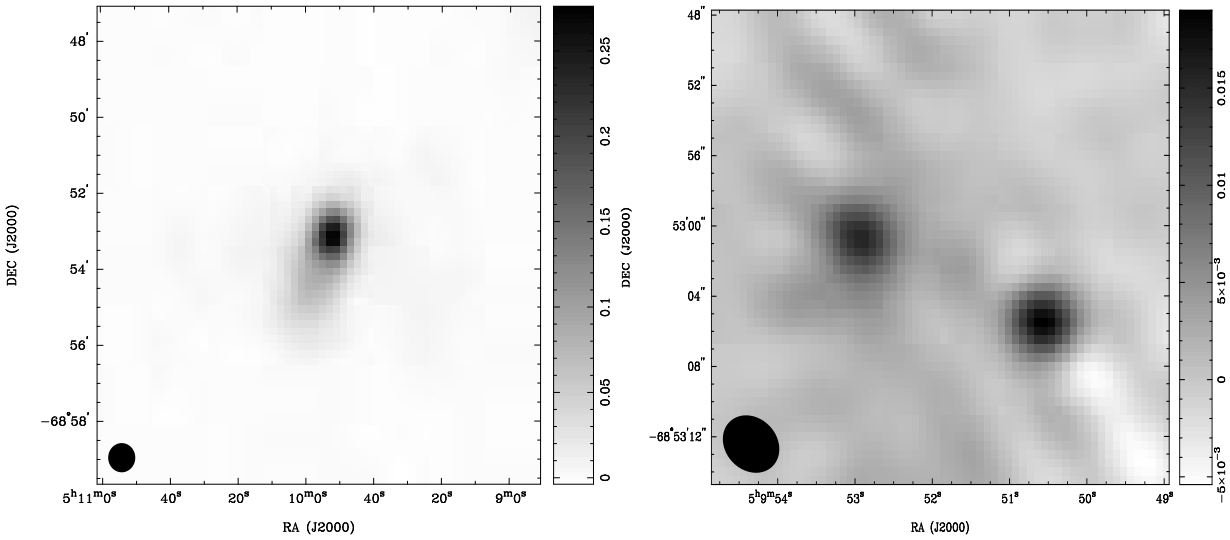

Figure 5.22: The MOST 843 MHz (left) and ATCA 4790 MHz (right) total intensity images of 0510–689 in the Large Magellanic Cloud. The intensity units are in Jy/beam.

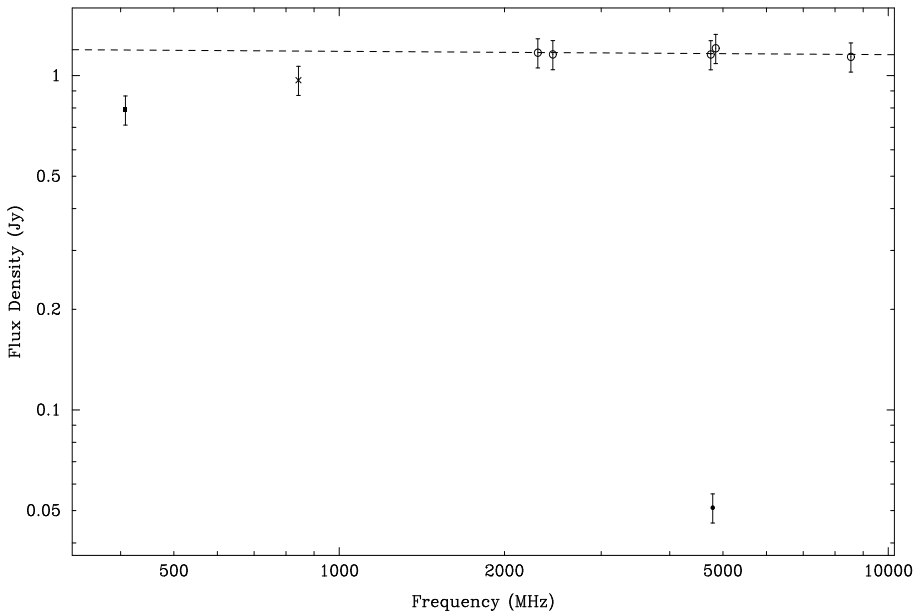

Figure 5.23: The radio spectrum of 0510–689 in the Large Magellanic Cloud.

0513–692 (Figures 5.24 and 5.25) The MOST 843 MHz image shows an extended dish-like region with a point-like object located on the north-eastern edge. The ATCA 4790 MHz image shows a slightly extended but nonetheless compact source at a position corresponding to the point-like object in the MOST image. The larger angular-scale extended emission imaged with the MOST is completely resolved out in the ATCA image. The integrated flux density at 843 MHz was determined by interactively selecting both the compact source and the diffuse extended emission giving a value of 287 mJy. The peak flux density of the compact source is around 28 mJy/beam. The integrated flux density of the object in the ATCA image is 9.1 mJy with a peak flux density of 4.6 mJy/beam.

The Parkes source B0513–6915 was detected only at 4.75 and 8.55 GHz with flux densities of 264 and 68 mJy respectively. As would be expected given the morphology of this source, the ATCA 5 GHz flux density is significantly below the Parkes value as the larger beam of the Parkes radio telescope would have included emission from the compact source and the large extended region. The object was not detected at the lower frequencies observed at Parkes, perhaps owing to confusion and the related difficulty in obtaining accurate source positions and flux densities. Surprisingly, this source is not listed in the MRC but has a flux density of 1.18 Jy in the MC4 catalogue. This source was not observed in the survey by Dickey et al. (1994).

Filipovic et al. (1998a) classify this source as a previously identified SNR and further classify it as being an evolved SNR. The previous classification was based on work by Mathewson et al. (1985). Whilst this object was not detected in X-rays using the *Einstein* satellite and was also not detected within about 10–15 arcmin of the ATCA position with the *ROSAT* HRI (Sasaki, Haberl & Pietsch 2000), the *ROSAT* PSPC does report a source within 1 arcmin of the ATCA determined position of the compact component. A compact H II region, DEM 109 (Henize: N112), is classified as a bright knot by DEM having dimensions of 0.6×0.6 arcmin. The H II region centroid lies only 5 arcsec away from the peak of the ATCA position. There is also a known infrared source, LI–LMC 636, which is most likely associated with the H II region, DEM 109. No detection was made with the PTI at 2.3 GHz.

Given the scatter of flux density values shown in Figure 5.25 a spectral index has not been determined. It is difficult to be certain about the classification of the compact source. Despite excellent positional agreement between a known H II region and the ATCA determined radio position, it may be a chance coincidence with the ATCA source being a weak background object. However, some of the observed 4790 MHz flux density may be intrinsic thermal emission from the H II region itself. Further observations are required over a range of interferometer spacings to image the compact and extended structure fully, in order to determine the nature of the compact source with certainty.

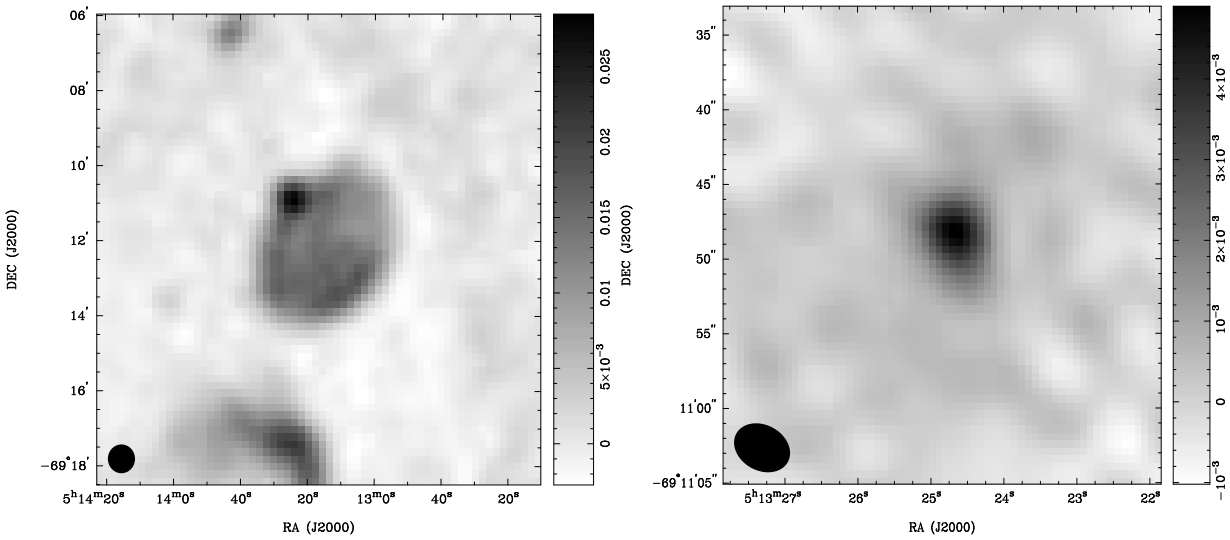

Figure 5.24: The MOST 843 MHz (left) and ATCA 4790 MHz (right) total intensity images of 0513–692 in the Large Magellanic Cloud. The intensity units are in Jy/beam.

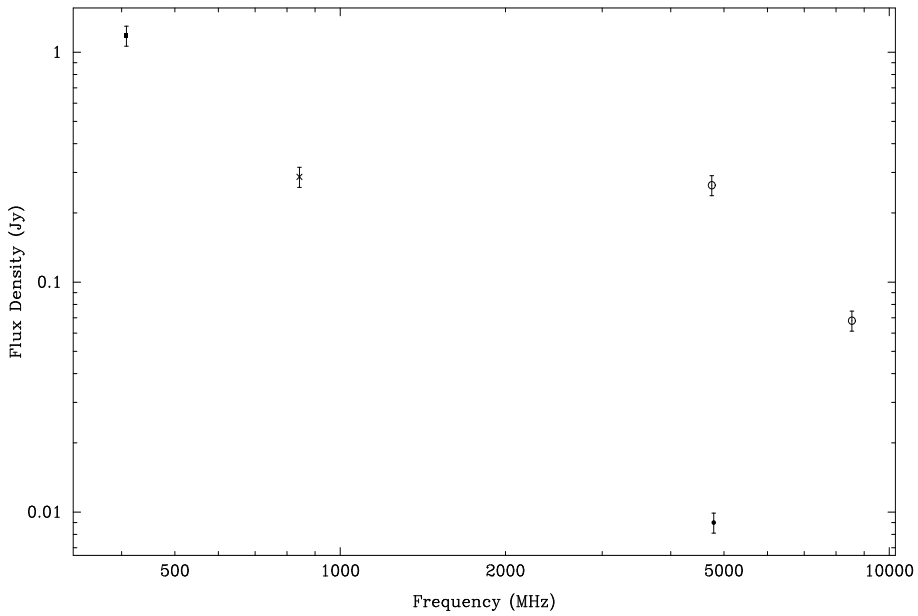

Figure 5.25: The radio spectrum of 0513–692 in the Large Magellanic Cloud.

0514–676 (Figures 5.26 and 5.27) The MOST image shows a single, compact source with a peak flux density of 253 mJy/beam and an integrated flux density of 279 mJy. The full 70 arcmin MOST image shows that this object is located in a region with little extended emission. There is a strong compact source (with flux density greater than 2 Jy/beam) located 15 arcmin to the north east. The 4790 MHz ATCA image shows a cluster of three weak and relatively compact sources with the strongest having a peak flux density of 11 mJy/beam. The integrated flux densities are 16, 14 and 4 mJy. The three sources lie within a circle of diameter ~ 15 arcsec.

No detection of this object is reported in any of the Parkes surveys published by Filipovic and coworkers. Although the source would have sufficient flux density to be detected at 1.40 GHz it is probable that confusion from the strong source located to the north east would have made the measurement of this source particularly difficult at Parkes. This object is catalogued in the MRC with a flux density of 740 mJy at 408 MHz. No known X-ray emission has been reported from this object.

A spectral index of $\alpha = -(1.24 \pm 0.03)$ has been determined from a fit to all three data points (with the ATCA 4790 MHz flux density being the sum of the integrated flux densities of the three individual sources). The integrated flux density ratio of the two strongest sources is less than 1.2, and together with their small separation (10 arcsec) the criteria of Magliocchetti et al. (1998) suggest that these may be components of the same source. The same criteria suggest that the third source is probably unrelated.

The good fit to the spectrum and source morphology (particularly at 4790 MHz) suggests that this is most likely an extragalactic background source.

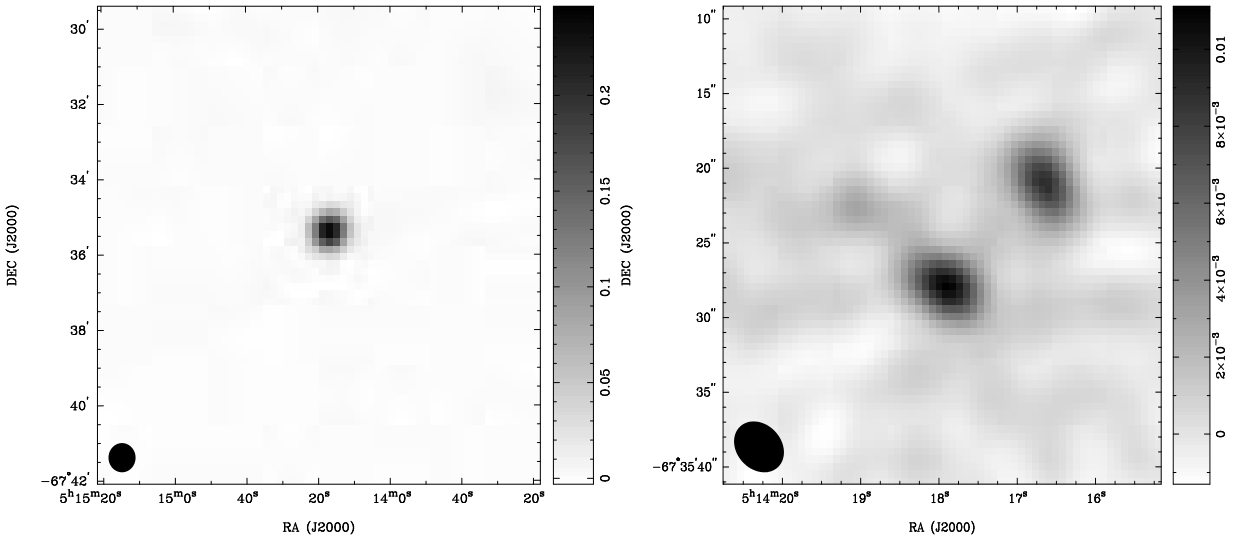

Figure 5.26: The MOST 843 MHz (left) and ATCA 4790 MHz (right) total intensity images of 0514–676 in the Large Magellanic Cloud. The intensity units are in Jy/beam.

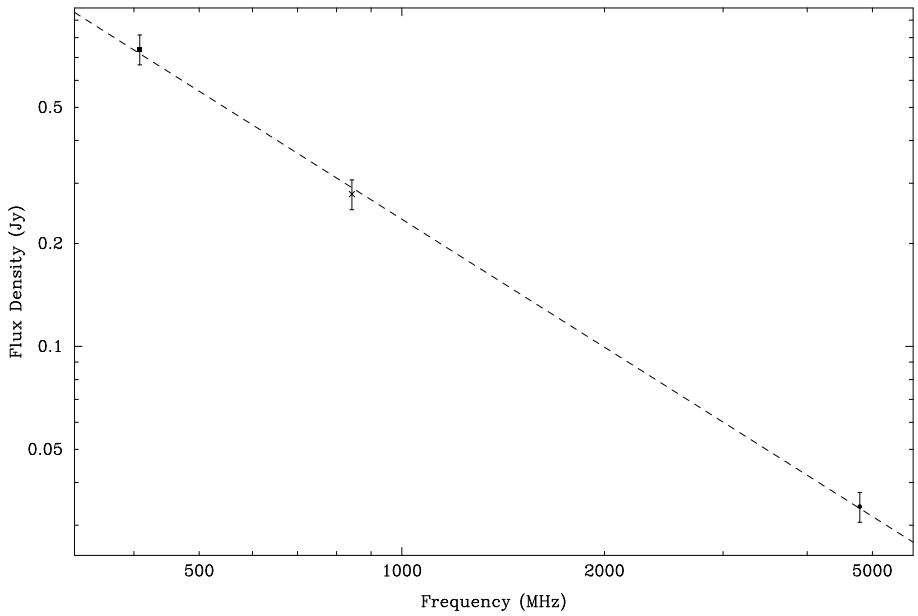

Figure 5.27: The radio spectrum of 0514–676 in the Large Magellanic Cloud.

0515–660 (Figures 5.28 and 5.29) The MOST image shows a compact source with a peak flux density of 499 mJy/beam and integrated flux density of 539 mJy with the deconvolved source dimensions being slightly larger than the synthesized beam. The ATCA image shows an elongated (or "head-tail") source with a peak flux density of 45 mJy/beam at 4790 MHz. The integrated flux density of the entire region of emission is 71 mJy.

The object has an MRC 408 MHz flux density of 1.070 Jy. The Parkes source B0515–6601 is detected at a number of frequencies, with a flux density of 77 mJy at 4.75 GHz and 70 mJy at 4.85 GHz. These values agree with the ATCA determined value of 71 mJy. The ATCA source was previously classified as a background source by Dickey et al. (1994) as part of their identification of sources used for 21 cm absorption studies of the Magellanic System. They denoted this object by J0515–659 with their 1419 MHz continuum position having excellent position agreement with the ATCA data presented here. The difference in source nomenclature is due to MOST B1950.0 source identifications being used for the sources reported here. A *ROSAT* PSPC X-ray source is located within 6 arcsec in declination and 2.5 s in right ascension of the ATCA determined position. No infrared emission is detected.

A spectral index of $\alpha = -(1.09 \pm 0.05)$ was determined from 8 data points with only the Parkes 1.40 GHz value being excluded. It is unclear why this value is significantly lower than both the ATCA 1419 MHz flux density and that predicted from the spectrum.

The spectral index, H I absorption and source morphology support the previous classification of this object as a background source.

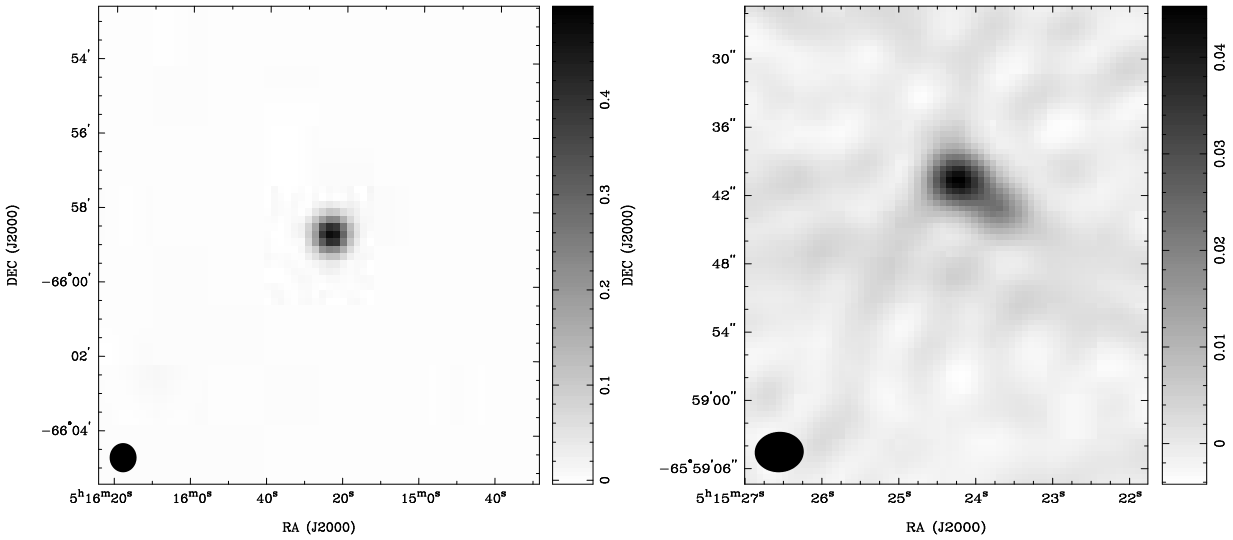

Figure 5.28: The MOST 843 MHz (left) and ATCA 4790 MHz (right) total intensity images of 0515–660 in the Large Magellanic Cloud. The intensity units are in Jy/beam.

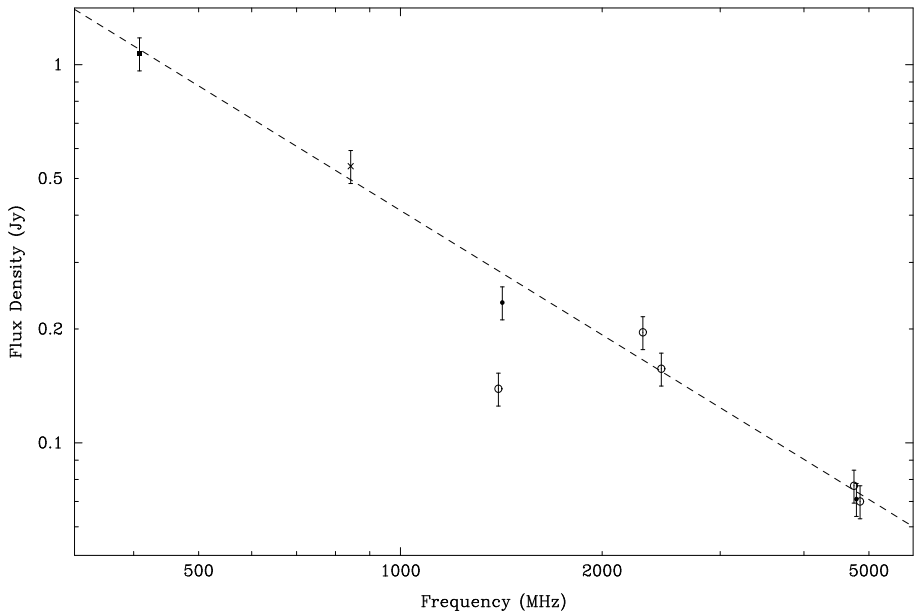

Figure 5.29: The radio spectrum of 0515–660 in the Large Magellanic Cloud.

0515–674 (Figures 5.30 and 5.31) This is the strongest compact source in the LMC. The integrated flux density at 843 MHz is 2.576 Jy and easily dominates the MOST field that contains this source. At 4790 MHz an integrated flux density of 417 mJy was determined.

The 408 MHz flux density from the MRC is 3.770 Jy. The source was detected at all frequencies in the Parkes surveys with flux densities of 728 and 790 mJy at 4.75 and 4.85 GHz respectively. These values are significantly higher than the ATCA value determined from my observations. Filipovic and coworkers note that the H II region, DEM 117, is located in the vicinity of this source. The H II region is categorized as very faint by Davies, Elliott & Meaburn (1976) and has a position around 1 arcmin away from the ATCA position determined here. It is likely that thermal emission from this source may contribute to the flux density determined from the Parkes observations. No infrared emission is detected from this object. The *ROSAT* PSPC survey (Haberl & Pietsch 1999) detect a source that has excellent positional agreement with the ATCA position determined here; the discrepancy is around 3.4 arcsec in declination with negligible difference in right ascension.

All available data were used to calculate a spectral index of $\alpha = -(0.80 \pm 0.08)$ which is consistent with the spectrum of a background source. Observations with the PTI at 2.3 GHz also show that this source in compact and relatively strong with an uncalibrated flux density of around 2.2 Jy. Brief H I spectral line observations conducted with the ATCA showed strong absorption at the expected velocity of the LMC. Based on these observations this object can be confidently classified as a background source.

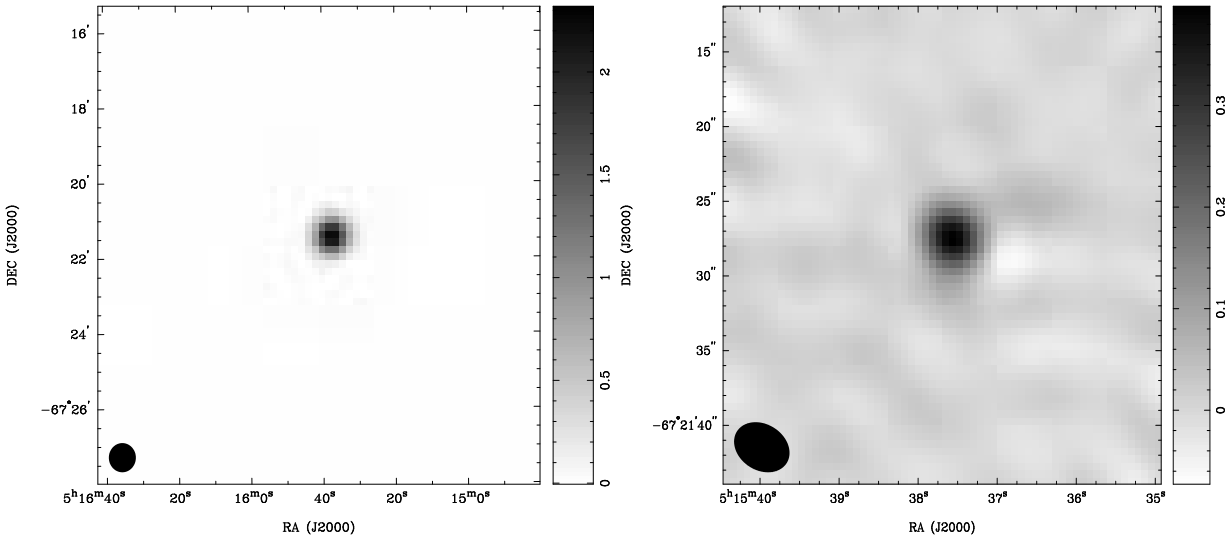

Figure 5.30: The MOST 843 MHz (left) and ATCA 4790 MHz (right) total intensity images of 0515–674 in the Large Magellanic Cloud. The intensity units are in Jy/beam.

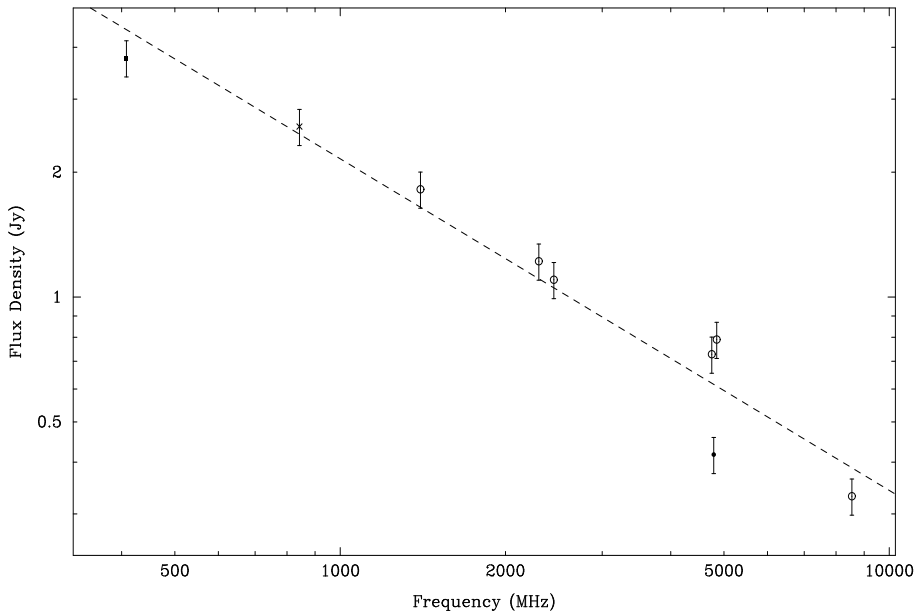

Figure 5.31: The radio spectrum of 0515–674 in the Large Magellanic Cloud.

0517–718 (Figures 5.32 and 5.33) A relatively compact source is revealed at both frequencies. The peak flux density from the MOST 843 MHz image is 483 mJy/beam and the integrated flux density is 535 mJy. The ATCA 4790 MHz peak flux density is 181 mJy/beam and the integrated flux density is 200 mJy. As there is some slight extension visible in the ATCA image automated source fitting was not used.

The source is listed in the MC4 catalogue with a flux density of 580 mJy at 408 MHz. This source was detected at all frequencies in the Parkes surveys and has flux densities of 264 and 275 mJy at 4.75 and 4.85 GHz respectively which are slightly greater than the value determined from the ATCA. It should also be noted that the Parkes 2.30 and 2.45 GHz flux densities of 510 and 314 mJy differ by a significant amount given that the frequencies are relatively close. In addition, the Parkes 1.40 GHz flux density is 537 mJy is similar to the Parkes 2.30 GHz flux density. This may be due to confusion at the two lowest Parkes frequencies, intrinsic source variability or other unknown instrumental factors. Dickey et al. (1994) also observed this source and detected absorption in its direction. They determined a continuum flux density at 1419 MHz of 353 mJy.

Whilst no infrared emission has been detected from this area, X-ray emission has been detected from the source 517.4–7149 as reported by Wang et al. (1991). However, the X-ray source is 3 arcmin away from the ATCA position and there must be some doubt as to whether the X-ray emission is coincident with the compact radio source. Haberl & Pietsch (1999) catalogued an X-ray source (number 1315) which is almost 2 arcmin away from the ATCA position. The two X-ray sources have a position difference in declination of around 4 arcmin suggesting that they are different sources.

A spectral index of $\alpha = -(0.40 \pm 0.07)$ was determined from the full dataset. The PTI 2.3 GHz observations shows multiple strong fringes suggesting source structure at a much smaller angular scale than detected with the ATCA.

The spectral index, structure, presence of H I absorption and the PTI detection suggest that this source is most likely a flat-spectrum extragalactic background source.

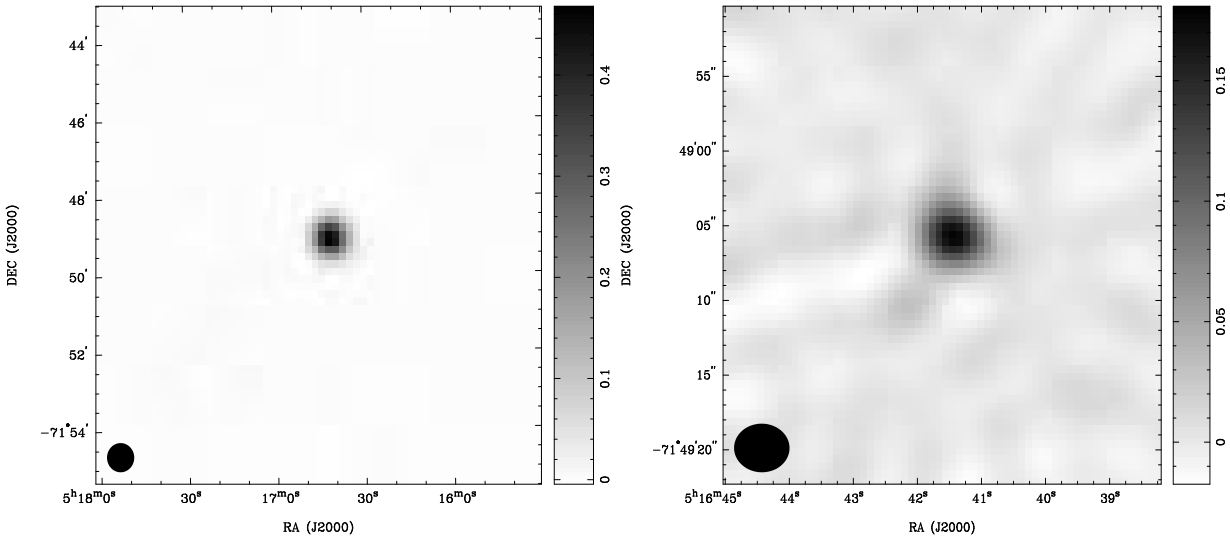

Figure 5.32: The MOST 843 MHz (left) and ATCA 4790 MHz (right) total intensity images of 0517–718 in the Large Magellanic Cloud. The intensity units are in Jy/beam.

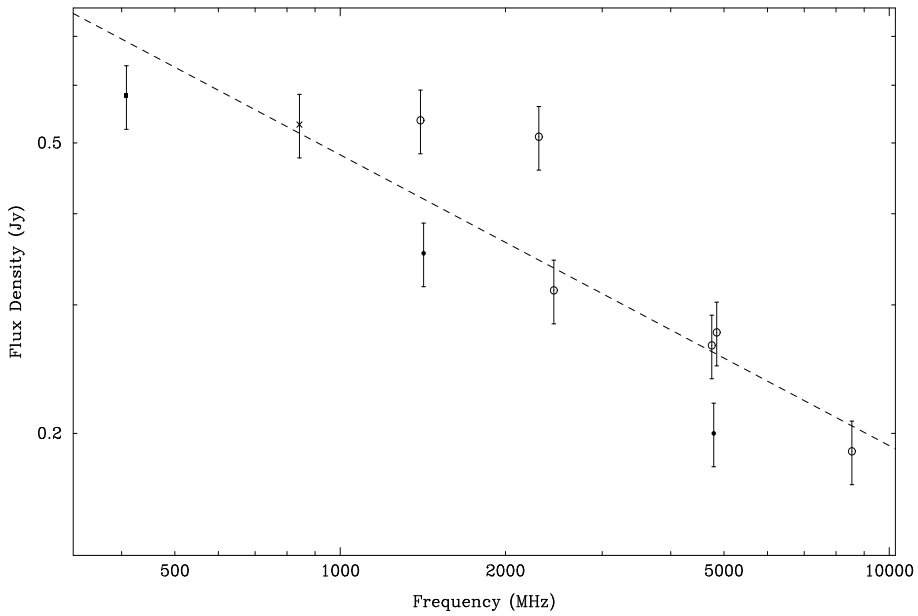

Figure 5.33: The radio spectrum of 0517–718 in the Large Magellanic Cloud.

0518–679 (Figures 5.34 and 5.35) The MOST image shows an isolated, compact source with peak and integrated flux densities of 293 mJy/beam and 332 mJy respectively. The ATCA image shows a complex morphology with the peak flux in the image being a little over 11 mJy/beam. The source, which is compact at the angular resolution of the MOST, is made up of a number of components; two weak and relatively compact components lie to the east of the field and a stronger and elongated source lies to the west. In addition there appears to be faint and diffuse extended emission linking all three sources. The combined flux density of this region is 43 mJy.

The source 0518–679 is listed as having an integrated flux density of 350 mJy in the MC4 catalogue, significantly lower than their listed peak flux density of 550 mJy; it is unclear as to why this is the case. The Parkes source B0518–6759 was detected at all observed frequencies with flux densities of 126 and 112 mJy at 4.75 and 4.85 GHz respectively. Filipovic and coworkers identify this source with the known H II region DEM 129 (Henize: N36) catalogued as having dimensions of 3×3 arcmin and consisting primarily of a bright central knot. Marx, Dickey & Mebold (1997) detect this source with the ATCA at 1380 and 2378 MHz with flux densities of 52 and 19 mJy respectively. However, the 2378 MHz flux density is significantly lower than the ATCA 4790 MHz flux density determined here which may be as a result of their source fitting procedure in which a single gaussian was fitted to the patch of emission. At 2.3 GHz it is probable that the object is beginning to be resolved into a number of distinct components similar to what is observed with the ATCA at 4790 MHz. No X-ray or infrared emission has been detected at the position of this source.

Given the scatter of flux densities, it is a difficult task to select which values to include in a computation of the spectral index. The morphology of the ATCA 4790 MHz image suggests that the compact source is being resolved into a number of discrete components. This hypothesis is supported by the 5 and 8 GHz flux densities from Parkes, which are clustered into the lower right quadrant of Figure 5.35. Taking only the 408 MHz, MOST 843 MHz and the 1.40 and 2.45 GHz Parkes values, a spectral index of $\alpha = -(0.08 \pm 0.13)$ has been determined, which is characteristic of an H II region.

From this single high angular resolution observation it is not possible to determine the nature of the compact emission observed at 4790 MHz. It is reasonable to expect that most of the observed emission is actually part of the H II region due to its diffuse extended morphology. The possibility remains that the compact source may be a weak background object unassociated with the H II region itself.

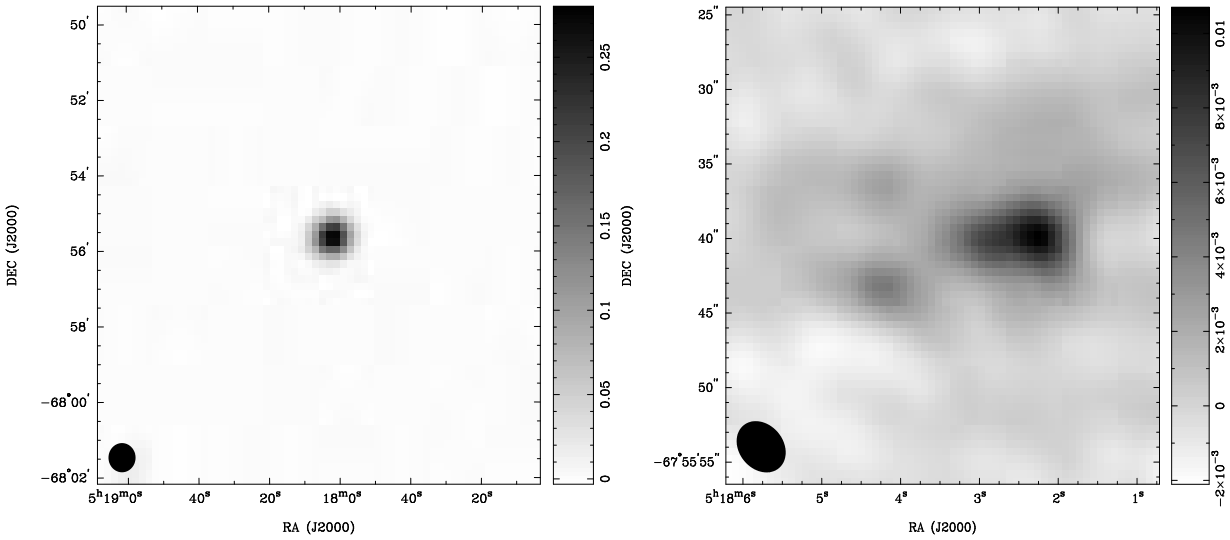

Figure 5.34: The MOST 843 MHz (left) and ATCA 4790 MHz (right) total intensity images of 0518–679 in the Large Magellanic Cloud. The intensity units are in Jy/beam.

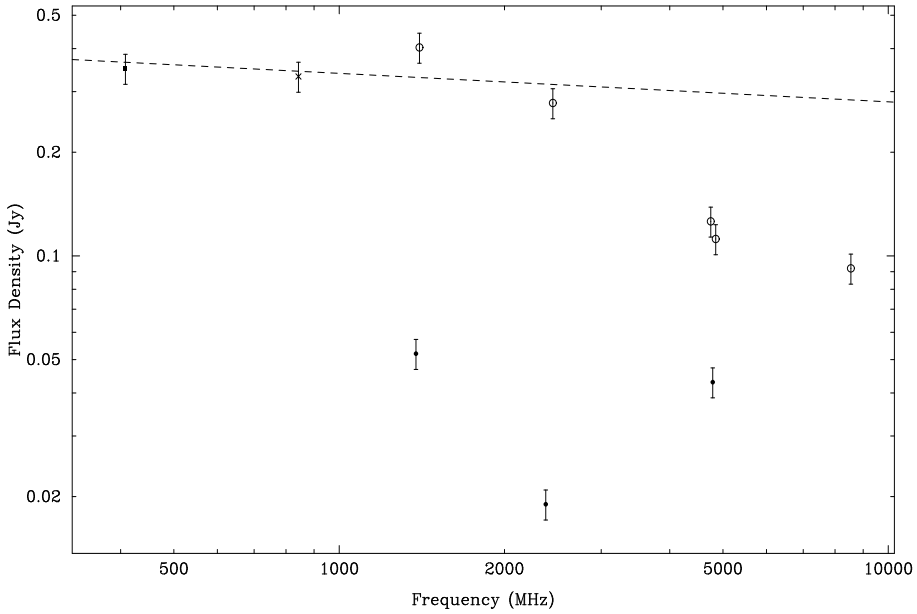

Figure 5.35: The radio spectrum of 0518–679 in the Large Magellanic Cloud.

0518–696 (Figures 5.36 and 5.37) The images at both frequencies reveal a compact source with some slight extension visible in the ATCA image. The peak and integrated flux densities at 843 MHz are 560 mJy/beam and 588 mJy respectively. The ATCA 4790 MHz integrated flux density is 102 mJy, determined interactively to include the slight extension visible on the TV display. An inspection of the full 70 arcmin MOST image reveals extended emission on a scale of arcminutes corresponding to the faint diffuse emission visible to the south-east of the MOST image. There is also some other diffuse emission surrounding the compact source.

This source appears in the MRC with a flux density of 1.040 Jy. Parkes source B0518–6937 lies within an arcminute of the ATCA position, but was only detected at 8.55 GHz with a flux density of 107 mJy. The source was observed in the survey of Dickey et al. (1994) with a 1419 MHz continuum flux density of 330 mJy and H I absorption was detected. The source was detected at both 1380 and 2378 MHz by Marx, Dickey & Mebold (1997) with flux densities of 326 and 259 mJy respectively; the flux density at the lower of these frequencies has good agreement with the 1419 MHz value. The ATCA position is around 8 arcmin north of the H II region DEM 134 (Henize: N120). An X-ray source 519.1–6943 (Wang et al. 1991) is located over 4 arcmin to the south of the ATCA position and is probably coincident with the SNR located near DEM 134. Similarly, the *ROSAT* PSPC survey also detects a source at a similar position to that reported by Wang et al. (1991) and is identified as the SNR in N120.

Excluding the Parkes 8.55 GHz flux density results in a spectral index of $\alpha = -(0.92 \pm 0.06)$, typical of an extragalactic background source. The sole Parkes value is significantly greater than that which would be expected from the extrapolated spectrum. This is probably due to the larger Parkes beam including a significant flux density contribution from the large region of extended emission located to the south of 0518–696.

Although this object is located near two H II region and a known SNR, the high angular resolution ATCA data suggests that this source is unrelated to these objects and is a compact extragalactic background source.

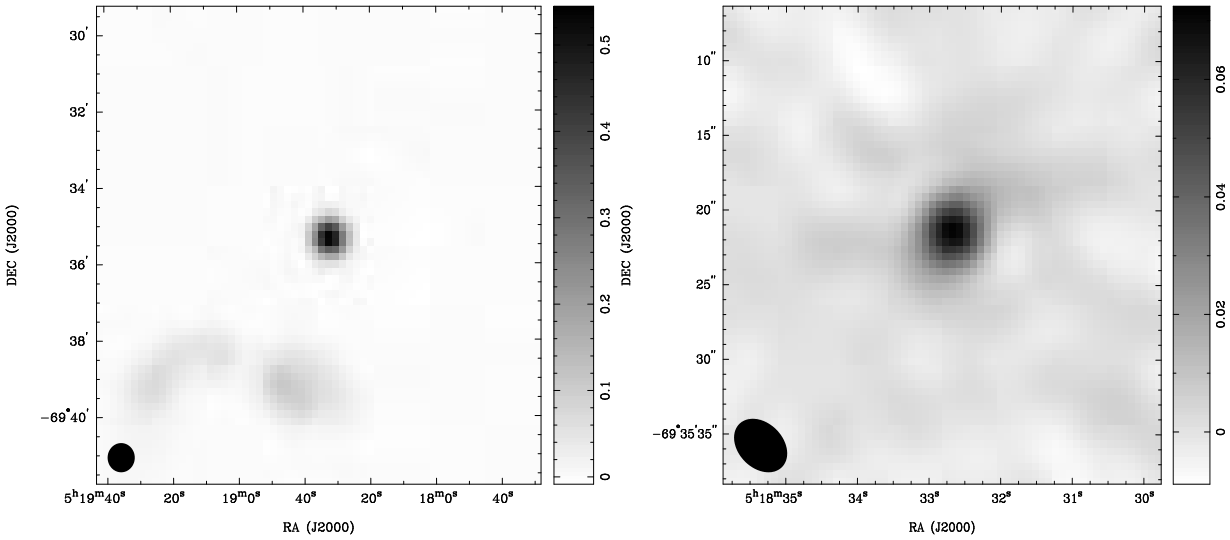

Figure 5.36: The MOST 843 MHz (left) and ATCA 4790 MHz (right) total intensity images of 0518–696 in the Large Magellanic Cloud. The intensity units are in Jy/beam.

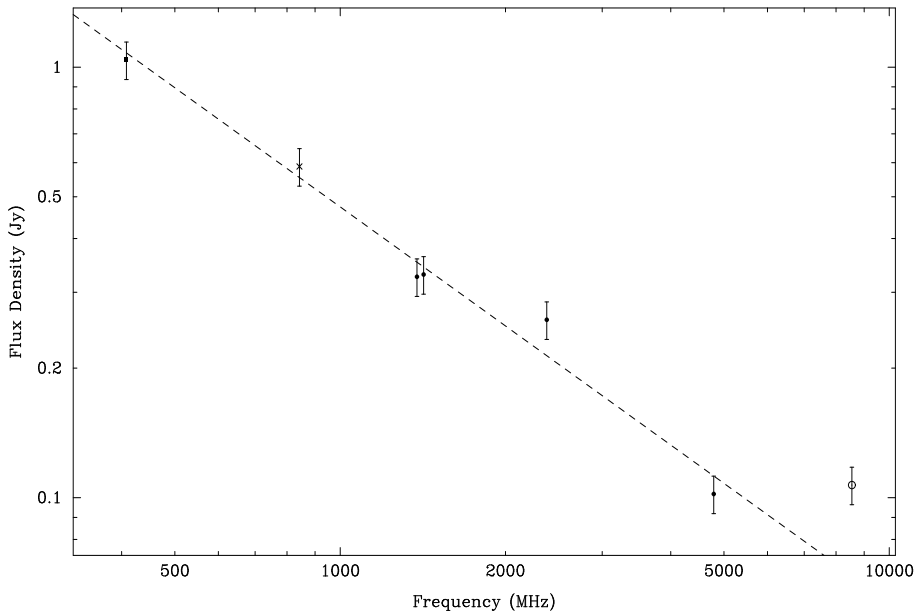

Figure 5.37: The radio spectrum of 0518–696 in the Large Magellanic Cloud.

0524–708 (Figures 5.38 and 5.39) The top panel of Figure 5.38 shows the MOST of image of this source which reveals an apparent double source structure. Treating these two sources as a single entity for the purpose of the determination of integrated flux density gives a value of 1.774 Jy. The peak from the stronger of the two sources is 705 mJy/beam. The ATCA 4790 MHz observations resolve the two objects into individual sources as shown in the lower panel of this figure. The image on the left corresponds to the northern component of the MOST image and has a peak flux density of 40 mJy/beam and an integrated flux density of 80 mJy. The ATCA image of the southern component is shown on the right of the lower panel and has a slightly larger peak flux density of 49 mJy/beam with an integrated flux density of 81 mJy.

A flux density of 2.350 Jy is listed in the 408 MHz MRC and the source B0524–7053 was detected at all frequencies in the Parkes surveys; it is noted as being extended only at 2.30 GHz. There is no X-ray or infrared emission detected from these sources. The source was resolved into the two components in both the H I survey of Dickey et al. (1994) and the continuum survey of Marx, Dickey & Mebold (1997). Dickey et al. (1994) determined 1419 MHz continuum flux densities of 195 and 207 mJy and Marx, Dickey & Mebold (1997) list 1380 MHz flux densities of 225 and 245 mJy and 2378 MHz flux densities of 144 and 156 mJy. Dickey et al. (1994) note that the first of these sources shows H I absorption whereas the second shows no absorption and they suggest that this may be due a sharp spatial boundary for the cloud seen in absorption towards the first of the sources.

Excluding both ATCA values results in a spectral index of $\alpha = -(0.88 \pm 0.07)$. It should be noted that the flux densities determined from the Parkes surveys in the 5 GHz band are around 100 mJy greater than those determined with the ATCA and this trend is repeated in the 1.4 GHz band. This suggests that the ATCA observations have detected a compact feature in each component and have not included all the emission from large angular scales.

It appears likely that this is an extragalactic double-lobed radio source and that the ATCA is only sensitive to a "bright spot" in each component. This is supported by the spectrum which is typical of background sources, and by the H I absorption seen in the direction of one component.

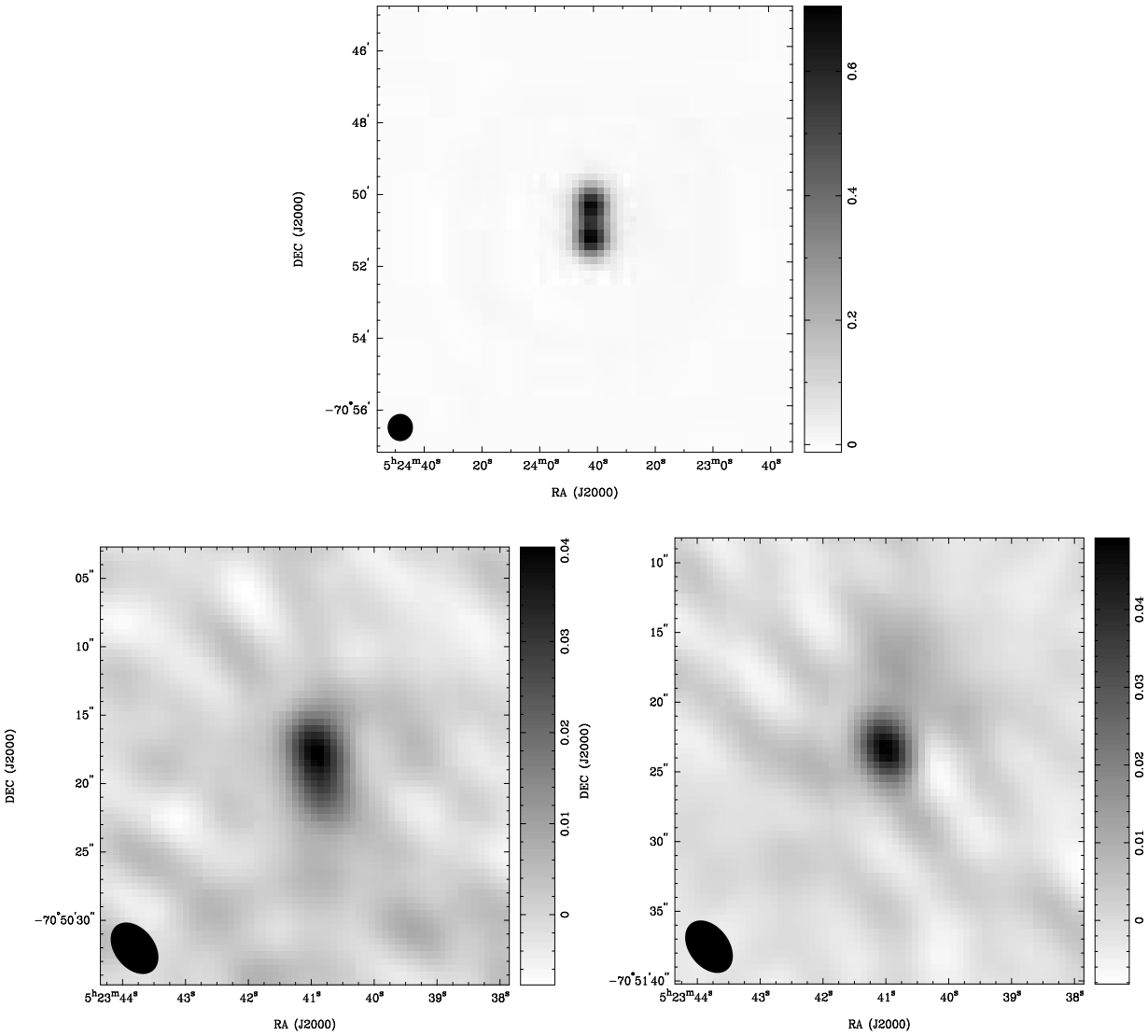

Figure 5.38: The MOST 843 MHz (top) and ATCA 4790 MHz (bottom left and right) total intensity images of 0524–708 in the Large Magellanic Cloud. The intensity units are in Jy/beam.

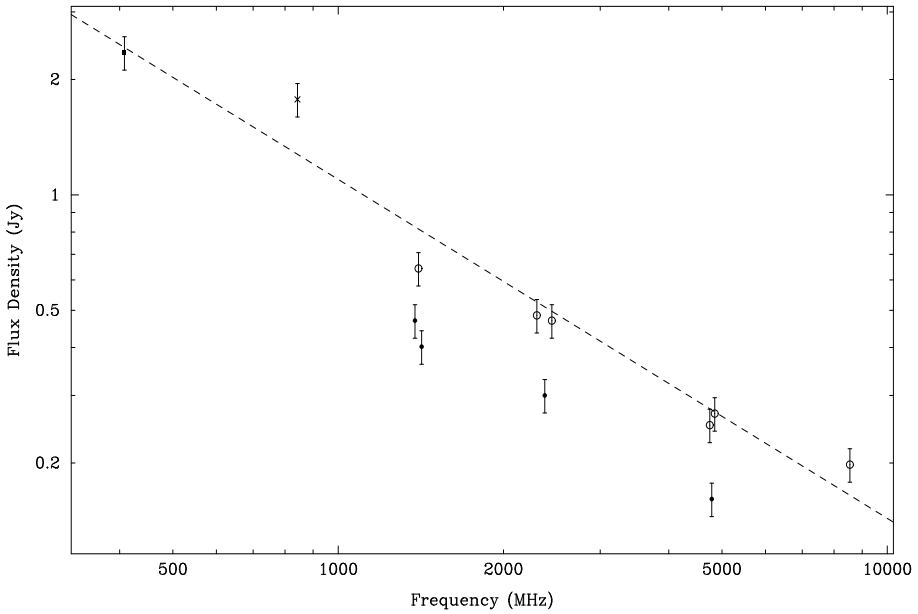

Figure 5.39: The radio spectrum of 0524–708 in the Large Magellanic Cloud.

This page intentionally left blank to maintain formatting.

0526–658 (Figures 5.40 and 5.41) The MOST image shows a compact source with a fainter source to the immediate north and another very faint source some distance away to the north-west. The integrated flux density of the compact source and the weaker adjacent source combined is 408 mJy at 843 MHz. The ATCA 4790 MHz image shows a source slightly extended to the north, with the region having an integrated flux density of 54 mJy.

The source has a catalogued flux density of 640 mJy in the MC4 catalogue. The Parkes survey detected the source B0526–6551 at 2.30, 2.45, 4.75 and 4.85 GHz; at the latter two frequencies, flux densities of 138 and 108 mJy were determined. These values are around twice that detected with the ATCA at a similar frequency. The Parkes source has been identified with N49D (Henize 1956); no X-ray or infrared emission has been detected from this object. Dickey et al. (1994) report a 1419 MHz continuum flux density of 121 mJy for this source, with a number of absorption components which is expected given that this is a region associated with a complex pattern of Hα filaments and H II regions.

The morphology of the MOST and ATCA images suggests that the compact source may be superimposed on the extended emission. Assuming this is the case, the choice of flux densities from which to calculate the spectral index needs to be undertaken with care. It is likely the flux densities from Parkes will include the core component, extended emission and other sources within the beam. Thus, excluding the Parkes values and using the *peak* flux density from the MOST, a spectral index of $\alpha = -(1.03 \pm 0.15)$ was determined which is typical of a relatively steep spectrum background source. Weak PTI 2.3 GHz fringes were detected at the ATCA position with an approximate flux density of 60 mJy.

Based on source morphology, the radio spectrum, PTI detection and the H I absorption results, the compact component is likely to be a background source coincidently superimposed on the H II region.

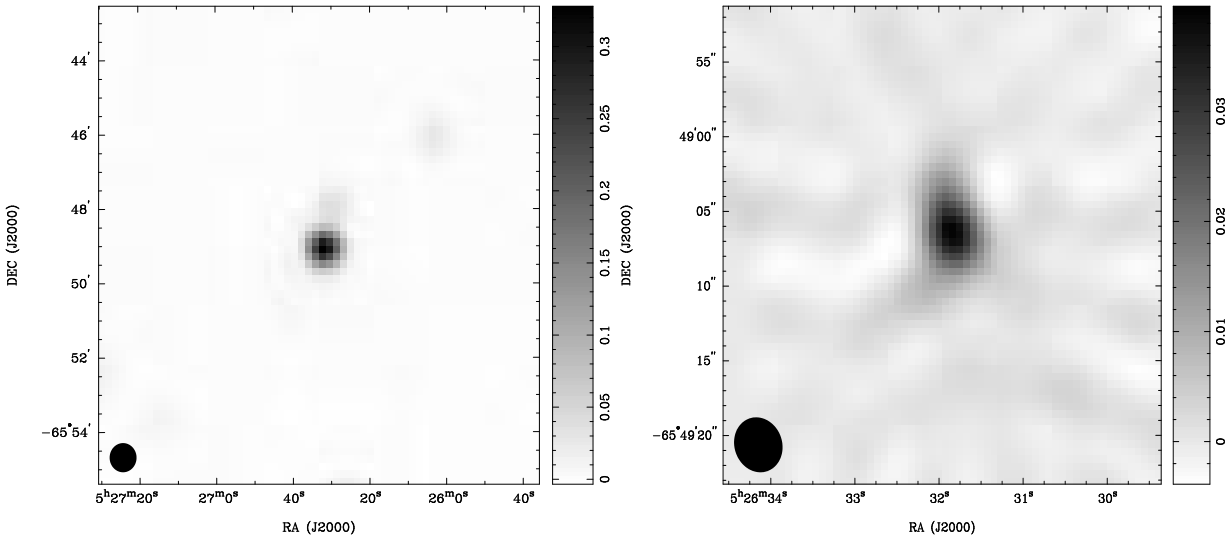

Figure 5.40: The MOST 843 MHz (left) and ATCA 4790 MHz (right) total intensity images of 0526–658 in the Large Magellanic Cloud. The intensity units are in Jy/beam.

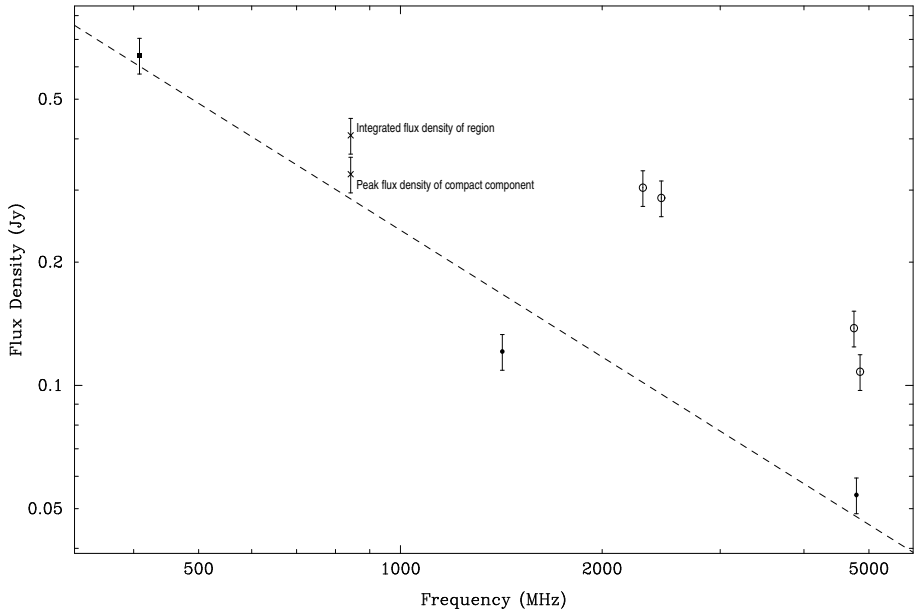

Figure 5.41: The radio spectrum of 0526–658 in the Large Magellanic Cloud.

0526–659 (Figures 5.42 and 5.43) The MOST 843 MHz image shows a strong, compact source with some faint extension to the north-west whereas the ATCA image has almost completely resolved this source into two weak, compact sources and some fainter diffuse emission on the eastern edge of the sub-image. The two regions of emission are separated by around 50 arcsec. The "patchy" appearance of the ATCA image is because the low peak flux densities accentuate the baselevel when a linear transfer function is applied. The peak and integrated flux densities at 843 MHz are 291 mJy/beam and 401 mJy respectively. At 4790 MHz the integrated flux densities for each region have been determined separately by interactively selecting the region of interest. The flux density of the compact source and diffuse emission on the eastern edge of the field is 47 mJy. The compact source located near the western edge of the field has a flux density of 11 mJy.

A flux density of 530 mJy is listed in the MC4 catalogue. The Parkes source B0526–6558 lies within 2 arcsec of the peak in the MOST position but was detected in the Parkes surveys at only 4.75 GHz with a flux density of 119 mJy, and it may be associated with N49C (Henize 1956). Although no X-ray emission was detected, the infrared source LI–LMC1042(1067) is probably associated with the Parkes radio source according to (Filipovic et al. 1998c).

Excluding only the ATCA 4790 MHz from the determination of the spectral index gives a value of $\alpha = -(0.63 \pm 0.07)$. I conclude that around 50% of the 5 GHz emission from this source is from structure with an angular scale of greater than 30 arcsec and is resolved out by the ATCA.

The source morphology revealed with the ATCA suggests that this may be a double-lobed radio galaxy background to the LMC. However, the separation of the two regions of emission is near the limits defined by Magliocchetti et al. (1998) for components to be members of a "double source". Further ATCA observations over a range of baselines and frequencies are needed to sample the larger scale structure.

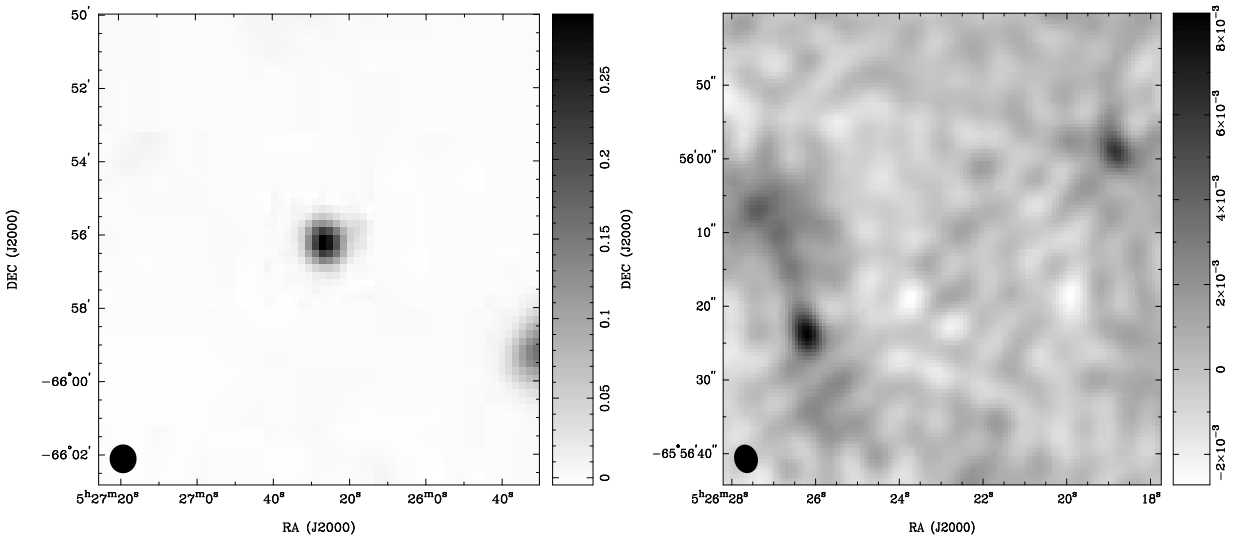

Figure 5.42: The MOST 843 MHz (left) and ATCA 4790 MHz (right) total intensity images of 0526–659 in the Large Magellanic Cloud. The intensity units are in Jy/beam.

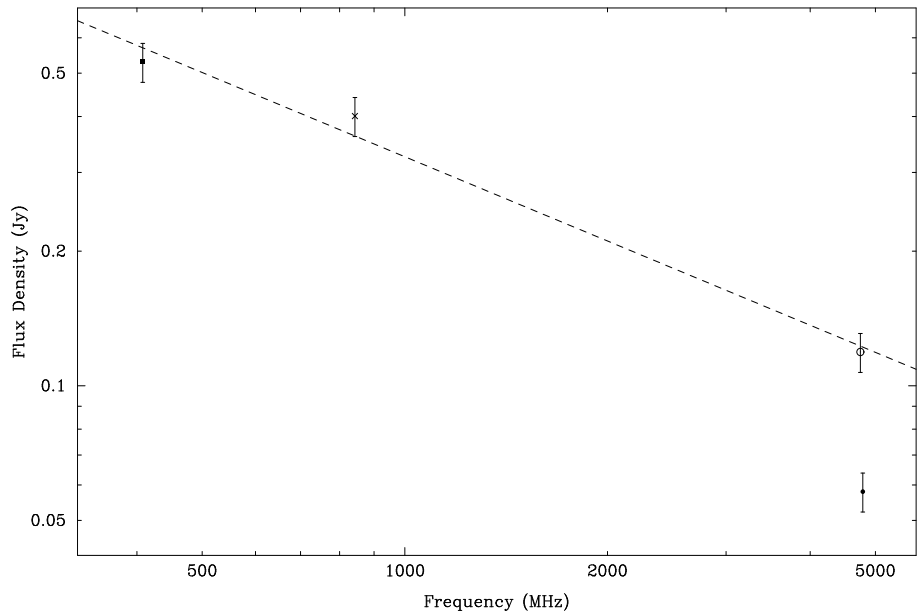

Figure 5.43: The radio spectrum of 0526–659 in the Large Magellanic Cloud.

0527–651 (Figures 5.44 and 5.45) A compact source was observed at both frequencies. The MOST 843 MHz source has an integrated flux density of 654 mJy and the ATCA 4790 MHz source has an integrated flux density of 187 mJy.

The flux density given in the MRC at 408 MHz for this object is 1.080 Jy. The Parkes source B0528–6506 was detected at a number of frequencies with a 4.75 GHz flux density of 193 mJy which agrees well with the ATCA value determined here. Dickey et al. (1994) give a continuum flux density of 431 mJy at 1419 MHz, consistent with the value of 417 mJy determined from the Parkes observations. There appears to be no H I absorption towards this source although emission is observed. No X-ray or infrared emission is detected. A spectral index of $\alpha = -(0.69 \pm 0.03)$ was determined from all available data. Fringes were also detected with the PTI at 2.3 GHz.

Based on the radio spectrum and morphology this is probably a compact background source.

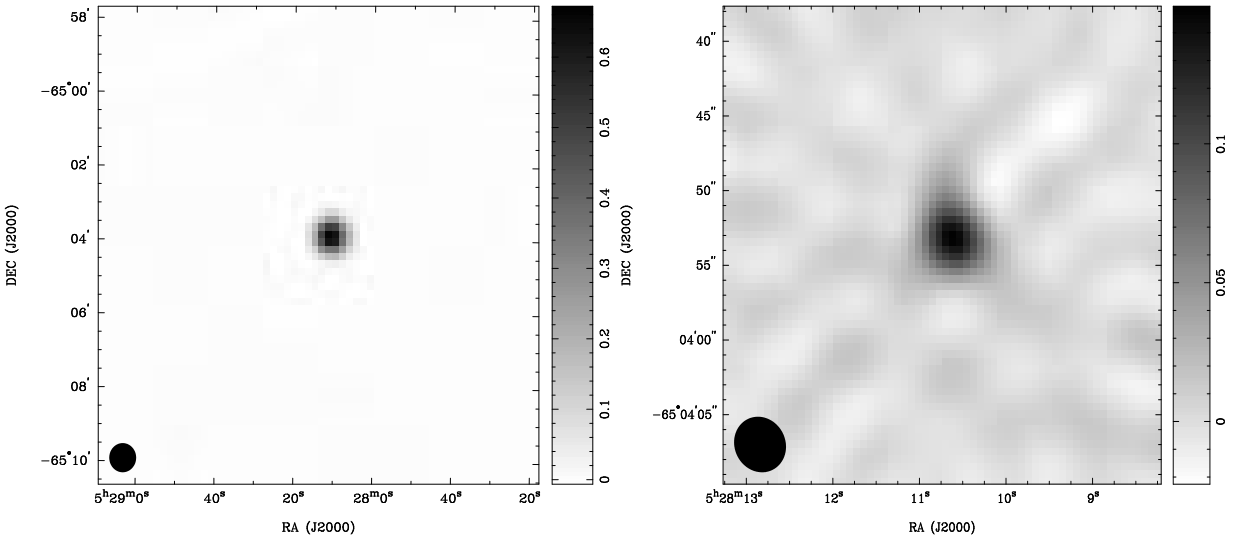

Figure 5.44: The MOST 843 MHz (left) and ATCA 4790 MHz (right) total intensity images of 0527–651 in the Large Magellanic Cloud. The intensity units are in Jy/beam.

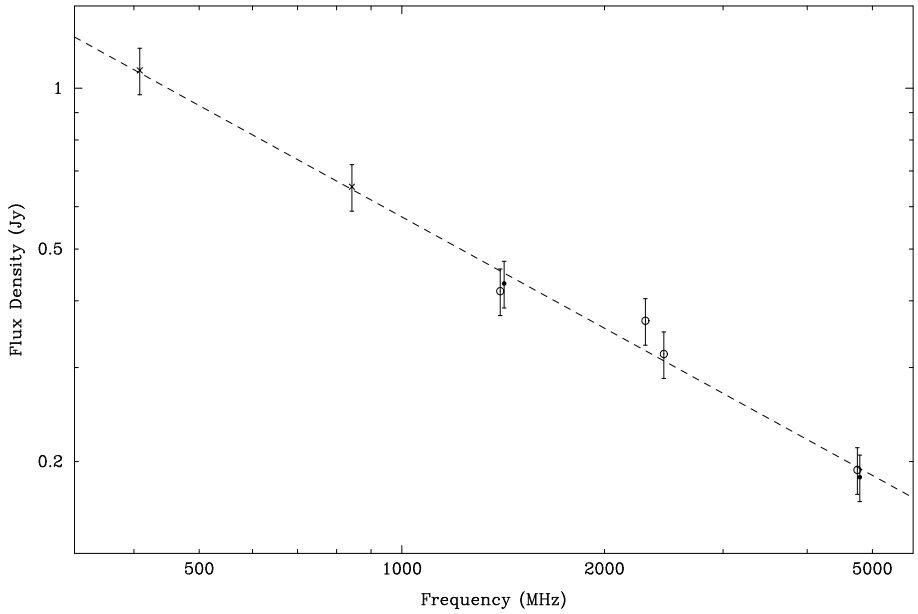

Figure 5.45: The radio spectrum of 0527–651 in the Large Magellanic Cloud.

0528–692 (Figures 5.46 and 5.47) The MOST image reveals a compact source on the eastern edge of a faint but complete "ring" of emission. The integrated flux density at 843 MHz of the compact source and "ring" combined is 83 mJy. The ATCA image shows a weak and slightly extended compact source with a position of the peak some 10 arcsec from the centroid of the compact source in the MOST image. The integrated flux density at 4790 MHz is 3.2 mJy.

Given the 843 MHz flux density, the expected 408 MHz flux density from this object would be below the catalogue limits of both the MC4 and MRC and no source is listed in these catalogues. Parkes source B0528–6914 observed in the surveys by Filipovic and coworkers is located within 15 arcsec of the ATCA position. The Parkes flux densities at 4.75 and 4.85 GHz are 75 and 73 mJy respectively; the source was only detected in the 5 and 8 GHz bands. Filipovic et al. (1998a) classify this source as an evolved SNR with a radio spectral index of $\alpha = -(0.44 \pm 0.03)$. The source is catalogued with a flux density of 15 mJy at 1380 MHz in the survey of Marx, Dickey & Mebold (1997). An X-ray source, 528.1–6915 is catalogued by Wang et al. (1991) with a position some 30 arcsec from the emission peak in the ATCA image. The *ROSAT* PSPC survey detected what is presumably the same X-ray source. The catalogued *ROSAT* source position lies only 11 arcsec from the ATCA object. The X-ray source is identified with the SNR and is coincident with the H II region DEM 210. Davies, Elliott & Meaburn (1976) describe this Hα nebulosity as being scattered.

A spectral index of $\alpha = -(0.09 \pm 0.02)$ was determined from the MOST and Parkes data and the fit to these values is shown by the dashed line in Figure 5.47. It is not surprising that the ATCA 4790 MHz value is significantly less than the Parkes flux densities (at a similar frequency) given that the ATCA will only be sensitive to emission on angular scales less than about 30 arcsec. The faint ring of emission visible in the MOST image has a diameter of around 2 arcmin. Taking the flux density of the compact component at 843 MHz (45 mJy) and the ATCA values gives a spectral index of $\alpha = -(1.51 \pm 0.21)$ and is shown by the dotted line in Figure 5.47. Neither of these values agree with that determined by Filipovic et al. (1998a). The lower frequency Parkes results are not catalogued and this is probably due to confusion leading to significant position and flux density uncertainties at 1.4 and 2.3 GHz.

It is difficult to be certain as to the nature of this source with the limited high angular resolution radio data available. The spectral index of the compact component suggests that this may be an an extragalactic background object. Further ATCA observations, over a range of baselines, but particularly at 1.4 GHz, are needed to image the compact and extended components and thus classify the source with some degree of certainty.

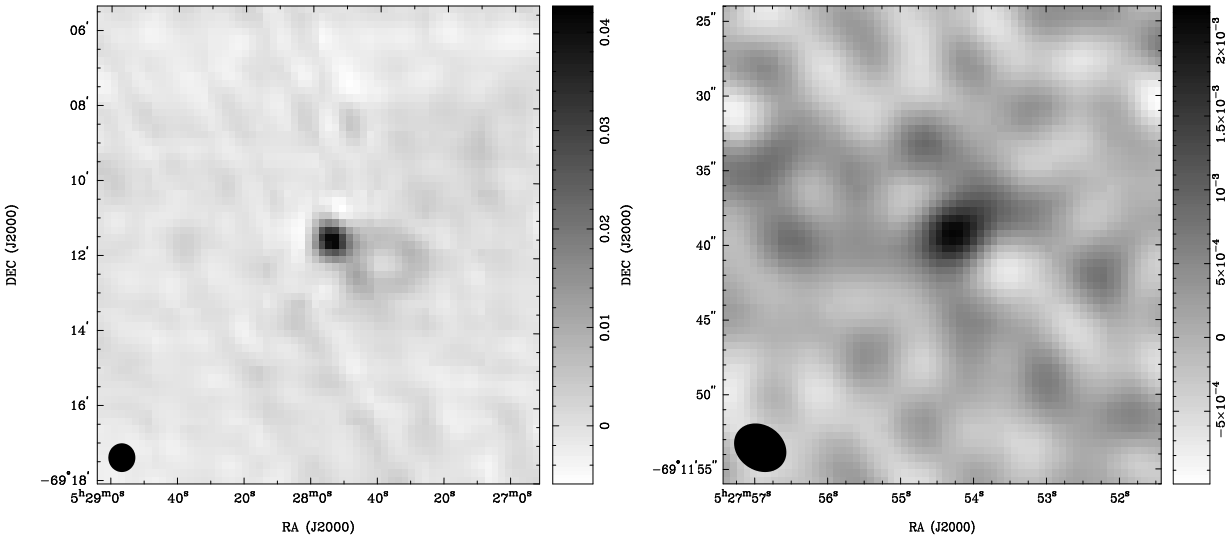

Figure 5.46: The MOST 843 MHz (left) and ATCA 4790 MHz (right) total intensity images of 0528–692 in the Large Magellanic Cloud. The intensity units are in Jy/beam.

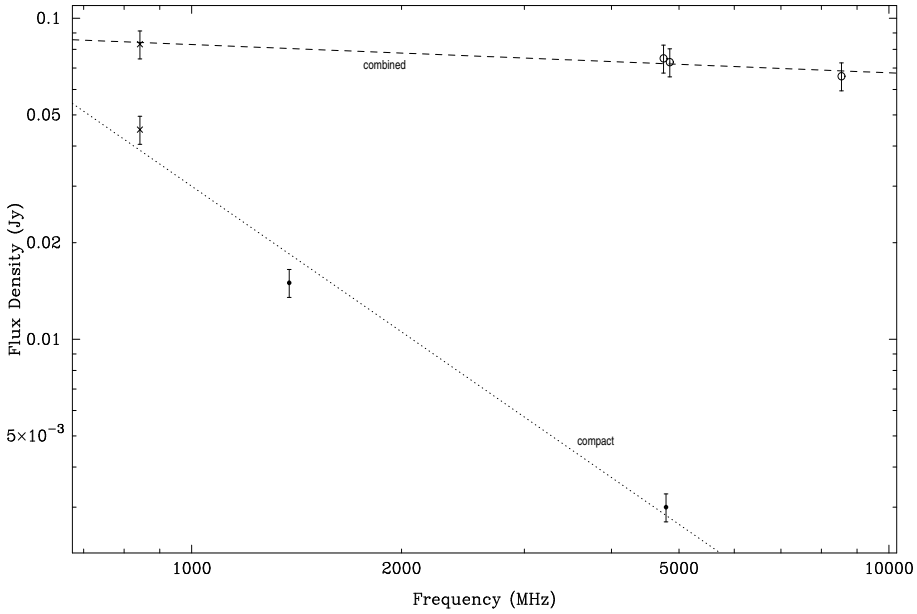

Figure 5.47: The radio spectrum of 0528–692 in the Large Magellanic Cloud. The dashed line shows the fit to the MOST and Parkes data, with the slope of the dotted line giving the spectral index of the compact component.

0530–678 (Figures 5.48 and 5.49) The peak and integrated flux densities determined from the MOST 843 MHz image are 333 and 375 mJy respectively and a number of weaker and slightly extended sources are visible in the field. Peak and integrated flux densities of 43 and 62 mJy were determined from the ATCA 4790 MHz image. There is possible slight extension to the source at 4790 MHz.

This source is listed in the MC4 catalogue at 408 MHz with a flux density of 500 mJy. The Parkes source B0529–6752 was detected at a number of frequencies with a flux density of around 89 and 90 mJy at 4.75 and 4.85 GHz, somewhat higher than determined with the ATCA. This may be due to the larger Parkes beam including emission from the weaker sources visible in the MOST image. No X-ray or infrared emission was detected from this object. Marx, Dickey & Mebold (1997) determine flux densities of 188 and 101 mJy at 1380 and 2378 MHz respectively and Dickey et al. (1994) determine a flux density of 155 mJy at 1419 MHz. Both ATCA determined flux densities in the 1.4 GHz band are significantly lower than the Parkes value of 265 mJy determined at a similar frequency. This difference may be due to similar reasons to the discrepancy observed in the 5 GHz band. No H I absorption was seen in the direction of this source. PTI observations at 2.3 GHz shows two distinct components with approximate peak flux densities of 38 and 45 mJy.

Excluding the two ATCA flux densities, a spectral index of $\alpha = -(0.76 \pm 0.05)$ has been computed which is consistent with that expected for background sources. The spectral index, source morphology and PTI detection suggests that this is likely a compact background source.

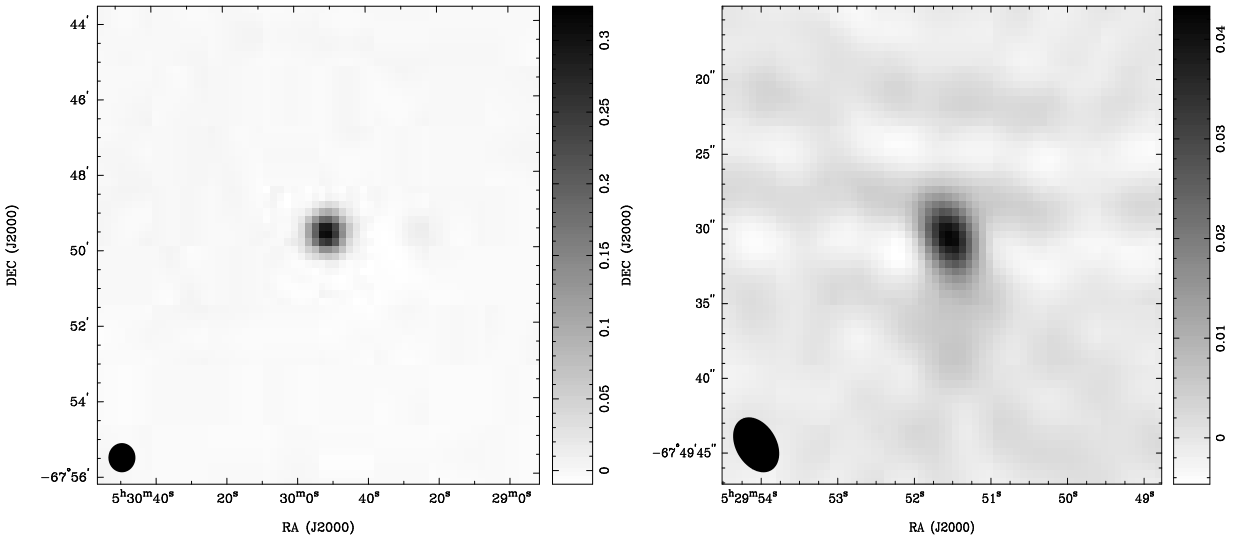

Figure 5.48: The MOST 843 MHz (left) and ATCA 4790 MHz (right) total intensity images of 0530–678 in the Large Magellanic Cloud. The intensity units are in Jy/beam.

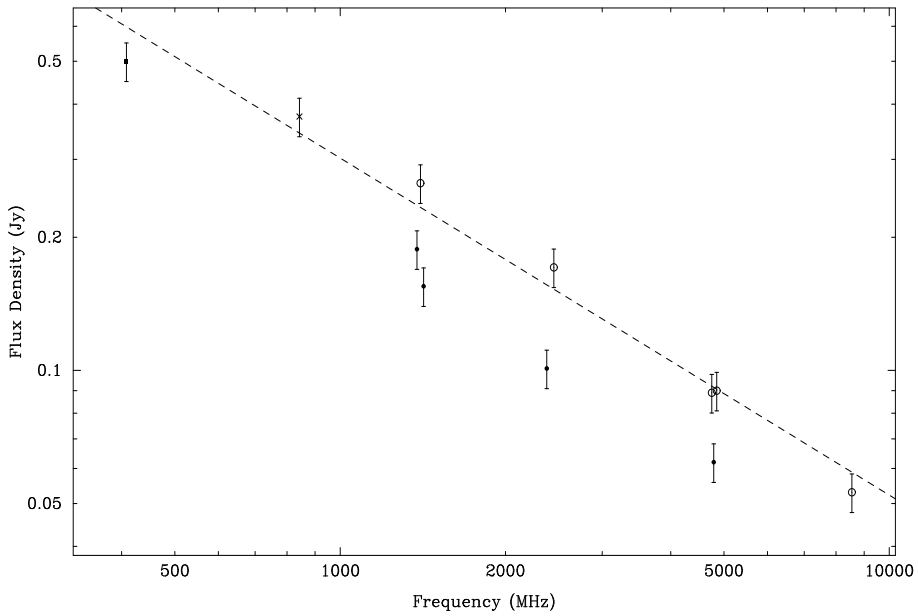

Figure 5.49: The radio spectrum of 0530–678 in the Large Magellanic Cloud.

0532–675 (Figures 5.50 and 5.51) The MOST image shows a complex morphology with knots located at the north and south extremities of the area of emission separated by about 3 arcmin with fainter emission appearing to connect these knots in an arc-like structure. The strongest source has a peak flux density of 52 mJy/beam and the integrated flux density of the entire region is 270 mJy. The ATCA image shows a relatively weak source with some extension to the north-east at a position coincident with the strongest knot of the MOST image. The peak and integrated flux densities at 4790 MHz are 3.1 mJy/beam and 5.3 mJy respectively.

The source has a flux density of 370 mJy in the 408 MHz MC4 catalogue. The nearest source found in the Parkes survey, B0532–6734, was only detected at 4.75 GHz with a flux density of 93 mJy. The position agreement is good with a difference of less than 15 arcsec between the ATCA and Parkes positions. X-ray source 532.5–6734 is listed in the catalogue by Wang et al. (1991) and the *ROSAT* PSPC detects the same object. In both cases, the positional agreement is good with a difference in declination of well under 2 arcmin. This was identified by Wang et al. (1991) as SNR 0532–675 and is classified as an SNR by Filipovic et al. (1998a), although the entry is flagged as being probable but not certain. IRAS source LI–LMC1288 has been identified by Filipovic et al. (1998c) as being an infrared counterpart of the Parkes source B0532–6734. There is a significant and very bright filamentary H II region located some 8 arcmin away from the ATCA position with dimensions of 12×7 arcmin (Davies, Elliott & Meaburn 1976).

A spectral index of $\alpha = -(0.57 \pm 0.04)$ has been determined from 408, 843 MHz and Parkes data and the fit to these data is shown by the dashed line in Figure 5.51. This value is in excellent agreement with the value $\alpha = -(0.56 \pm 0.12)$ reported by Filipovic and coworkers determined primarily from published data. As the angular extent of the source is around 3 arcmin it is not surprising that the ATCA has resolved out much of the larger angular-scale emission leading to a lower than predicted flux density at 4790 MHz. The spectral index of the compact component is $\alpha = -1.6$ determined from the MOST and ATCA data and the slope is shown by the dotted line in Figure 5.51.

The classification of this object remains uncertain. The spectrum of the compact component suggests that it may be an extragalactic background source. Further ATCA observations over a range of baselines and frequencies are required to image this larger scale structure and determine the nature of the extended emission.

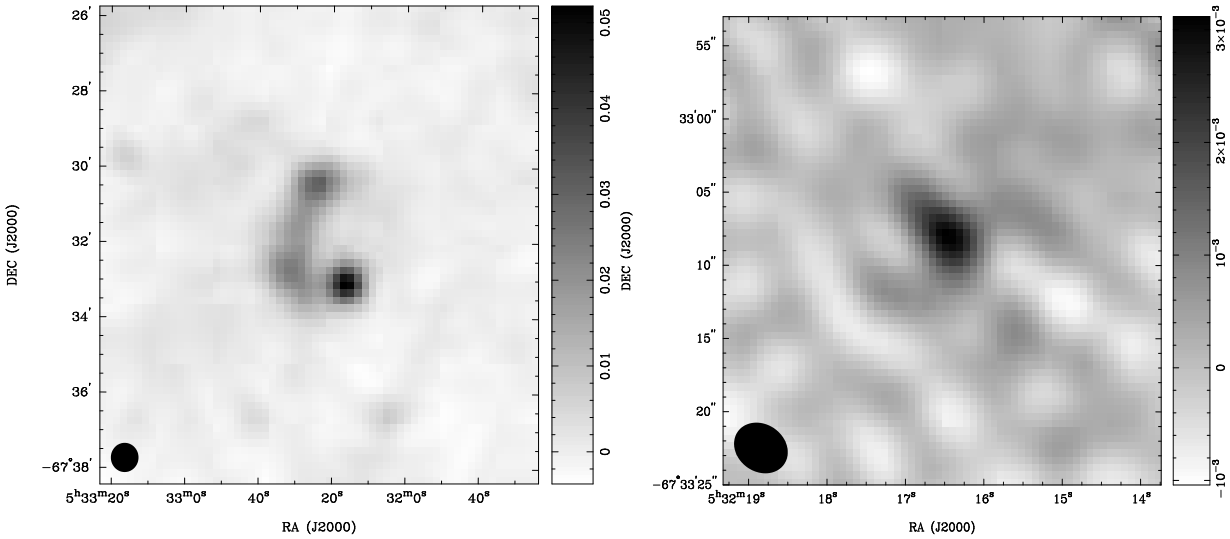

Figure 5.50: The MOST 843 MHz (left) and ATCA 4790 MHz (right) total intensity images of 0532–675 in the Large Magellanic Cloud. The intensity units are in Jy/beam.

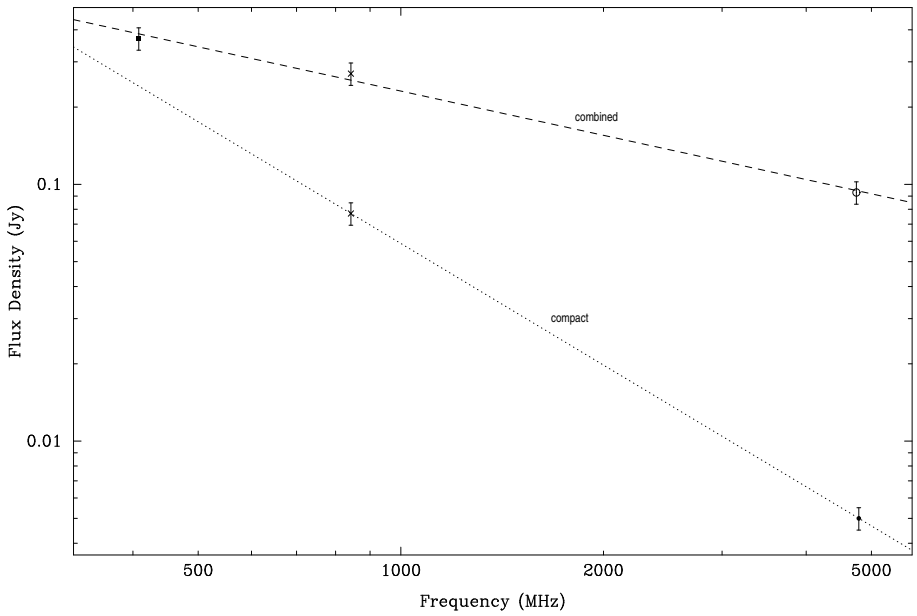

Figure 5.51: The radio spectrum of 0532–675 in the Large Magellanic Cloud. The dashed line shows the fit to the 408 MHz, MOST and Parkes data, with the slope of the dotted line giving the spectral index of the compact component.

0533–725 (Figures 5.52 and 5.53) The MOST image shows a compact source with 843 MHz peak and integrated flux densities of 526 mJy/beam and 534 mJy respectively. The ATCA 4790 MHz image shows two relatively compact sources with the northern source the stronger. The integrated flux density of both sources combined is 78 mJy with the stronger source having a peak flux density of 44 mJy/beam.

A 408 MHz flux density of 900 mJy is given in the MRC. The corresponding Parkes source B0533–7233 was detected at a number of the Parkes survey frequencies with flux densities of 101 and 110 mJy at 4.75 and 4.85 GHz respectively. This is a little higher than the ATCA determined value, possibly reflecting a contribution from other sources or regions of extended diffuse emission within the larger Parkes beam, however the difference is not significant. No X-ray and infrared emission was detected from this object.

Using all the available data a spectral index of $\alpha = -(0.92 \pm 0.06)$ was determined which is typical of a steep spectrum background source. This object is probably an extragalactic background source.

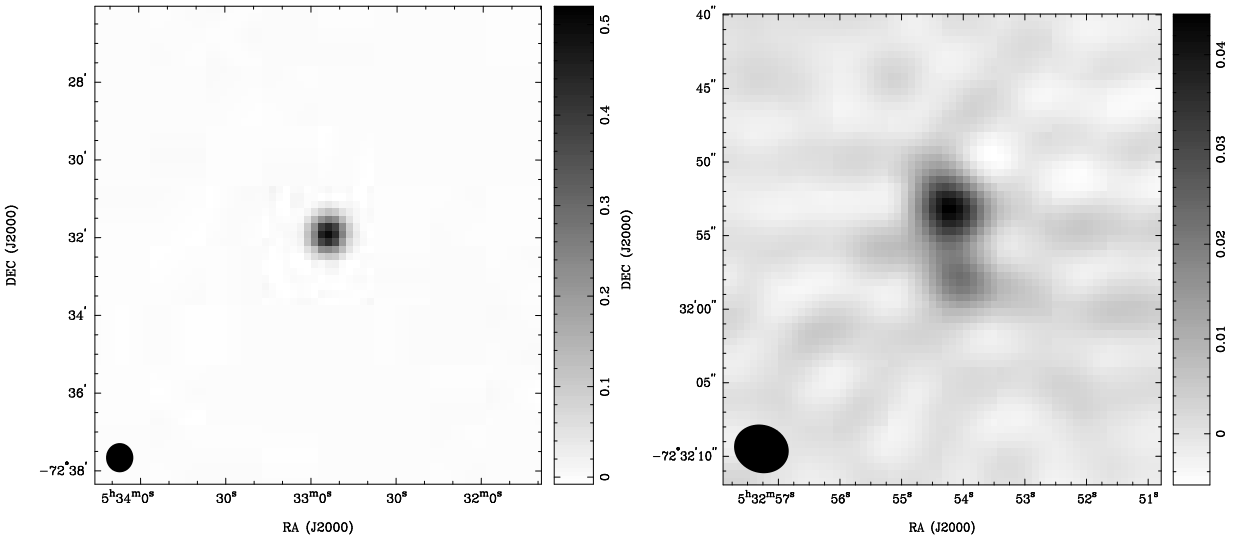

Figure 5.52: The MOST 843 MHz (left) and ATCA 4790 MHz (right) total intensity images of 0533–725 in the Large Magellanic Cloud. The intensity units are in Jy/beam.

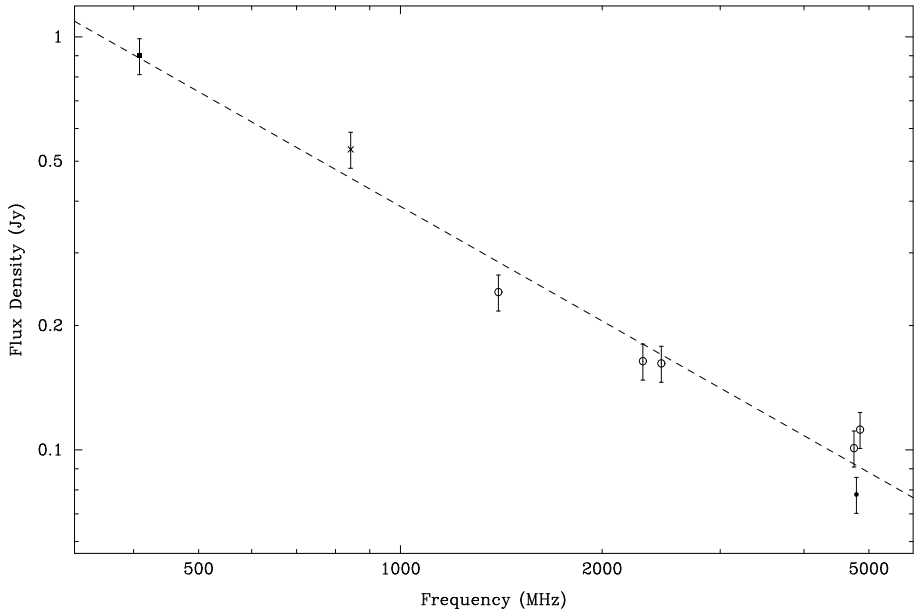

Figure 5.53: The radio spectrum of 0533–725 in the Large Magellanic Cloud.

0534–720 (Figures 5.54 and 5.55) The MOST 843 MHz image shows an arc of extended emission, one arm of which points towards a compact source lying 2–3 arcmin away. The integrated flux density at 843 MHz of the compact source can be determined independently of the extended region and this gives a value of 38 mJy. Combining both the compact source and the arc of extended emission as a single area gives and integrated flux density of 200 mJy. The ATCA 4790 MHz image is of the compact source with a peak flux density of 12.3 mJy/beam and an integrated flux density of 14.2 mJy.

The source is listed in the MC4 catalogue with a flux density of 220 mJy. The Parkes source B0534–7204 is located within about an arcminute of the ATCA position although there is a difference of around 1 arcmin between the Parkes positions at the various frequencies. The source was detected with Parkes at 2.45, 4.75 and 4.85 GHz with flux densities of 147, 103 and 93 mJy respectively. Filipovic et al. (1998a) classifies this source as a probable but not certain SNR which had not previously been identified. There was no X-ray emission from this region recorded in the *Einstein* survey of the LMC or in the *ROSAT* position sensitive proportional counter survey of the LMC. The object lies outside the region surveyed by DEM in their Hα survey of the LMC. The PTI 2.3 GHz observations suggest a marginal detection with a flux density of approximately 30 mJy.

Including all data except the ATCA 4790 MHz value results in a spectral index of $\alpha = -(0.34 \pm 0.05)$ with the fit to these data indicated by the dashed line in Figure 5.55. This agrees well with the value determined by Filipovic and coworkers of $\alpha = -(0.32 \pm 0.04)$. The flux density determined with the ATCA is significantly lower than the comparable Parkes values as only the compact source is imaged with the ATCA with the larger scale structure being resolved out. Taking the flux density of just the compact source at 843 MHz (38 mJy) and the 4790 MHz integrated flux density of 14.2 mJy gives a spectral index of $\alpha \sim -0.6$, shown by the dotted line in Figure 5.55.

Given the complex morphology imaged with the MOST it is difficult to classify this source with certainty. However, it appears likely that the compact source may be an extragalactic background object. Further ATCA observations are required to image the extended region to determine the nature of this object. The detection of polarized emission from this region would help confirm the tentative identification of this source as an SNR.

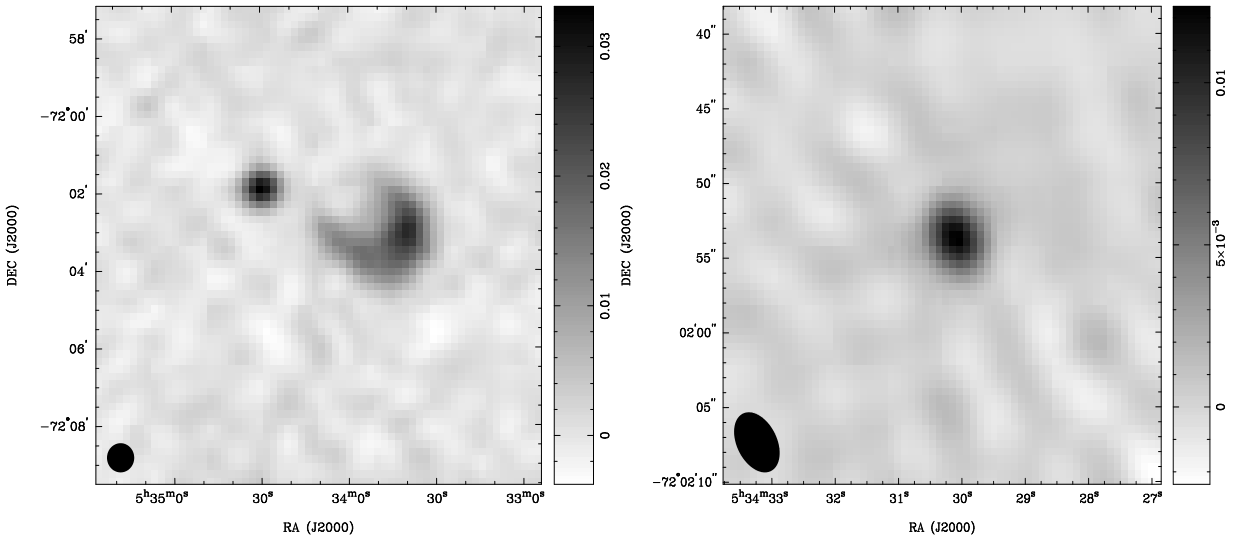

Figure 5.54: The MOST 843 MHz (left) and ATCA 4790 MHz (right) total intensity images of 0534–720 in the Large Magellanic Cloud. The intensity units are in Jy/beam. The dashed line shows the fit to the 408 MHz, MOST and Parkes data, with the slope of the dotted line giving the spectral index of the compact component.

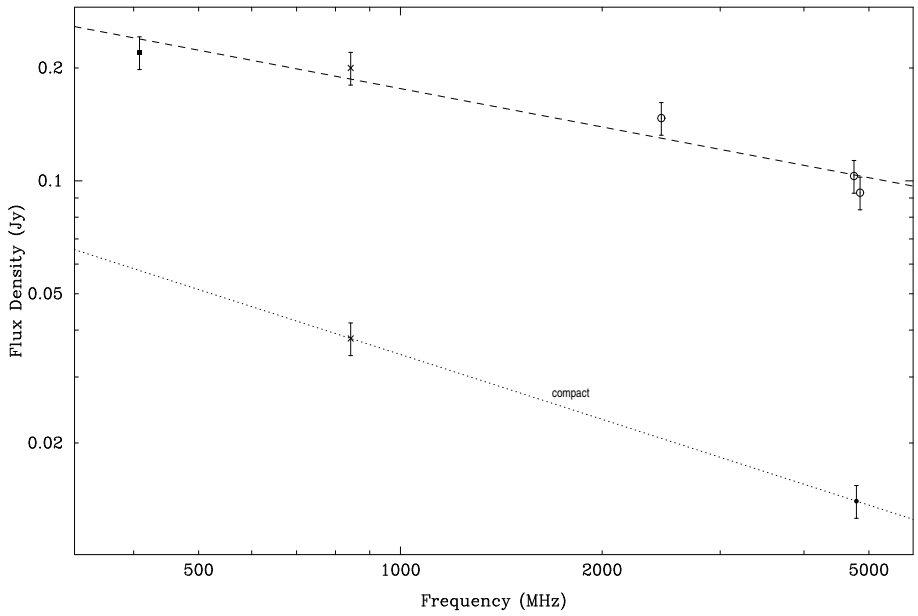

Figure 5.55: The radio spectrum of 0534–720 in the Large Magellanic Cloud. The dashed line shows the fit to the 408 MHz, MOST and Parkes data, with the slope of the dotted line giving the spectral index of the compact component.

0535–676 (Figures 5.56 and 5.57) The MOST image shows a slightly extended source embedded in a area of diffuse extended emission with further diffuse emission towards the eastern edge of the field. The ATCA image shows a compact source surrounded by diffuse emission which is of such low surface brightness that its spatial extent is difficult to determine. The integrated flux densities are 1.786 Jy at 843 MHz and 9.4 mJy at 4790 MHz.

This strong source is catalogued in the MRC with a flux density of 1.150 Jy. The same source has a flux density of 1.610 Jy in the MC4 catalogue. The reason for this difference is unknown. The Parkes source B0535–6736 was detected at all observed frequencies with flux densities of > 1 Jy over the full observed frequency range. The flux densities at the two nearby frequencies of 4.75 and 4.85 GHz are 1.454 and 2.267 Jy respectively which although somewhat surprising suggests possible calibration or instrumental issues, particularly as the 4.85 GHz value is from the PMN catalogue of Wright et al. (1994). The Parkes source was identified with the H II region DEM 241 (Henize: N59A) which is described as containing knots and having an angular extent of 8×8 arcmin. The infrared source LI–LMC1367 (Filipovic et al. 1998c) appears to be associated with this object. X-ray emission was detected in the *ROSAT* PSPC survey within 9 arcsec of the ATCA position. As this source was extended at 4790 MHz it was not selected as a candidate for the H I absorption study conducted by Dickey et al. (1994).

A spectral index of $\alpha = -(0.05 \pm 0.10)$ was determined by taking the MC4 408 MHz value, the MOST 843 MHz value and the full set of Parkes flux densities. This is characteristic of an H II region. Given the extended nature of the emission seen in the MOST images (of order 5 arcmin) and similar extended emission in the ATCA image it is not surprising that the ATCA flux density is significantly lower than single dish measurements and than that expected from the spectrum based on these and lower frequency values. Clearly a significant fraction of the flux at angular scales greater than 30 arcsec has not been sampled with the ATCA.

Both the morphology, particularly at 843 MHz, and spectrum support the identification of this source with the H II region.

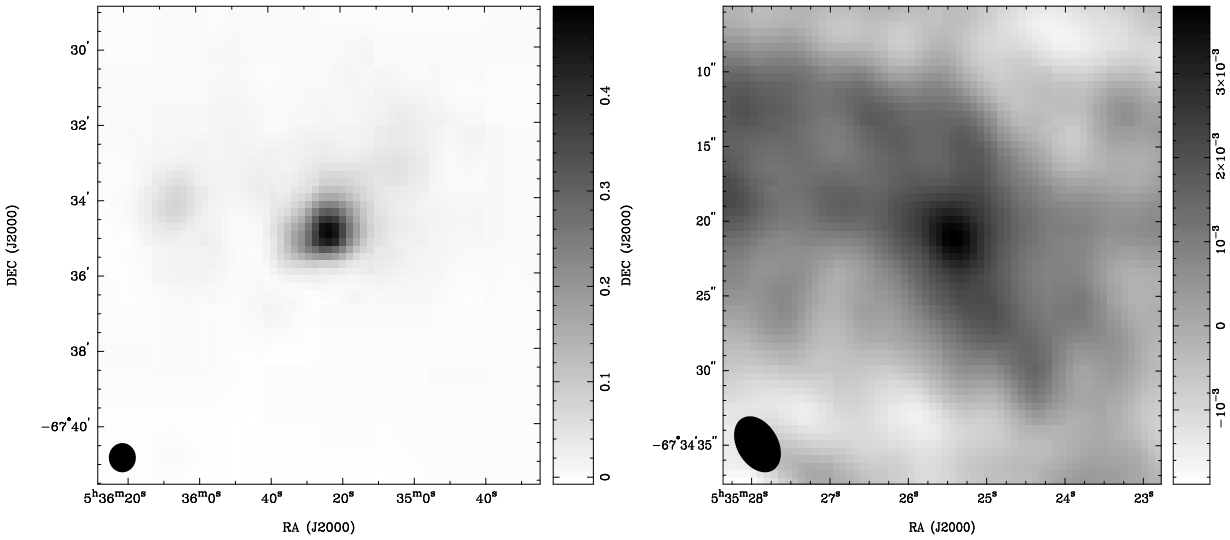

Figure 5.56: The MOST 843 MHz (left) and ATCA 4790 MHz (right) total intensity images of 0535–676 in the Large Magellanic Cloud. The intensity units are in Jy/beam.

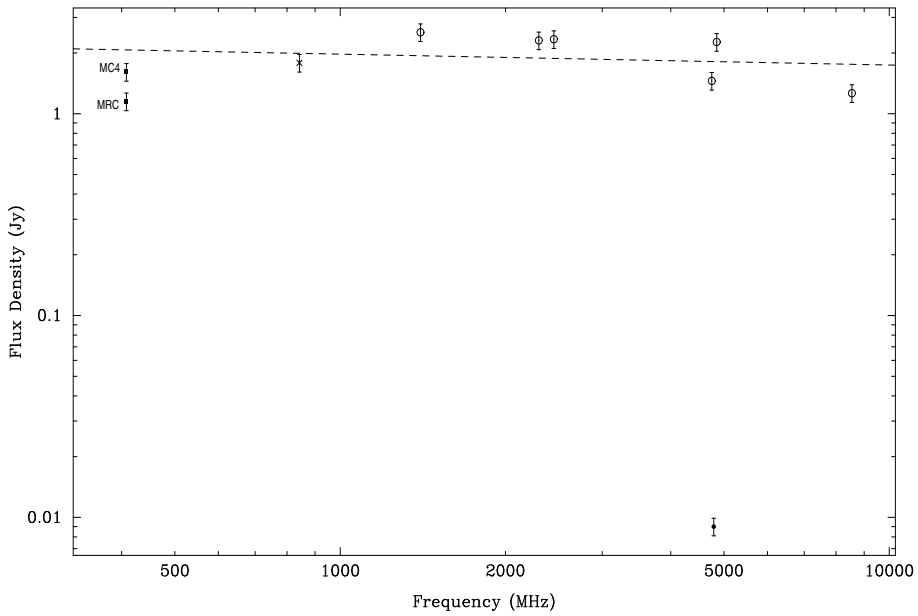

Figure 5.57: The radio spectrum of 0535–676 in the Large Magellanic Cloud.

0537–692 (Figures 5.58 and 5.59) This source is located to the south-west of the large 30-Doradus complex which dominates the full 70 arcmin MOST field. The compact source to the east of the large "ring" of emission was the target chosen for the ATCA observations. The compact source has an integrated flux density of around 235 mJy at 843 MHz. Including this source with the large extended region gives a combined integrated flux density of 2.132 Jy; the peak flux density in this MOST image is 156 mJy/beam. The ATCA image resolves out much of the larger scale structure and the source image corresponds to the compact MOST source. This source is extended at 4790 MHz and has an integrated flux density of 51 mJy.

Comparison with data from lower angular resolution instruments is difficult for this object given its proximity to the strong, extended 30-Doradus region. Parkes source B0537-6914 is located within an arcminute of the ATCA 4790 MHz position but is marked as "extended" and is only catalogued at 8.55 GHz with a flux density of just over 1.5 Jy. This source would have significant flux contributions from the extended nearby region and from part of 30-Doradus itself. Flux densities of 174 and 116 at 1380 and 2378 MHz were determined in the ATCA continuum survey of Marx, Dickey & Mebold (1997). Dickey et al. (1994) observed the source at 1419 MHz and obtained an integrated flux density of 125 mJy; a number of deep H I absorption components are observed in the direction of this source. Dickey et al. (1994) states that this source is located in the south-west part of DEM 263 (Henize: N157), which is the large and bright H II region corresponding to the centre of the emission from 30-Dor. The nearest X-ray source determined in the re-analysis of the *Einstein* data by Wang et al. (1991) is 536.8–6914, located less than 2 arcmin from the compact source. This is the known SNR, N157B. Similarly, *ROSAT* PSPC survey source 866 is also associated with the known SNR in N157B.

As can be seen from Figure 5.59 the flux densities fall into two distinct regions of the graph. The upper region contains the MOST and Parkes 8.55 GHz flux densities from the combined emission from the compact source and large "ring" structure and the lower region shows the two ATCA values representing the flux density primarily from the compact source. The spectral index determined from the MOST and Parkes data is $\alpha \sim -0.2$ (indicated by the dashed line) which is typical of an an H II region or SNR. The flux density from the compact component at 843 MHz (235 mJy) together with the ATCA determined values gives a spectral index of $\alpha = -(0.84 \pm 0.13)$, indicated by the dotted line in Figure 5.59. This steeper spectrum corresponds to the compact core component and is typical of extragalactic background sources. The 2.3 GHz PTI detects two distinct, although weak, compact components each having a flux density of approximately 20 mJy.

Higher angular resolution observations are required to image both the compact source and region of extended emission and to better understand if the compact source is related to the region of extended emission. The spectral index of the compact object suggests that it may be an extragalactic background source.

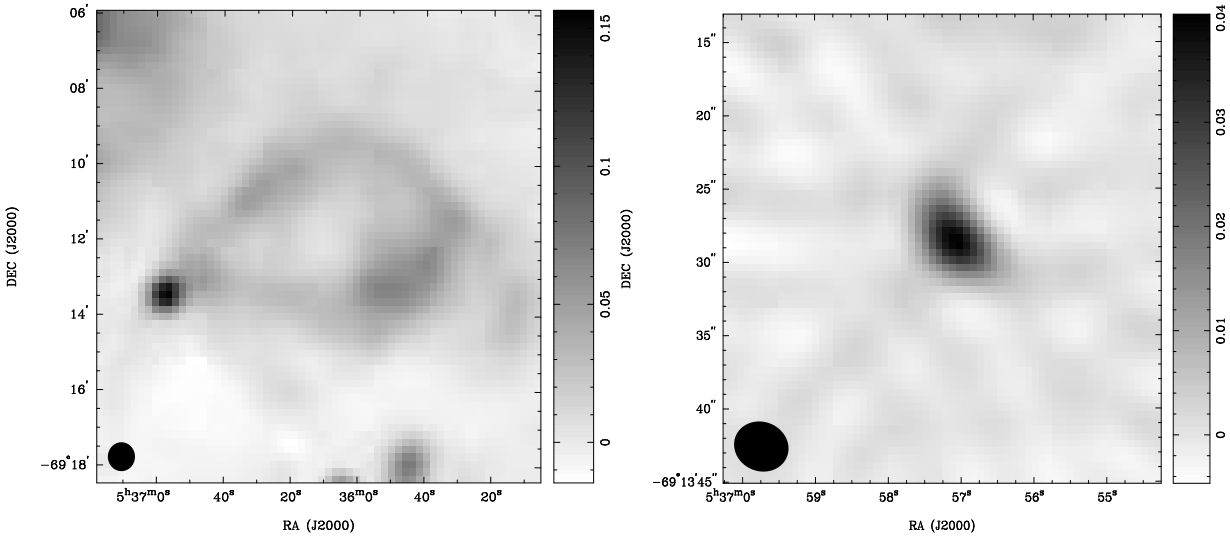

Figure 5.58: The MOST 843 MHz (left) and ATCA 4790 MHz (right) total intensity images of 0537–692 in the Large Magellanic Cloud. The intensity units are in Jy/beam. The dashed line shows the fit to the MOST and Parkes data, with the slope of the dotted line giving the spectral index of the compact component.

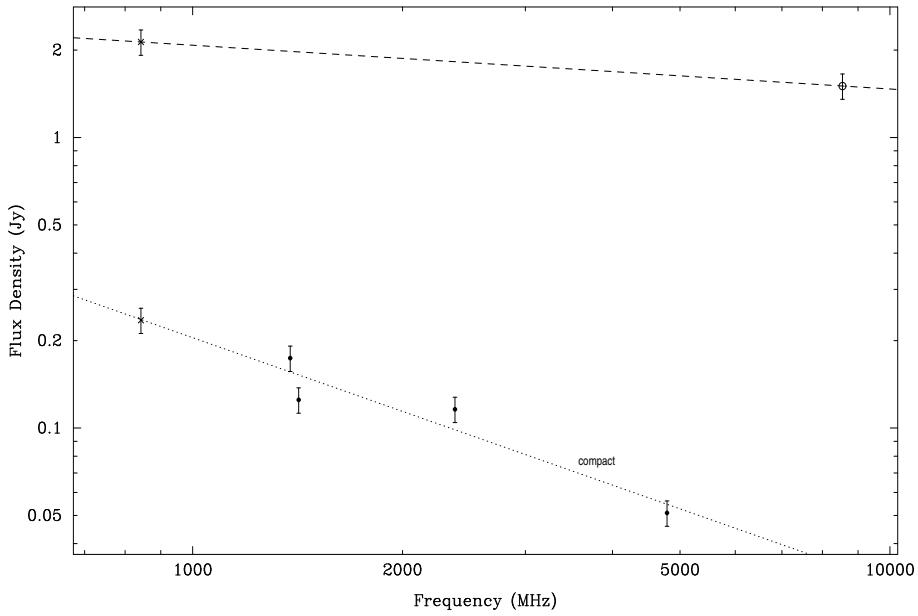

Figure 5.59: The radio spectrum of 0537–692 in the Large Magellanic Cloud. The dashed line shows the fit to the integrated flux density at 843 MHz of the extended region and compact source combined and the Parkes data. The slope of the dotted line gives the spectral index of the compact component.

0540–696 (Figures 5.60 and 5.61) The MOST 843 MHz image shows a compact source with some extension and the full 70 arcmin MOST field suggests that this object is embedded in a large extended region of emission covering > 10 arcmin in declination. The peak and integrated flux densities at 843 MHz are 572 mJy/beam and 1.522 Jy respectively. The ATCA 4790 MHz image shows a slightly extended source with some diffuse emission to the south-west with peak and integrated flux densities of 78 mJy/beam and 179 mJy respectively. This source appears to be unrelated to the nearby known SNR, 0540–693 (Manchester, Staveley-Smith & Kesteven 1993).

The 408 MHz flux density listed in the MRC is 1.480 Jy. The Parkes source B0540–6940 was detected at a number of frequencies with flux densities > 1 Jy over the range of observed frequencies. The Parkes source has been identified with the H II region DEM 284 (Henize: N160A) and the infrared source LI–LMC1503 is also associated with this region (Filipovic et al. 1998c). The X-ray source 540.1–6946 (Wang et al. 1991) is located some 6 arcmin to the south of the position of the peak in the ATCA image; the *ROSAT* PSPC source 1001 is coincident with 540.1–6946. The X-ray source is unrelated to the radio source. Marx, Dickey & Mebold (1997) list flux densities of 33 and 61 mJy at 1380 and 2378 MHz. This source was observed as part of the H I absorption studies carried out by Dickey et al. (1994) who report a 1419 MHz continuum flux density of 84 mJy which is around 2.5 times that determined at a similar frequency by Marx, Dickey & Mebold (1997). Dickey et al. (1994) also suggest that this source is intrinsic to the LMC and has previously been identified as a possible supernova remnant. Intrinsic source variability on timescales of a few years may explain the "scatter" in the ATCA flux densities.

Using only the Parkes data, a spectral index of $\alpha = -(0.18 \pm 0.08)$ was calculated which is consistent with that expected from H II regions. It is likely that the Parkes flux densities include contributions from surrounding areas of emission and that the ATCA observations under-estimate the true flux density given that there is significant emission with angular extent greater than 30 arcsec.

The extended morphology revealed in both images presented here supported the previous classification that the radio source is associated with the H II region, DEM 284. The ATCA 5 GHz source may be a background object.

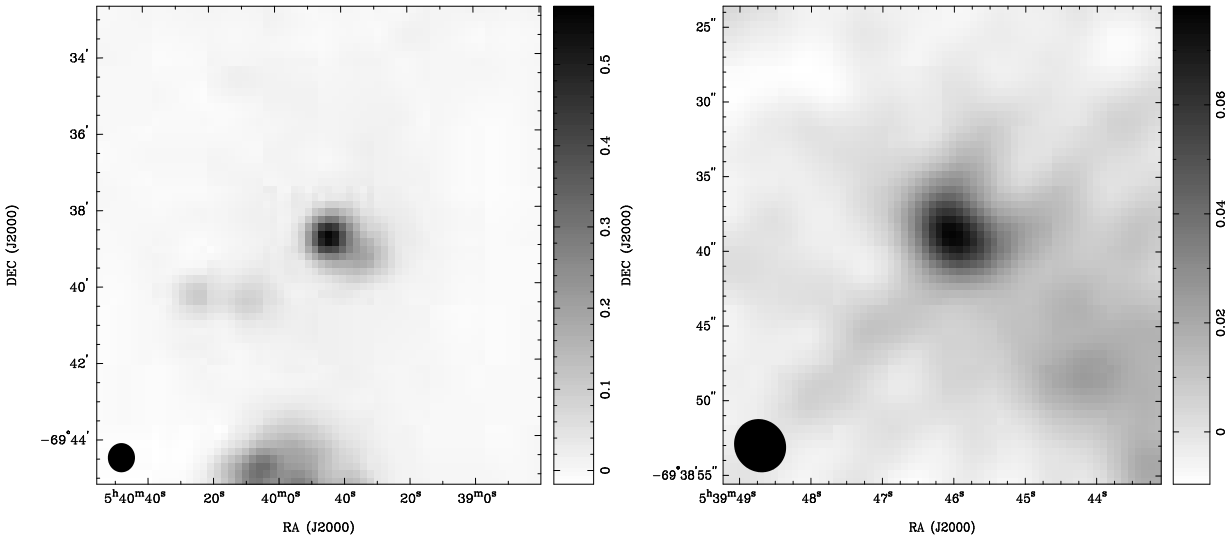

Figure 5.60: The MOST 843 MHz (left) and ATCA 4790 MHz (right) total intensity images of 0540–696 in the Large Magellanic Cloud. The intensity units are in Jy/beam.

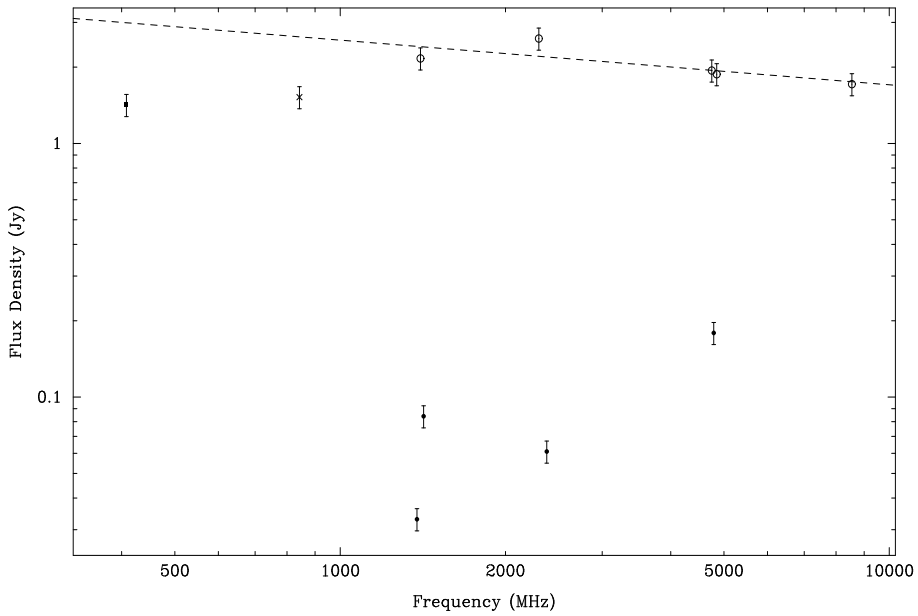

Figure 5.61: The radio spectrum of 0540–696 in the Large Magellanic Cloud.

0541–670 (Figures 5.62 and 5.63) Both the MOST and ATCA images show extended sources. The MOST image shows a source extended towards the north-east with a peak flux density of 33.5 mJy/beam and an integrated flux density of 51 mJy. The ATCA image shows three distinct weak sources in a clump. None of the three sources imaged with the ATCA has a peak flux density greater than 3 mJy/beam; the integrated flux densities of the three sources combined is about 6.4 mJy. Because of the low surface brightness the image appears to be somewhat patchy.

At 408 MHz this source is listed in the MC4 catalogue with a flux density of 300 mJy (the MRC has a flux density limit of 700 mJy). Parkes source B0541–6707, detected only in the 13 cm and 6 cm bands, is located at least 6 arcmin away (to the south of the MOST sub-image) from the position of 0541–670 and is unlikely to be associated with 0541–670. The full 70 arcmin MOST field shows a strong, compact source near the Parkes position. Thus the source observed here does not appear to have been detected in previous radio surveys most probably because of confusion from this stronger source within the Parkes beam. The *ROSAT* PSPC X-ray source 456 is located 20 arcsec from the centroid of the ATCA positions.

A spectral index of $\alpha = -(1.52 \pm 0.27)$ was determined from the three data points, and whilst there is some uncertainty in the fit, it suggests the presence of a steep spectrum extragalactic background source. Given the low flux density of the individual components in the ATCA image, it is difficult to apply the flux density ratio criteria of Magliocchetti et al. (1998) with confidence, but it is probable that these components are members of the one source.

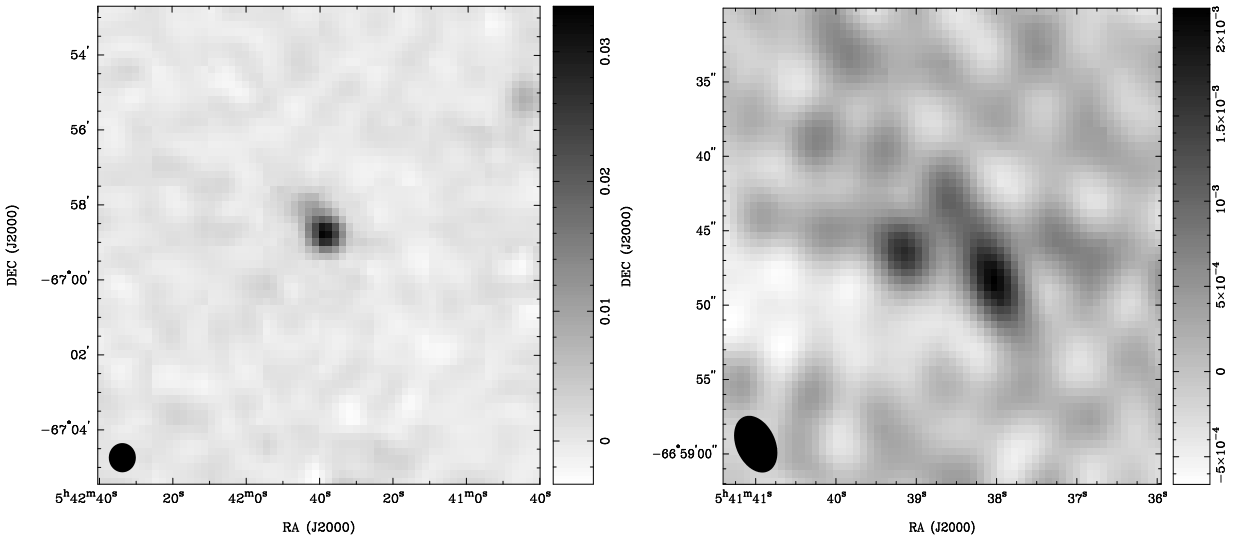

Figure 5.62: The MOST 843 MHz (left) and ATCA 4790 MHz (right) total intensity images of 0541–670 in the Large Magellanic Cloud. The intensity units are in Jy/beam.

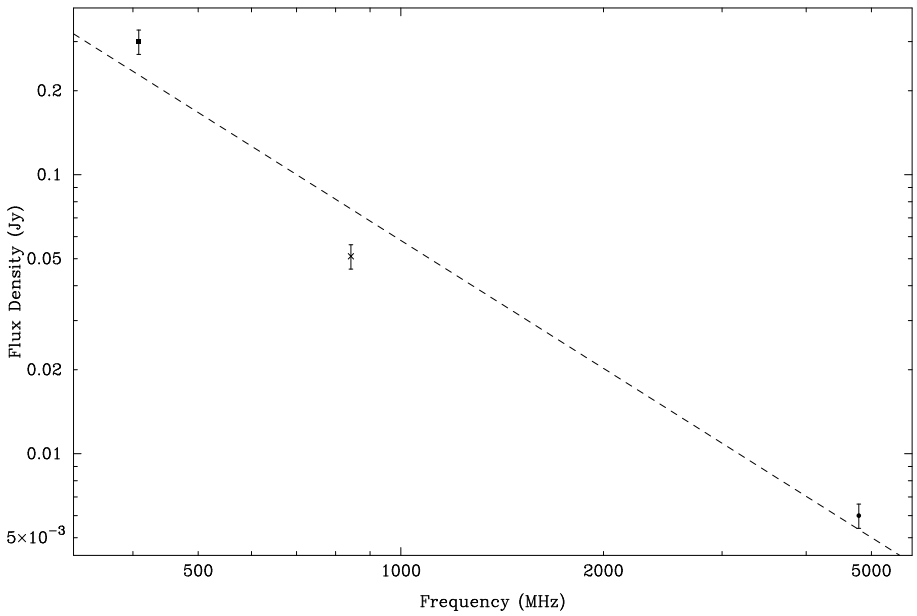

Figure 5.63: The radio spectrum of 0541–670 in the Large Magellanic Cloud.

0543–681 (Figures 5.64 and 5.65) The MOST image shows a compact source with a number of fainter compact sources to the south-west of the main source, visible on a graphics display but not easily seen here. These are are not artifacts of the observing or imaging process. The peak and integrated flux densities at 843 MHz are 340 mJy/beam and 387 mJy respectively. The ATCA image shows two compact patches of emission, with integrated flux densities of 15 and 13 mJy at 4790 MHz.

This object is listed in the MC4 catalogue with a flux density of 700 mJy. The Parkes source B0543-6808 is detected at a number of frequencies with flux densities of 58 and 47 mJy at 4.75 and 4.85 GHz respectively. Dickey et al. (1994) determine a flux density of 98 mJy at 1419 MHz and H I absorption is seen in the direction of this source. Flux densities of 128 and 76 mJy at 1380 and 2378 MHz were determined in the survey of Marx, Dickey & Mebold (1997). No X-ray or infrared emission has been detected from this object.

A spectral index of $\alpha = -(1.08 \pm 0.06)$ was determined by selecting only the 408, 843, 4750 and 4850 MHz data. This is typical of a steep spectrum background source. The ATCA 5 GHz flux densities are well below the corresponding Parkes flux densities (Filipovic et al. 1995). This situation also applies to the 1.4 GHz data. This suggests that the ATCA is detecting a compact core component whilst the Parkes telescope is sampling this core component together with emission from larger angular scale structure.

The radio spectrum, morphology and H I absorption suggests that 0543–681 can be classified as a background source. The two sources may be components of the same object.

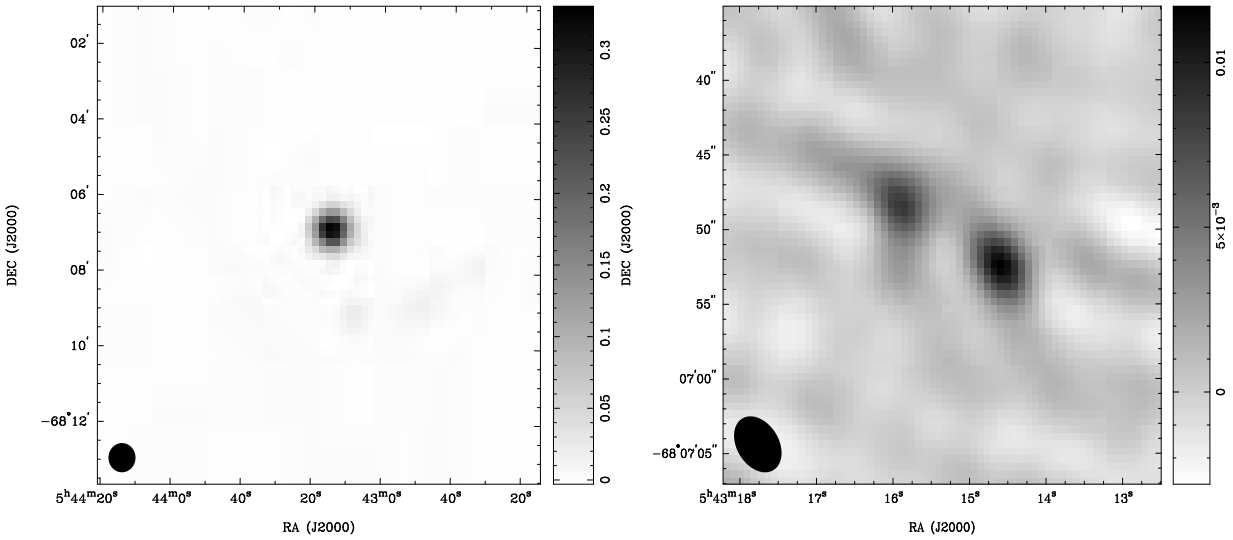

Figure 5.64: The MOST 843 MHz (left) and ATCA 4790 MHz (right) total intensity images of 0543–681 in the Large Magellanic Cloud. The intensity units are in Jy/beam.

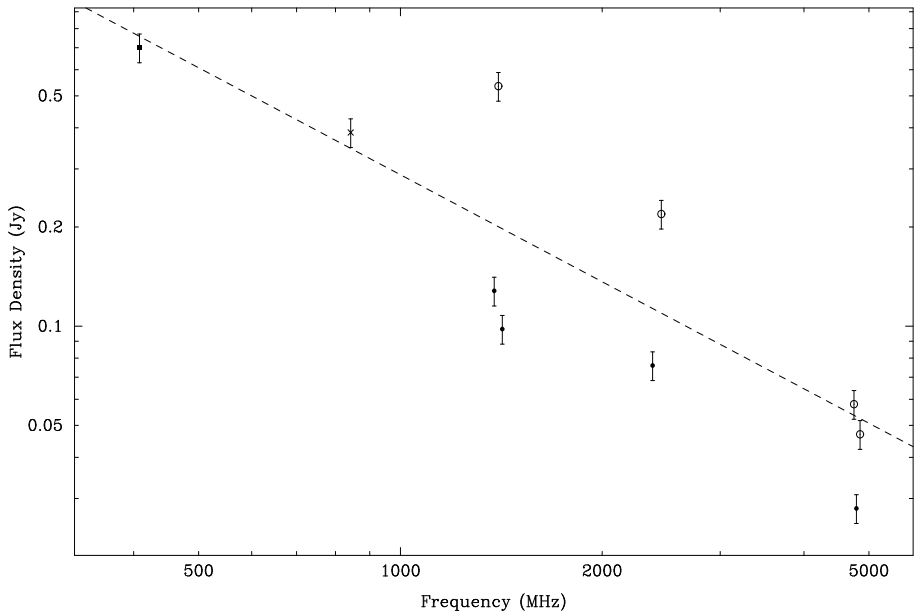

Figure 5.65: The radio spectrum of 0543–681 in the Large Magellanic Cloud.

0543–710 (Figures 5.66 and 5.67) The MOST image shows a slightly elongated source with peak and integrated flux densities of 196 mJy/beam and 255 mJy respectively. The ATCA image shows a complex structure having a morphology similar to a double-lobed radio galaxy. The integrated flux density at 4790 MHz, obtained by interactively selecting the areas of emission, is 14.5 and 8.8 mJy. The orientation of the double-lobed structure seen in the ATCA image corresponds with the angle of the extension that is visible in the MOST image.

This source has a MC4 catalogued flux density of 370 mJy at 408 MHz. The source B0543–7105 was detected only in the 5 and 8 GHz bands at Parkes. The reported Parkes flux density of 131 mJy in the 5 GHz band is significantly greater than the ATCA value, determined from the observations reported here. Marx, Dickey & Mebold (1997) determine a 1380 MHz flux density of 58 mJy. Given the complex structure imaged with the ATCA, it is reasonable to assume that much of the diffuse and extended emission associated with this source has not been sampled with the ATCA. No infrared emission has been detected from this source. X-ray emission was detected from a *ROSAT* PSPC source located some 11 arcsec from the ATCA 4790 MHz position.

Excluding the ATCA 1380 and 4790 MHz flux densities, a spectral index of $\alpha = -(0.39 \pm 0.02)$ has been determined with a good fit to the selected data. It is unclear why this source was not detected in the 20 and 13 cm bands at Parkes, given the slope of the radio spectrum and the fact that the MOST image of the area shows that the source is located in a relatively isolated region.

Although this source is likely to be a distant double-lobed radio galaxy located behind the LMC, further ATCA multi-configuration (with both short and long interferometer spacings) observations at 5 GHz are required to fully image the complex structure.

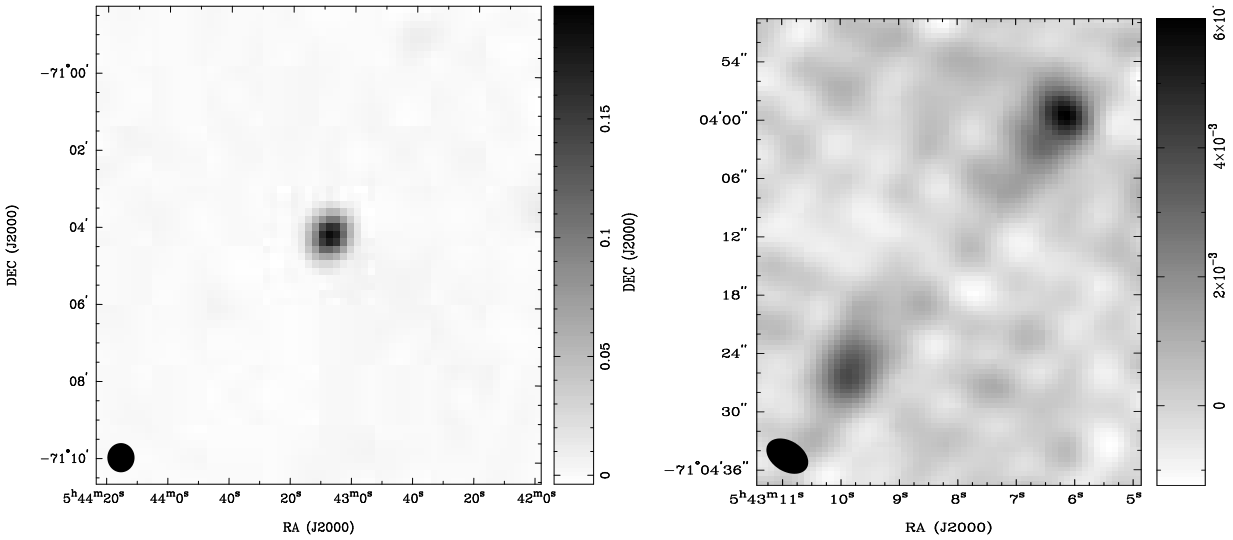

Figure 5.66: The MOST 843 MHz (left) and ATCA 4790 MHz (right) total intensity images of 0543–710 in the Large Magellanic Cloud. The intensity units are in Jy/beam.

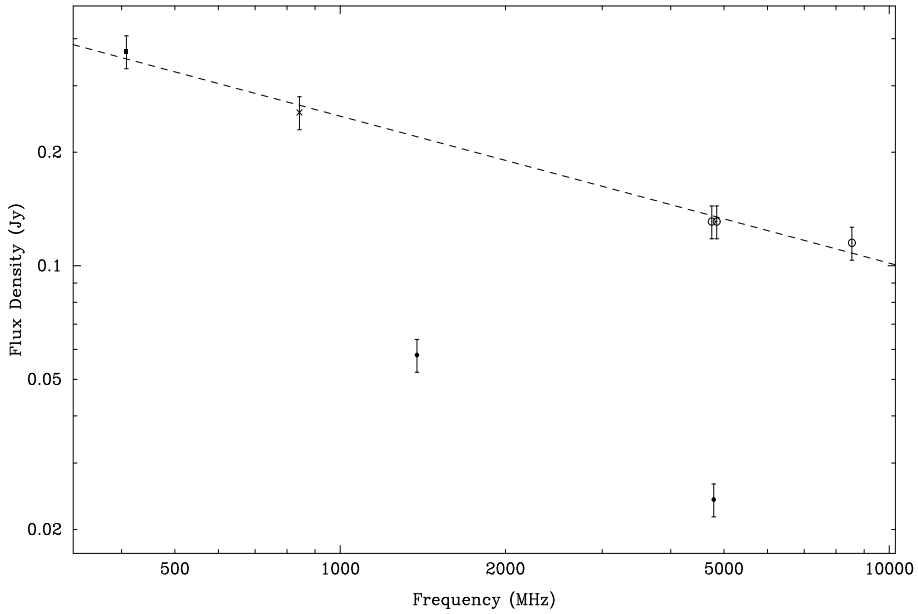

Figure 5.67: The radio spectrum of 0543–710 in the Large Magellanic Cloud.

0545–649 (Figures 5.68 and 5.69) The MOST 843 MHz image show a compact source with peak and integrated flux densities of 683 mJy/beam and 715 mJy respectively. The ATCA image shows a compact source with some slight extension. The ATCA source has deconvolved dimensions of 4.91×3.69 arcsec and an integrated flux density of 204 mJy.

A flux density of 1.330 Jy is given in the MRC. The source B0545–6454 was detected at all frequencies in the Parkes survey apart from at 8.55 GHz. The Parkes flux densities at 4.75 and 4.85 GHz are 295 and 289 mJy respectively, somewhat larger than the ATCA value of 204 mJy. Dickey et al. (1994) list a 1419 MHz flux density of 419 mJy, apparently 100 mJy lower than that found by Filipovic and coworkers in the Parkes surveys. No absorption is seen in the H I observations.

Excluding the ATCA 1419 and 4790 MHz flux density values, a spectral index of $\alpha = -(0.60 \pm 0.04)$ has been determined. Recomputing the spectral index with the full dataset changes the slope by a negligible amount and increases the fitting error only slightly. Strong fringes were seen on the PTI at 2.3 GHz, with an approximate flux density of 234 mJy.

Based on the morphology, spectrum and location of the source in relation to the main area of the LMC, this is most likely a core-dominated discrete background source.

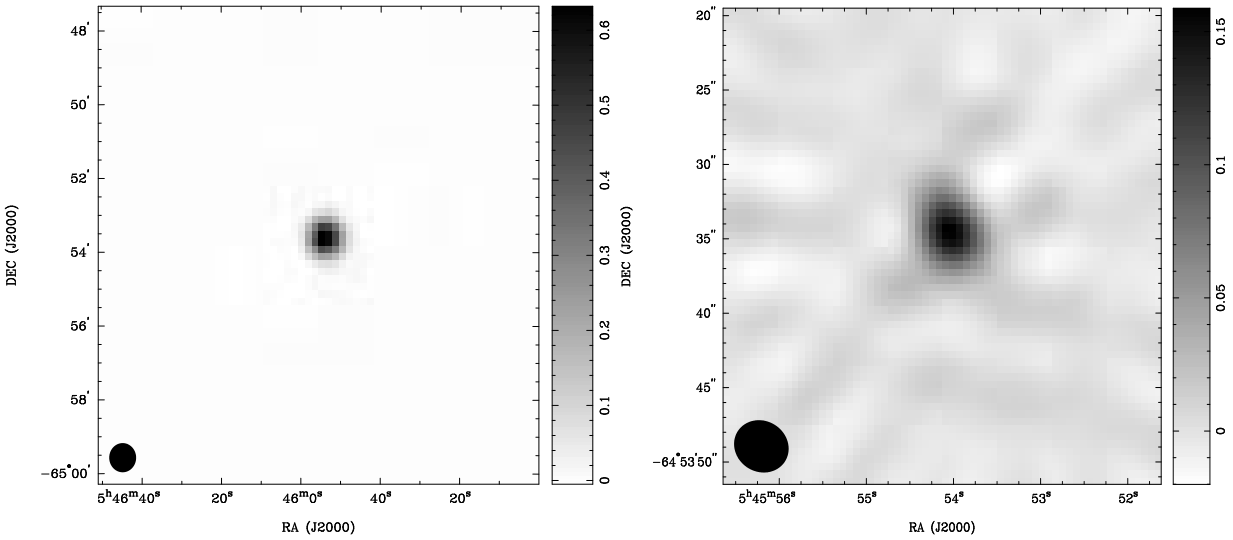

Figure 5.68: The MOST 843 MHz (left) and ATCA 4790 MHz (right) total intensity images of 0545–649 in the Large Magellanic Cloud. The intensity units are in Jy/beam.

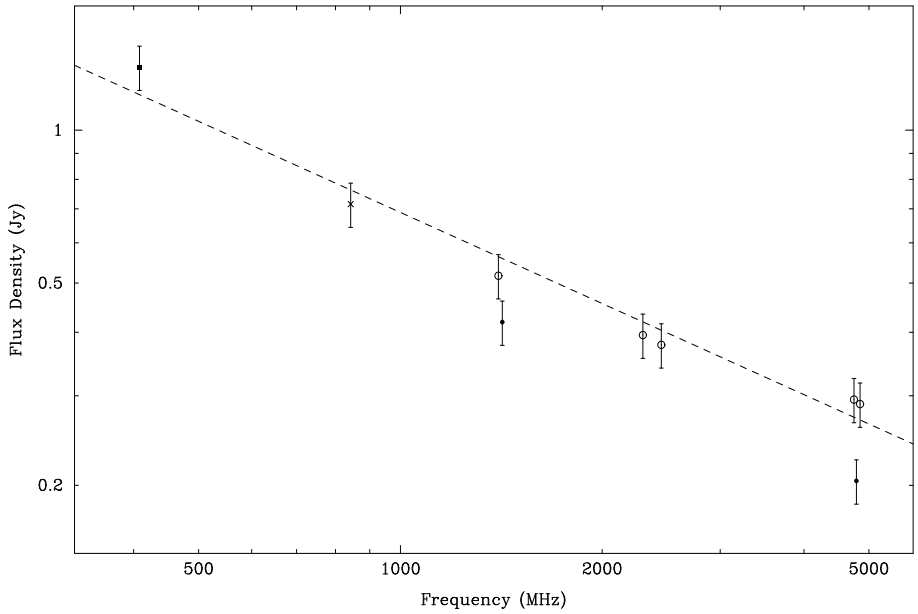

Figure 5.69: The radio spectrum of 0545–649 in the Large Magellanic Cloud.

0545–719 (Figures 5.70 and 5.71) The MOST 843 MHz image shows a discrete source with dimensions slightly larger than the synthesized beam and an integrated flux density of 410 mJy. The ATCA 4790 MHz image shows a significantly weaker source with an integrated flux density of 49 mJy and a peak flux density of 39 mJy/beam. There is a possible extension to the north-east.

This source has a 408 MHz MC4 catalogue flux density of 610 mJy. Parkes source B0545–7156 has good positional agreement with the ATCA position. It was not detected at 1.40 GHz although it was detected at all other observed Parkes frequencies; it is marked as being extended in the 2.3 GHz band. A flux density of 101 mJy is given at 4.75 GHz, double the ATCA determined value. Whilst Filipovic and coworkers did not detect this source in the 20 cm band, Dickey et al. (1994) report a flux density of 205 mJy at 1419 MHz and identify this as a background source.

Excluding both ATCA values and the two Parkes values at 2.3 GHz results in a spectral index of $\alpha = -(0.74 \pm 0.03)$. It is unclear as to why the Parkes 2.3 GHz values are significantly higher than the spectrum indicates. Confusion or unknown observing problems may explain these greater than expected values. The slope of the spectrum suggests that the ATCA 4790 MHz observations are imaging a compact core component and resolving out any larger scale diffuse emission. The PTI observations at 2.3 GHz support the presence of a compact component as fringes were seen with an approximate flux density of 130 mJy.

The observations presented here support the identification by Dickey et al. (1994) that this source is a background object with a significant compact core.

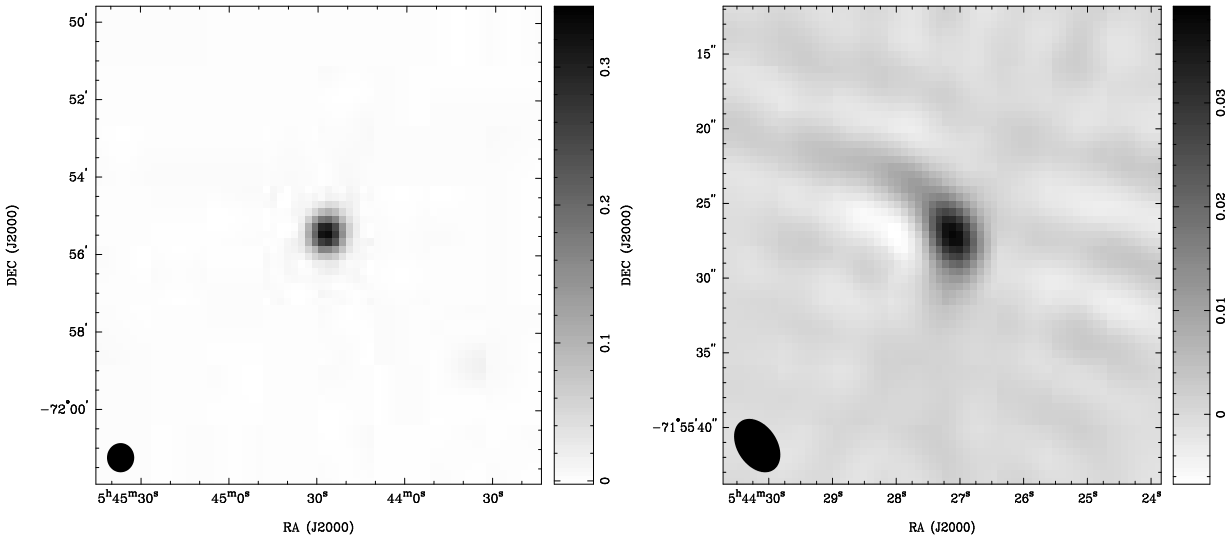

Figure 5.70: The MOST 843 MHz (left) and ATCA 4790 MHz (right) total intensity images of 0545–719 in the Large Magellanic Cloud. The intensity units are in Jy/beam.

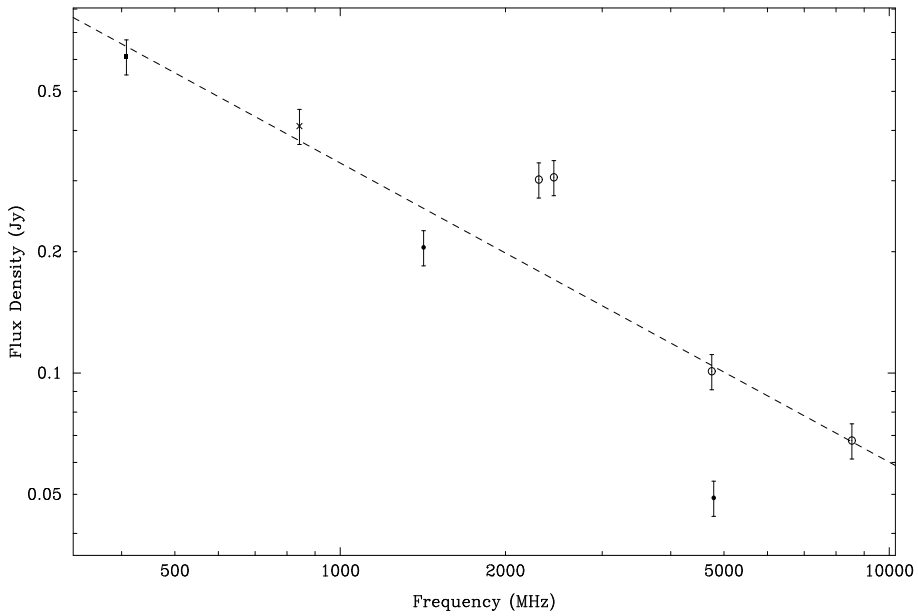

Figure 5.71: The radio spectrum of 0545–719 in the Large Magellanic Cloud.

0547–677 (Figures 5.72 and 5.73) The MOST 843 MHz image shows an isolated, compact source with peak and integrated flux densities of 147 mJy/beam and 185 mJy respectively. The ATCA 4790 MHz source shows an extension to the south-east; the peak and integrated flux densities are 29 mJy/beam and 40 mJy respectively.

The source is listed in the MC4 catalogue with a flux density of 270 mJy. The Parkes source B0547–6746 has relatively good positional agreement with the ATCA position and was detected at 2.45, 4.75, 4.85 and 8.55 GHz with flux densities of 126, 63, 69 and 48 mJy respectively. Whilst the ATCA-determined flux density is somewhat lower that then Parkes values they are comparable, particularly as the MOST image reveals two weaker compact sources to the south of 0547–677 which would be included in the flux density determined from the Parkes observations. Dickey et al. (1994) observed this source as part of their H I absorption line study of the LMC and obtained a 1419 MHz continuum flux density of 81 mJy. Marx, Dickey & Mebold (1997) determined continuum flux densities of 90 and 69 mJy at 1380 and 2378 MHz respectively. The ATCA 1.4 GHz flux densities are significantly lower than even the 2.45 GHz value obtained at Parkes. X-ray source 547.9–6746 (Wang et al. 1991) has excellent positional agreement with the ATCA 4790 MHz source with a difference of around 15 arcsec.

Excluding only the ATCA data, a spectral index of $\alpha = -(0.57 \pm 0.05)$ was calculated which agrees well with the value of $\alpha = -(0.58 \pm 0.05)$ determined by Filipovic et al. (1998a). Filipovic and coworkers classify this object as a background source based on the study of Dickey et al. (1994). The ATCA values are lower than expected from the spectrum, suggesting the presence of a compact steeper spectrum core. This suggestion is supported by a weak 2.3 GHz PTI detection observed at the ATCA position with an approximate flux density of 37 mJy.

The data presented here support the earlier classification of this object as an extragalactic background source with a compact core component.

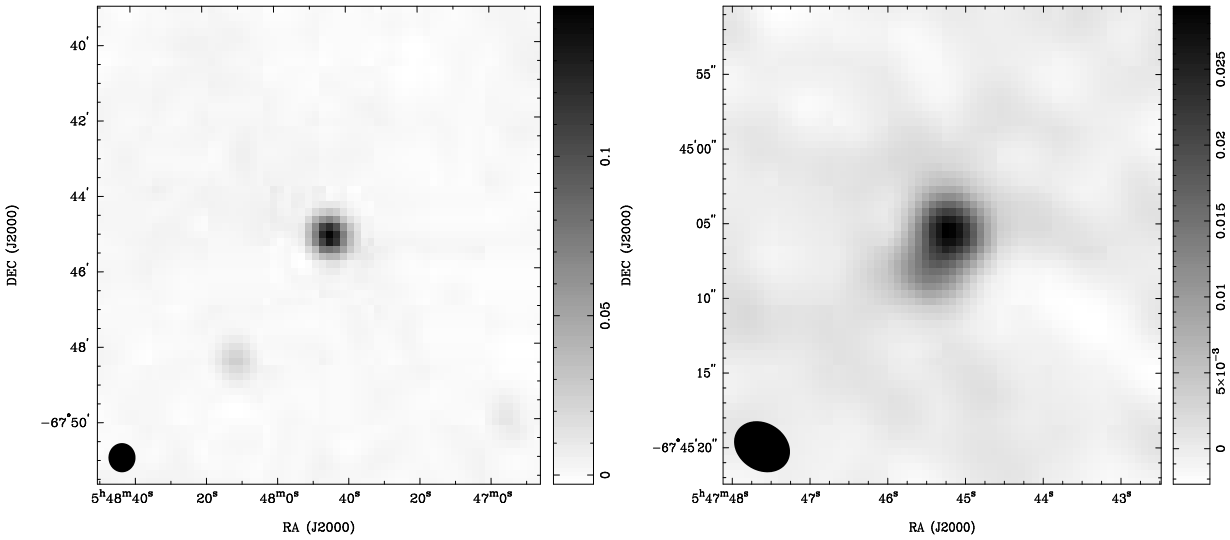

Figure 5.72: The MOST 843 MHz (left) and ATCA 4790 MHz (right) total intensity images of 0547–677 in the Large Magellanic Cloud. The intensity units are in Jy/beam.

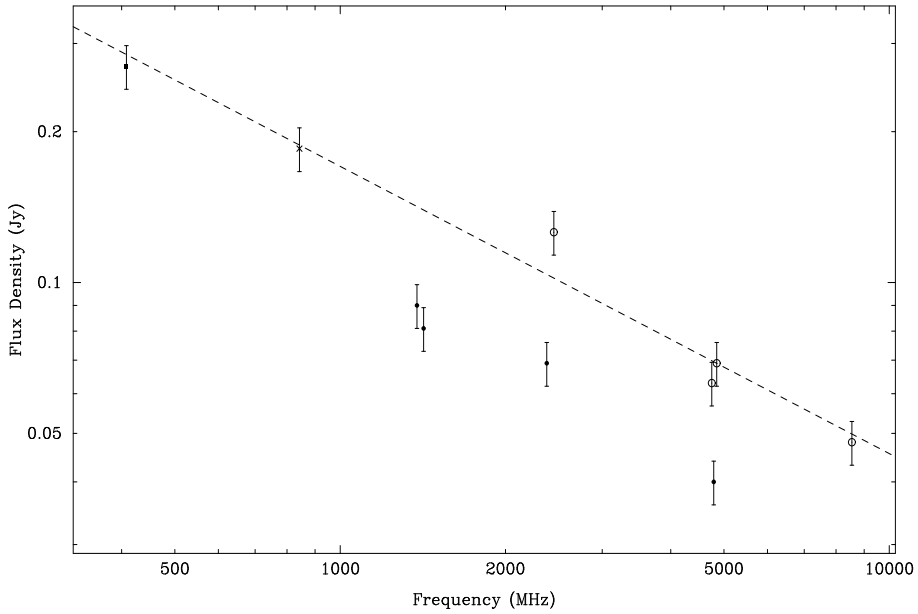

Figure 5.73: The radio spectrum of 0547–677 in the Large Magellanic Cloud.

0547–704 (Figures 5.74 and 5.75) The MOST 843 MHz image shows a relatively strong and slightly extended source (deconvolved dimensions of 50.7 × 43.0 arcsec) with a peak flux density of 196 mJy/beam and an integrated flux density of 218 mJy. The ATCA 4790 MHz image shows two slightly extended sources both of which have peak flux densities of less that 10 mJy/beam and a combined integrated flux density of 15 mJy. The full 70 arcmin MOST field containing this object shows that it is located in an area of the LMC that is only lightly populated with radio sources. It does not appear to be associated with any region of diffuse extended emission or located near to any known supernova remnants.

This object was not detected at any frequency in the Parkes radio surveys. The MC4 catalogue gives a 408 MHz flux density of 300 mJy. It is not clear as to why this source was not detected at least in the 20 cm band at Parkes (where a flux density of around 100 mJy may be expected), unless confusion made identification difficult. The continuum survey of Marx, Dickey & Mebold (1997) lists flux densities of 83 and 30 mJy at 1380 and 2378 MHz respectively. The nearest X-ray source listed in the *ROSAT* PSPC is located 40 arcsec away in declination and some 3 minutes of time in right ascension from the ATCA-determined position and is probably not related to the ATCA object.

Taking the flux densities at 408 and 843 MHz gives a spectral index of $\alpha \sim -0.4$. Excluding only the 408 MHz value results in a spectral index of $\alpha = -(1.55 \pm 0.18)$, with the fit to these data indicated by the dashed line in Figure 5.75. Given that the source appears slightly extended at 843 MHz, it is possible that there is some extended emission that has not been sampled with the ATCA.

The two components which are separated by 12 arcsec may be related (e.g. the two lobes of a radio galaxy) as both the separation and flux density ratio criteria of Magliocchetti et al. (1998) are satisfied (the components have integrated flux densities of 5.6 and 9.4 mJy). Based on the limited amount of data available we tentatively classify this object as an extragalactic background source.

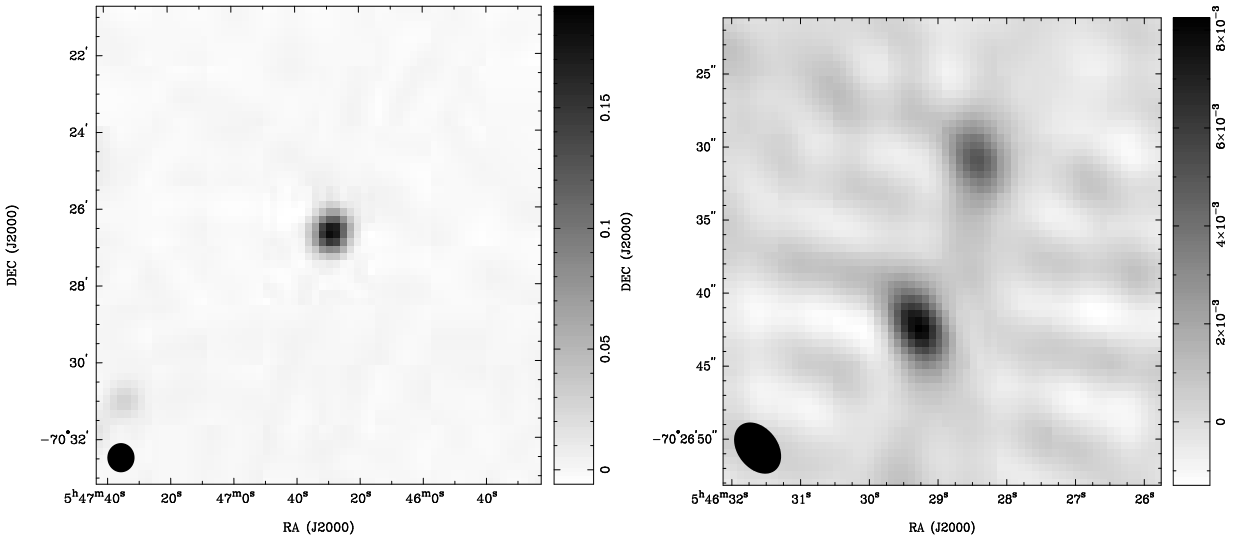

Figure 5.74: The MOST 843 MHz (left) and ATCA 4790 MHz (right) total intensity images of 0547–704 in the Large Magellanic Cloud. The intensity units are in Jy/beam.

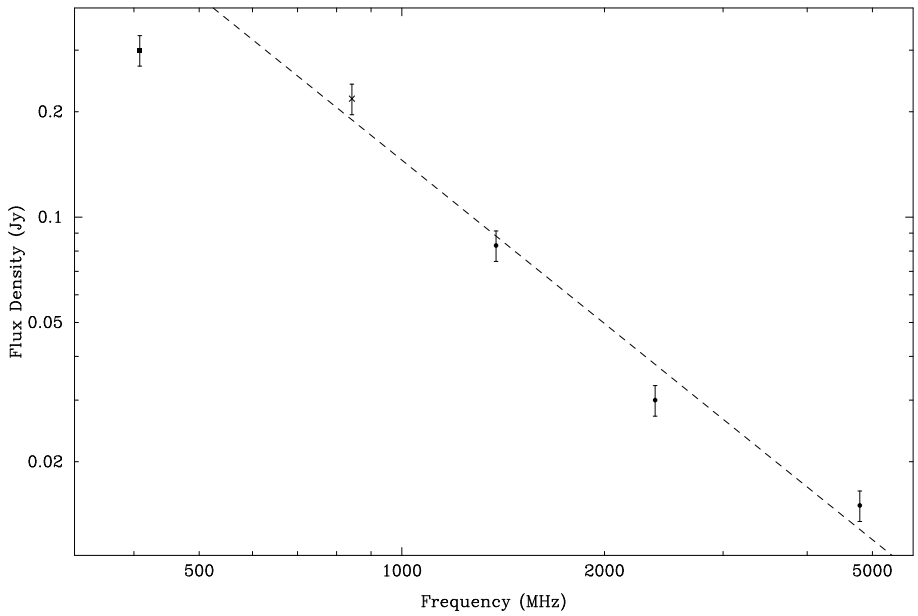

Figure 5.75: The radio spectrum of 0547–704 in the Large Magellanic Cloud.

0550–684 (Figures 5.76 and 5.77) The MOST image shows a compact source located on the edge of a half-shell of diffuse emission. The compact source has an integrated flux density of 145 mJy whereas the compact source and the extended region combined have an integrated flux density of 651 mJy at 843 MHz. The ATCA 4790 MHz image shows two sources with perhaps some faint diffuse emission between them. The peak position of the compact source in the MOST image lies between the two weak sources in the ATCA image, suggesting that the compact MOST source has been resolved into two components and some diffuse emission with the ATCA. The integrated flux densities of the two ATCA sources are 7.5 and 3.9 mJy.

Whilst this source is not listed in the MRC, a flux density of 980 mJy is given in the MC4 catalogue. Parkes source B0550–6823 appears, within uncertainties, coincident with the extended region rather than the compact source itself. The source is relatively strong and was detected over the full range of observed frequencies; the 4.75 and 4.85 GHz flux densities are 388 and 562 mJy respectively. The large difference in flux density between these two closely-spaced Parkes frequencies is hard to explain as is the fact that the 4.85 GHz flux density is greater than the 4.75 GHz value whereas the general trend from 1.40 GHz through to 8.55 GHz is one of decreasing flux density with increasing frequency. Marx, Dickey & Mebold (1997) determine a 1380 MHz flux density of 48 mJy. The large discrepancy between the Parkes and ATCA values at 1.4 and 5 GHz is due to the ATCA not sampling emission on larger angular scales. No detection was made of this object with the PTI at 2.3 GHz. The *ROSAT* All Sky Survey X-ray source LMC RASS 309 appears to be coincident with this object. There are some large-scale, faint optical filaments catalogued as DEM 328 in this area but these do not mimic the morphology imaged by the MOST.

Excluding the ATCA 4790 MHz value, a spectral index of $\alpha = -(0.33 \pm 0.07)$ was determined and the fit to these data is indicated by the dashed line in Figure 5.77. This compares favourably with the spectral index of $\alpha = -(0.37 \pm 0.06)$ determined by Filipovic et al. (1998a) who classified this object as a possible SNR. Taking the flux density of the compact component at 843 MHz (145 mJy), the Marx, Dickey & Mebold (1997) 1380 MHz flux density and the combined integrated flux density determined with the ATCA at 4790 MHz of 11.4 mJy, a spectral index of $\alpha = -(1.37 \pm 0.25)$ is obtained and shown as the dotted line in Figure 5.77.

Given the limited range of available data it is difficult to be certain about the previous identification of this source as a possible SNR. The morphology of the extended diffuse emission visible in the MOST image can be considered characteristic of an SNR. It is uncertain whether the compact source is part of the extended region or simply a coincident background object. Further observations over a range of frequencies and angular scales are required in order to image the extended region.

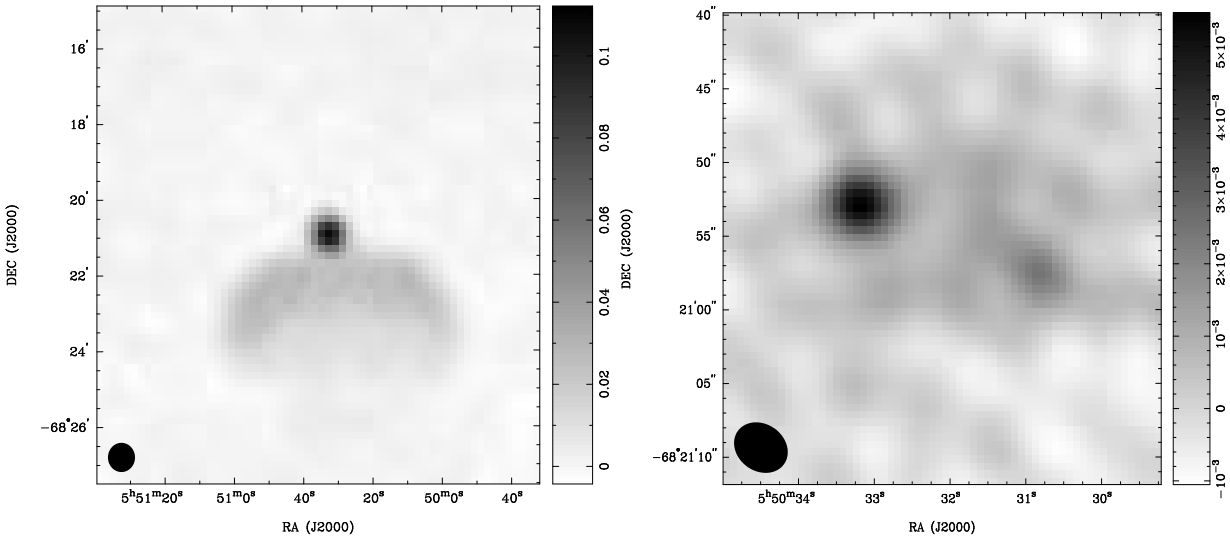

Figure 5.76: The MOST 843 MHz (left) and ATCA 4790 MHz (right) total intensity images of 0550–684 in the Large Magellanic Cloud. The intensity units are in Jy/beam.

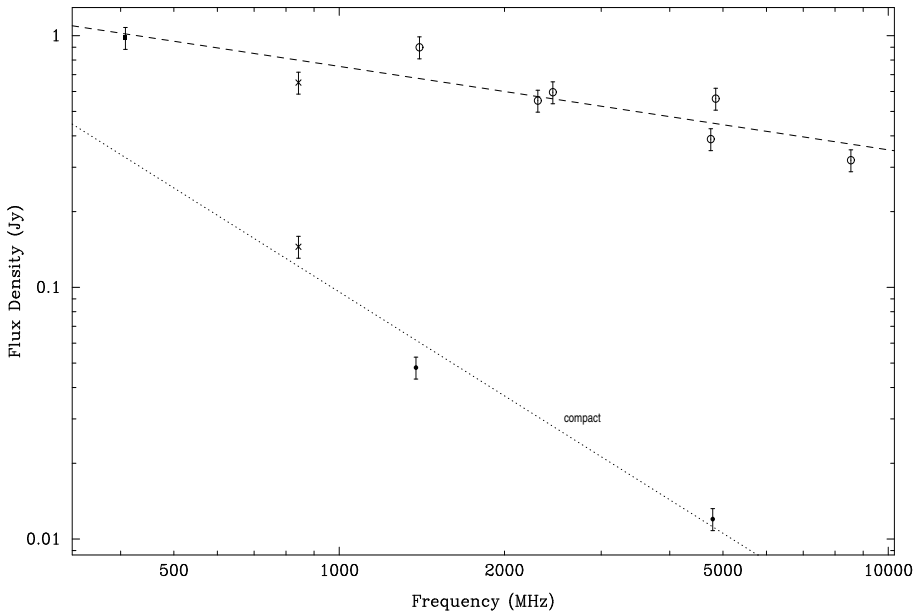

Figure 5.77: The radio spectrum of 0550–684 in the Large Magellanic Cloud. The dashed line shows the fit to the 408 MHz, MOST and Parkes data, with the slope of the dotted line giving the spectral index of the compact component.

0552–682 (Figures 5.78 and 5.79) The MOST 843 MHz image shows a compact source with peak and integrated flux densities of 346 mJy/beam and 360 mJy respectively. The ATCA 4790 MHz image shows a compact source with some slight elongation along the major axis. A peak flux density of 47 mJy/beam and integrated flux density of 51 mJy were determined from the interactive fitting procedure.

This source is not listed in the 408 MHz MRC, but appears in the MC4 catalogue with a flux density of 720 mJy. Parkes observations failed to detect this source at 1.40 GHz but do detect B0552–6815 at higher frequencies. Flux densities of 93 and 118 mJy at 4.75 and 4.85 GHz were reported from the Parkes observations, roughly double that determined with the ATCA at 4790 MHz. Dickey et al. (1994) give a 1419 MHz flux density of 182 mJy with H I absorption seen in the direction of this source. Similarly, Marx, Dickey & Mebold (1997) list a 1380 MHz flux density of 178 mJy.

Using only the 408, 843 MHz and Parkes 4.75 GHz values, a spectral index of $\alpha = -(0.82 \pm 0.04)$ has been computed which is typical of background sources. Based on the source morphology, spectrum and presence of H I absorption, this source is probably an extragalactic background source.

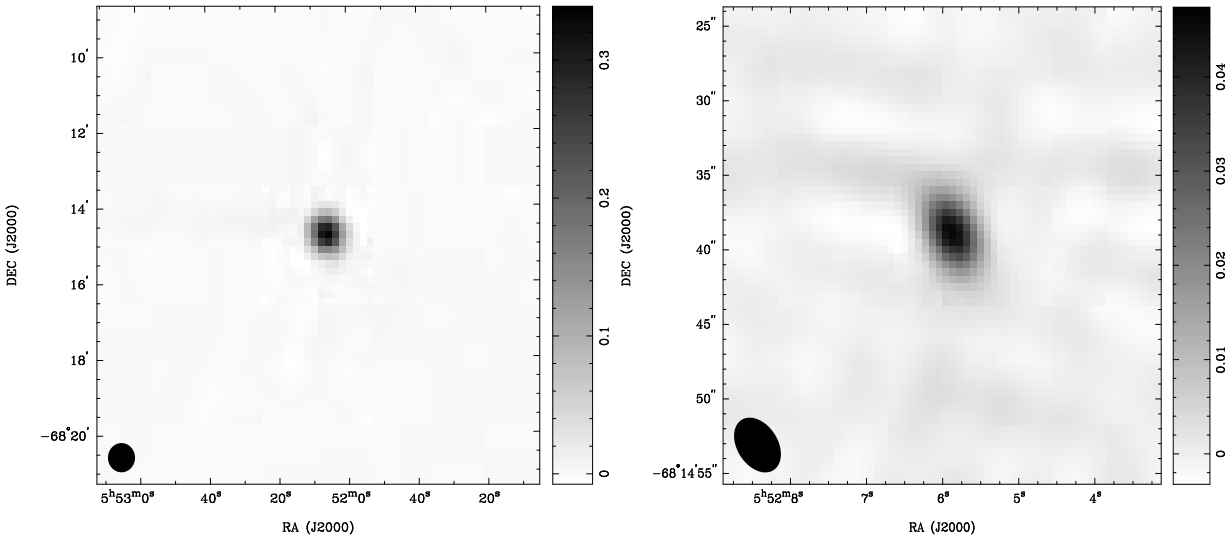

Figure 5.78: The MOST 843 MHz (left) and ATCA 4790 MHz (right) total intensity images of 0552–682 in the Large Magellanic Cloud. The intensity units are in Jy/beam.

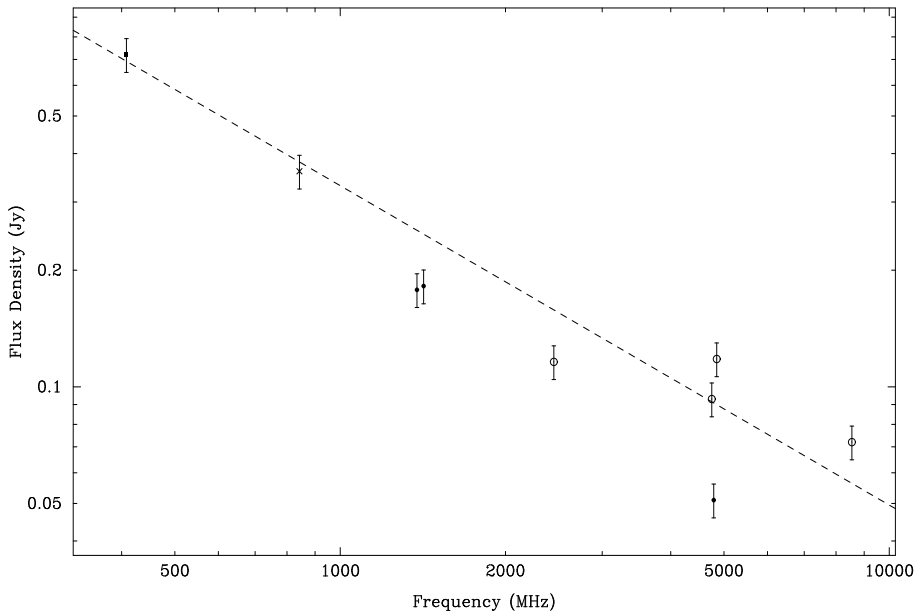

Figure 5.79: The radio spectrum of 0552–682 in the Large Magellanic Cloud.

0552–703 (Figures 5.80 and 5.81) Both the MOST and ATCA images exhibit an extended morphology. The source is clearly extended at the angular resolution of the MOST, and the improved angular resolution of the ATCA reveals two clearly resolved extended components. The peak and integrated flux densities at 843 MHz are 419 mJy/beam and 852 mJy respectively. The integrated flux densities of the two regions from the ATCA 4790 MHz observations are 92 and 77 mJy.

The 408 MHz flux density given in the MRC is 1.270 Jy. The Parkes source B0552–7022 has good positional agreement with the ATCA-determined position and was detected at all observed frequencies. Flux densities of 268 and 254 mJy were determined at 4.75 and 4.85 GHz. These are significantly greater than the combined integrated flux density of 169 mJy from the ATCA. Given the complex morphology revealed by the higher angular resolution ATCA observations the ATCA would not have fully sampled the larger scale emission at angular scales greater than 30 arcsec at this frequency. Marx, Dickey & Mebold (1997) list a 1380 MHz continuum flux density of 56 mJy which is significantly lower than the ATCA 4790 MHz flux density. With only two ATCA data points it is difficult to be certain as to why this may be the case. No X-ray or infrared emission was detected from this object and it was not observed as part of the Dickey et al. (1994) H I survey which targeted only those sources which were relatively compact at 4790 MHz.

Using all the data apart from the ATCA values, a spectral index of $\alpha = -(0.67 \pm 0.04)$ was determined. This source is likely to be a lobe-dominated radio galaxy background to the LMC.

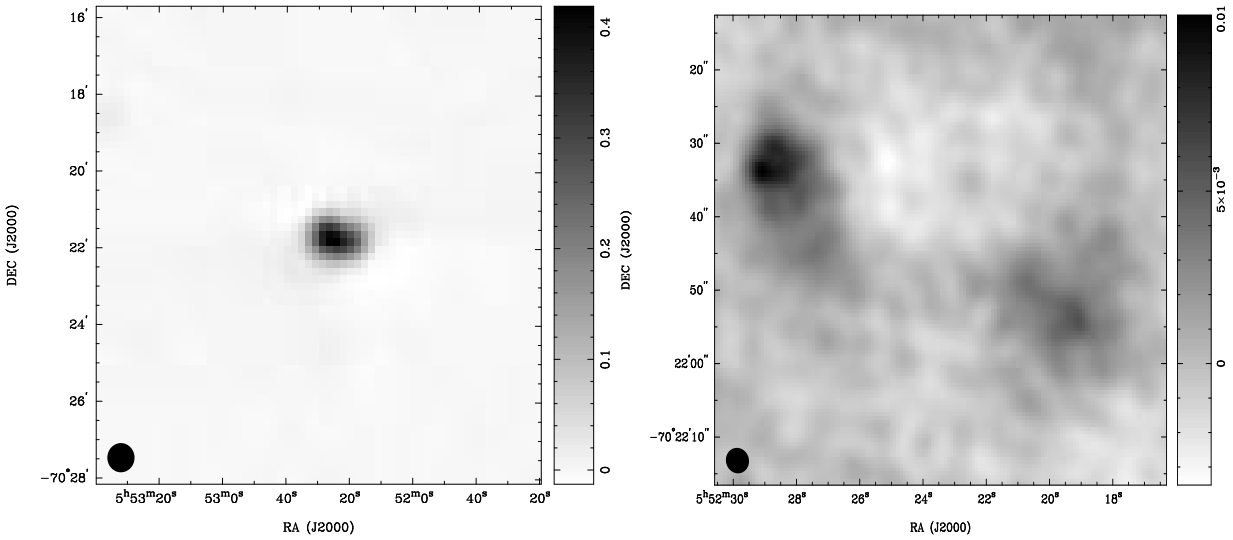

Figure 5.80: The MOST 843 MHz (left) and ATCA 4790 MHz (right) total intensity images of 0552–703 in the Large Magellanic Cloud. The intensity units are in Jy/beam.

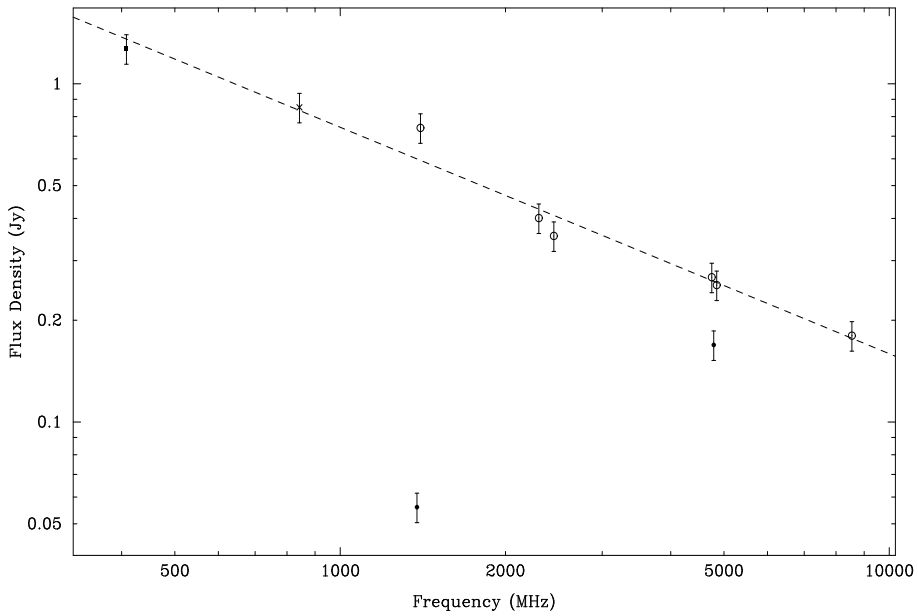

Figure 5.81: The radio spectrum of 0552–703 in the Large Magellanic Cloud.

0600–706 (Figures 5.82 and 5.83) A compact source is seen in the MOST image with peak and integrated flux densities of 839 mJy/beam and 871 mJy respectively. There is a fainter source on the eastern edge of the sub-image which is not discussed here. The ATCA image shows an extended source with a central brighter component. The integrated flux density at 4790 MHz is 133 mJy.

A 408 MHz flux density of 1.720 Jy is listed in the MRC. In the Parkes surveys the source B0600–7038 was only detected at 4.75 and 4.85 GHz with flux densities of 132 and 127 mJy respectively. This agrees with the ATCA flux density of 133 mJy determined here. This suggests that although the source is extended in the ATCA image, the radio emission and structure has been fully sampled. A 1419 MHz continuum flux density of 370 mJy is given by Dickey et al. (1994) although no H I absorption was seen towards the source. The *ROSAT* PSPC X-ray source 1175 lies within 25 arcsec of the centroid of the ATCA-determined position.

Using the full data-set a spectral index of $\alpha = -(1.04 \pm 0.05)$ was calculated which is within the expected range of a steep spectrum background source. The fit to the radio spectrum suggests that the 1419 MHz flux density may may be an under-estimate. Fringes were detected with the PTI at 2.3 GHz with an approximate flux density of 92 mJy suggesting the presence of a compact but relatively weak core.

The source is situated on the eastern edge of the LMC and its location, morphology and spectral index suggests that this object is probably a background source.

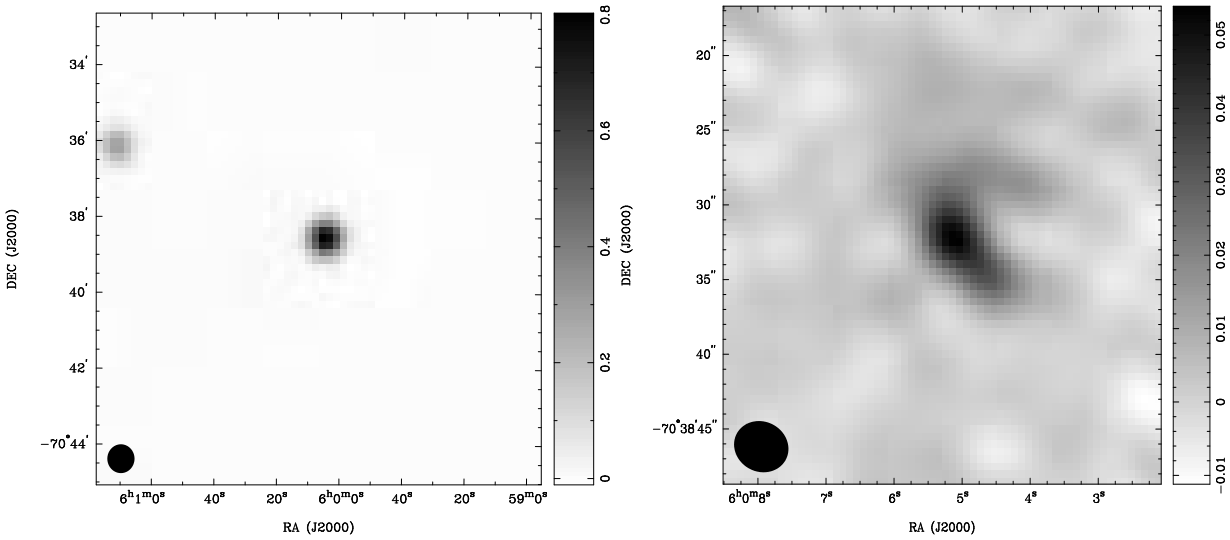

Figure 5.82: The MOST 843 MHz (left) and ATCA 4790 MHz (right) total intensity images of 0600–706 in the Large Magellanic Cloud. The intensity units are in Jy/beam.

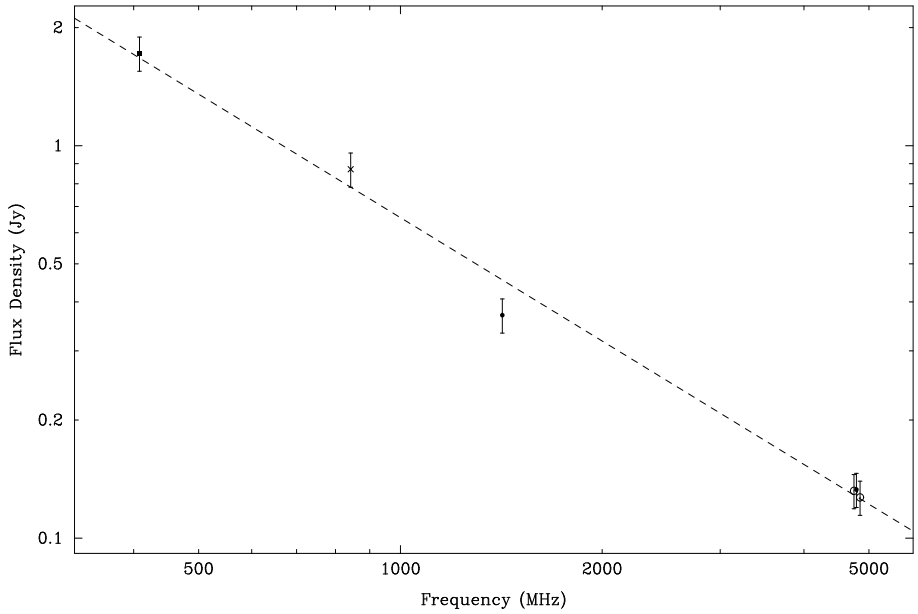

Figure 5.83: The radio spectrum of 0600–706 in the Large Magellanic Cloud.

Table 5.1: Comparison of the MOST 843 MHz, ATCA 1419 and 4790 MHz, Parkes survey data and X-ray observations of selected sources in the Large Magellanic Cloud. The reference column indicates if the tabulated data was taken from a published survey. B1950.0 positions are quoted if these are listed in the published catalogues; such positions have been precessed to obtain corresponding J2000.0 positions for the purposes of comparison.

Source	Frequency (GHz)	Source Position (B1950.0)	Source Position (J2000.0)	Integrated Flux Density (mJy)	Reference/ Notes
0440–665					
MOST #1	0.843		04 40 56.87 −66 24 23.0	889	
ATCA #1	4.79		04 40 56.72 −66 24 21.4	152	
ATCA #1	1.419		04 40 56.83 −66 24 23.7	360	Dickey
B0440–6630	1.40	04 40 53.7 −66 30 40	04 41 03.0 −66 25 01	451	Filipovic
B0440–6630	2.30	04 40 42.0 −66 29 08	04 40 51.6 −66 23 28	294	Filipovic
B0440–6630	2.45	04 40 45.2 −66 29 58	04 40 54.6 −66 24 18	323	Filipovic
B0440–6630	4.75	04 40 47.5 −66 30 34	04 40 56.9 −66 24 55	177	Filipovic
B0440–6630	4.85	04 40 45.4 −66 30 08	04 40 54.8 −66 24 28	173	Filipovic
0449–709					
MOST #1	0.843		04 49 03.50 −70 52 02.5	632	
ATCA #1	4.79		04 49 02.18 −70 51 48.5	71	
ATCA #2	4.79		04 49 03.40 −70 52 17.0	66	
B0449–7057	2.30	04 50 00.0 −70 57 29	04 49 29.6 −70 52 26	421	Filipovic
B0449–7057	4.75	04 49 28.2 −70 57 03	04 48 58.0 −70 51 58	151	Filipovic
B0449–7057	4.85	04 49 23.5 −70 57 07	04 48 53.3 −70 52 02	210	Filipovic
B0449–7057	8.55	04 49 38.4 −70 57 13	04 49 08.1 −70 52 09	63	Filipovic
0451–696					
MOST	0.843		04 51 13.79 −69 31 46.0	363	
ATCA #1	4.79		04 51 14.62 −69 36 48.0	13	
ATCA #2	4.79		04 51 13.87 −69 31 33.5	6	
ATCA #3	4.79		04 51 14.98 −69 31 22.9	4	
0454–649					
MOST #1	0.843		04 55 07.47 −64 50 19.3	1402	
ATCA #1	4.79		04 55 09.57 −64 50 15.9	35	
B0454–6454	1.40	04 54 37.3 −64 55 28	04 54 54.2 −64 50 46	1067	Filipovic
B0454–6454	2.30	04 54 53.5 −64 54 08	04 55 10.5 −64 49 28	894	Filipovic
B0454–6454	2.45	04 54 45.7 −64 54 53	04 55 02.6 −64 50 12	887	Filipovic
B0454–6454	4.75	04 54 48.3 −64 54 49	04 55 05.2 −64 50 08	448	Filipovic
0456–703					
MOST #1	0.843		04 56 08.53 −70 14 32.4	201	
ATCA #1	4.79		04 56 08.72 −70 14 33.4	76	
ATCA #1	1.419		04 56 08.80 −70 14 34.1	101	Dickey
B0456–7019	2.45	04 56 31.2 −70 19 22	04 56 05.6 −70 14 47	179	Filipovic
B0456–7019	4.75	04 56 30.9 −70 19 05	04 56 05.3 −70 14 30	103	Filipovic
B0456–7019	4.85	04 56 44.6 −70 19 42	04 56 18.9 −70 15 08	107	Filipovic
B0456–7019	8.55	04 56 33.8 −70 19 43	04 56 08.1 −70 15 08	100	Filipovic
0458–720					
MOST #1	0.843		04 57 56.30 −71 56 16.4	546	
ATCA #1	4.79		04 58 04.40 −71 56 35.0	10	
B0458–7201	1.40	04 59 11.5 −72 01 51	04 58 26.9 −71 56 26	424	Filipovic
B0458–7201	2.45	04 58 50.2 −72 00 52	04 58 05.9 −71 56 26	265	Filipovic
B0458–7201	4.75	04 58 46.3 −72 01 01	04 58 02.0 −71 56 35	189	Filipovic
B0458–7201	4.85	04 58 59.9 −72 01 08	04 58 15.5 −71 56 43	197	Filipovic

Table 5.1: (continued)

Source	Frequency (GHz)	Source Position (B1950.0)	Source Position (J2000.0)	Integrated Flux Density (mJy)	Reference/ Notes
0502–696					
MOST #1	0.843		05 02 01.08 −69 31 53.1	1389	
ATCA #1	4.79		05 01 59.82 −69 31 50.6	109	
B0502–6935	1.40	05 02 02.1 −69 35 29	05 01 42.3 −69 31 17	461	Filipovic
B0502–6935	2.30	05 02 27.8 −69 34 26	05 02 08.1 −69 13 16	424	Filipovic
B0502–6935	2.45	05 02 13.1 −69 35 54	05 01 53.2 −69 31 43	353	Filipovic
B0502–6935	4.75	05 02 20.9 −69 35 55	05 02 01.0 −69 31 45	139	Filipovic
B0502–6935	4.85	05 02 27.5 −69 36 30	05 02 07.4 −69 32 20	136	Filipovic
B0502–6935	8.55	05 02 28.1 −69 35 28	05 02 08.2 −69 31 18	53	Filipovic
0503–680					
MOST #1	0.843		05 02 58.96 −67 58 04.8	325	
ATCA #1	4.79		05 02 59.24 −67 58 01.8	17	
ATCA #2	4.79		05 02 58.62 −67 58 10.3	28	
B0503–6803	2.45	05 03 09.4 −68 02 31	05 03 02.7 −67 58 25	172	Filipovic
B0503–6803	4.75	05 03 14.9 −68 03 10	05 03 08.1 −67 59 04	82	Filipovic
B0503–6803	4.85	05 03 17.9 −68 01 42	05 03 11.3 −67 57 36	96	Filipovic
B0503–6803	8.55	05 03 10.7 −68 03 22	05 03 03.9 −67 59 16	66	Filipovic
0504–668					
MOST #1	0.843		05 05 01.01 −66 45 16.2	370	
ATCA #1	4.79		05 05 01.54 −69 45 16.5	20	
ATCA #2	4.79		05 05 00.44 −69 45 20.5	14	
B0505–6648	2.45	05 05 01.2 −66 48 37	05 05 03.6 −66 44 39	275	Filipovic
B0505–6648	4.75	05 05 28.0 −66 48 58	05 05 30.3 −66 45 02	61	Filipovic
B0505–6648	4.85	05 05 06.7 −66 48 56	05 05 09.1 −66 44 58	54	Filipovic
0505–681					
MOST #1	0.843		05 05 02.17 −68 03 23.8	129	
ATCA #1	4.79		05 04 50.77 −68 02 27.0	3	
B0505–6807	1.40	05 05 34.8 −68 05 46	05 05 27.3 −68 01 50	696	Filipovic
B0505–6807	2.30	05 05 03.9 −68 07 39	05 04 56.2 −68 03 41	311	Filipovic
B0505–6807	2.45	05 05 18.4 −68 06 58	05 05 10.7 −68 03 01	346	Filipovic
B0505–6807	4.75	05 04 57.2 −68 07 28	05 04 49.5 −68 03 29	306	Filipovic
B0505–6807	4.85	05 05 15.6 −68 07 15	05 05 07.9 −68 03 17	295	Filipovic
B0505–6807	8.55	05 05 06.9 −68 07 45	05 04 59.2 −68 03 47	349	Filipovic
0510–689					
MOST #1	0.843		05 09 53.08 −68 53 05.4	969	
ATCA #1	4.79		05 09 50.59 −68 53 05.4	19	
ATCA #2	4.79		05 09 52.93 −68 53 00.8	32	
B0510–6857	2.30	05 10 10.8 −68 57 15	05 09 55.2 −68 53 38	1171	Filipovic
B0510–6857	2.45	05 10 06.6 −68 56 55	05 09 51.1 −68 53 18	1157	Filipovic
B0510–6857	4.75	05 10 07.3 −68 57 20	05 09 51.7 −68 53 43	1156	Filipovic
B0510–6857	4.85	05 10 10.6 −68 57 08	05 09 55.0 −68 53 31	1207	Filipovic
B0510–6857	8.55	05 10 11.7 −68 57 02	05 09 56.2 −68 53 25	1138	Filipovic
0513–692					
MOST #1	0.843		05 13 23.91 −69 10 58.0	287	
ATCA #1	4.79		05 13 24.67 −69 10 48.3	9	
B0513–6915	4.75	05 13 33.7 −69 17 00	05 13 14.6 −69 13 37	264	Filipovic
B0513–6915	8.55	05 13 42.2 −69 14 55	05 13 23.4 −69 11 33	68	Filipovic
PSPC #835	X-ray		05 13 13.5 −69 11 30	–	Haberl

Table 5.1: (continued)

Source	Frequency (GHz)	Source Position (B1950.0)	Source Position (J2000.0)	Integrated Flux Density (mJy)	Reference/ Notes
0514–676					
MOST	0.843		05 14 16.89 −67 35 22.6	279	
ATCA #1	4.79		05 14 17.92 −67 35 27.8	16	
ATCA #2	4.79		05 14 16.67 −67 35 21.0	14	
ATCA #3	4.79		05 14 19.03 −67 35 22.7	4	
0515–660					
MOST #1	0.843		05 15 23.69 −65 58 39.0	539	
ATCA #1	4.79		05 15 24.26 −65 58 40.6	71	
ATCA #1	1.419		05 15 24.17 −65 58 41.6	235	Dickey
B0515–6601	1.40	05 15 32.8 −66 01 36	05 15 39.2 −65 58 23	139	Filipovic
B0515–6601	2.30	05 15 35.4 −66 02 15	05 15 41.8 −65 59 02	196	Filipovic
B0515–6601	2.45	05 15 22.2 −66 01 54	05 15 28.6 −65 58 40	157	Filipovic
B0515–6601	4.75	05 15 14.9 −66 01 06	05 15 21.4 −65 57 52	77	Filipovic
B0515–6601	4.85	05 15 04.9 −66 02 05	05 15 11.3 −65 58 50	70	Filipovic
0515–674					
MOST #1	0.843		05 15 37.36 −67 21 26.0	2576	
ATCA #1	4.79		05 15 37.58 −67 21 27.4	417	
B0515–6724	1.40	05 15 21.5 −67 25 20	05 15 17.8 −67 22 06	1819	Filipovic
B0515–6724	2.30	05 15 30.3 −67 24 50	05 15 26.6 −67 59 37	1220	Filipovic
B0515–6724	2.45	05 15 37.9 −67 24 43	05 15 34.2 −67 21 30	1101	Filipovic
B0515–6724	4.75	05 15 39.2 −67 24 37	05 15 35.5 −67 21 24	728	Filipovic
B0515–6724	4.85	05 15 41.5 −67 24 48	05 15 37.8 −67 21 35	790	Filipovic
B0515–6724	8.55	05 15 40.9 −67 24 21	05 15 37.2 −67 21 08	331	Filipovic
PSPC #524	X-ray		05 15 37.3 −67 21 24	–	Haberl
0517–718					
MOST #1	0.843		05 16 41.19 −71 49 04.3	535	
ATCA #1	4.79		05 16 41.45 −71 49 05.6	200	
ATCA #1	1.419		05 16 41.50 −71 49 05.7	353	Dickey
B0517–7151	1.40	05 17 37.3 −71 49 17	05 16 51.3 −71 46 11	537	Filipovic
B0517–7151	2.30	05 17 27.3 −71 51 37	05 16 40.9 −71 48 30	510	Filipovic
B0517–7151	2.45	05 17 30.7 −71 51 58	05 16 44.2 −71 48 51	314	Filipovic
B0517–7151	4.75	05 17 28.9 −71 52 07	05 16 42.4 −71 49 00	264	Filipovic
B0517–7151	4.85	05 17 34.9 −71 52 11	05 16 48.4 −71 49 05	275	Filipovic
B0517–7151	8.55	05 17 31.1 −71 51 56	05 16 44.6 −71 48 50	189	Filipovic
517.4–7149	X-ray	05 17 26.11 −71 49 16.1	05 16 40.19 −71 46 09.2	–	Wang
PSPC #1315	X-ray		05 15 10.6 −71 50 56	–	Haberl
0518–679					
MOST #1	0.843		05 18 02.28 −67 55 37.6	332	
ATCA #1	4.79		05 18 02.27 −67 55 39.7	32	
ATCA #2	4.79		05 18 04.22 −67 55 43.2	7	
ATCA #3	4.79		05 18 04.22 −67 55 36.7	4	
MDM 2	1.380		05 18 02.58 −67 55 42.3	52	Marx
MDM 2	2.378		05 18 02.61 −67 55 43.3	19	Marx
B0518–6759	1.40	05 18 19.8 −68 04 57	05 18 10.4 −68 01 55	403	Filipovic
B0518–6759	2.45	05 17 48.7 −68 01 32	05 17 39.8 −67 58 28	278	Filipovic
B0518–6759	4.75	05 18 11.7 −68 58 43	05 18 03.2 −67 55 41	126	Filipovic
B0518–6759	4.85	05 18 09.2 −68 59 07	05 18 00.6 −68 56 05	112	Filipovic
B0518–6759	8.55	05 18 24.6 −68 59 28	05 18 15.9 −67 56 27	92	Filipovic

Table 5.1: (continued)

Source	Frequency (GHz)	Source Position (B1950.0)	Source Position (J2000.0)	Integrated Flux Density (mJy)	Reference/ Notes
0518–696					
MOST #1	0.843		05 18 32.13 –69 35 19.1	588	
ATCA #1	4.79		05 18 32.68 –69 35 21.6	102	
ATCA #1	1.419		05 18 32.72 –69 35 21.7	330	
MDM 3	1.380		05 18 32.74 –69 35 22.8	326	Marx
MDM 3	2.378		05 18 32.72 –69 35 22.5	259	Marx
B0518–6937	8.55	05 18 58.9 –69 37 14	05 18 35.9 –69 34 15	107	Filipovic
519.1–6943	X-ray	05 19 04.48 –69 42 39.0	05 18 40.58 –69 39 40.1	–	Wang
PSPC #978	X-ray		05 18 43.4 –69 39 10	–	Haberl
0524–708					
MOST #1	0.843		05 23 40.34 –70 51 20.2	1774	
ATCA #1	4.79		05 23 40.95 –70 50 18.0	80	
ATCA #2	4.79		05 23 40.95 –70 51 23.5	81	
ATCA #1	1.419		05 23 40.93 –70 50 18.8	195	Dickey
ATCA #2	1.419		05 23 41.04 –70 51 23.2	207	Dickey
MDM 21	1.380		05 23 40.94 –70 50 20.9	225	Marx
MDM 21	2.378		05 23 40.86 –70 50 20.3	144	Marx
MDM 22	1.380		05 23 40.97 –70 51 22.3	245	Marx
MDM 22	2.378		05 23 41.01 –70 51 23.8	156	Marx
B0524–7053	1.40	05 24 21.9 –70 53 00	05 23 45.4 –70 50 23	643	Filipovic
B0524–7053	2.30	05 24 22.5 –70 53 26	05 23 45.9 –70 50 50	485	Filipovic
B0524–7053	2.45	05 24 19.2 –70 53 42	05 23 42.6 –70 51 05	470	Filipovic
B0524–7053	4.75	05 24 14.9 –70 53 28	05 23 38.3 –70 50 51	251	Filipovic
B0524–7053	4.85	05 24 20.4 –70 53 32	05 23 43.8 –70 50 55	269	Filipovic
B0524–7053	8.55	05 24 21.8 –70 53 27	05 23 45.2 –70 50 51	198	Filipovic
0526–658					
MOST #1	0.843		05 26 32.30 –65 49 05.3	408	
ATCA #1	4.79		05 26 31.84 –65 49 06.5	54	
ATCA #1	1.419		05 26 31.87 –65 49 07.0	121	Dickey
B0526–6551	2.30	05 26 54.6 –65 53 18	05 27 00.7 –65 50 54	304	Filipovic
B0526–6551	2.45	05 26 55.5 –65 52 51	05 27 01.7 –65 50 27	287	Filipovic
B0526–6551	4.75	05 26 24.9 –65 52 03	05 26 31.2 –65 49 37	138	Filipovic
B0526–6551	4.85	05 26 25.7 –65 51 19	05 26 32.1 –65 48 53	108	Filipovic
0526–659					
MOST #1	0.843		05 26 27.03 –65 56 19.2	401	
ATCA #1	4.79		05 26 26.21 –65 56 24.0	47	
ATCA #2	4.79		05 26 18.85 –65 55 59.0	11	
B0526–6558	4.75	05 26 33.4 –65 58 46	05 26 38.9 –65 56 20	119	Filipovic
0527–651					
MOST #1	0.843		05 28 10.67 –65 03 52.9	654	
ATCA #1	4.79		05 28 10.62 –65 03 53.1	187	
ATCA #1	1.419		05 28 10.65 –65 03 53.3	431	Dickey
B0528–6506	1.40	05 27 52.7 –65 06 14	05 28 04.0 –65 03 54	417	Filipovic
B0528–6506	2.30	05 28 06.2 –65 06 06	05 28 17.5 –65 03 47	367	Filipovic
B0528–6506	2.45	05 28 01.3 –65 06 17	05 28 12.5 –65 03 58	318	Filipovic
B0528–6506	4.75	05 28 03.2 –65 06 13	05 28 14.5 –65 03 54	193	Filipovic

Table 5.1: (continued)

Source	Frequency (GHz)	Source Position (B1950.0)	Source Position (J2000.0)	Integrated Flux Density (mJy)	Reference/ Notes
0528–692					
MOST #1	0.843		05 27 55.08 –69 11 29.6	83	
ATCA #1	4.79		05 27 54.29 –69 11 39.2	3	
MDM 33	1.380		05 27 54.56 –69 11 40.7	15	Marx
B0528–6914	4.75	05 28 01.2 –69 14 11	05 27 40.6 –69 11 51	75	Filipovic
B0528–6914	4.85	05 28 04.3 –69 14 04	05 27 43.7 –69 11 44	73	Filipovic
B0528–6914	8.55	05 28 08.4 –69 14 03	05 27 47.8 –69 11 43	66	Filipovic
528.1–6915	X-ray	05 28 04.34 –69 14 31.0	05 27 43,66 –69 12 11.0	–	Wang
PSPC #836	X-ray		05 27 43.4 –69 11 50	–	Haberl
0530–678					
MOST #1	0.843		05 29 51.25 –67 49 34.5	375	
ATCA #1	4.79		05 29 51.55 –67 49 30.3	62	
ATCA #1	1.419		05 29 51.55 –67 49 31.9	155	Dickey
MDM 38	1.380		05 29 51.64 –67 49 34.5	188	Marx
MDM 38	2.378		05 29 51.64 –67 49 33.6	101	Marx
B0529–6752	1.40	05 29 55.2 –67 51 38	05 29 46.2 –67 49 26	265	Filipovic
B0529–6752	2.45	05 29 54.8 –67 52 19	05 29 45.8 –67 50 07	171	Filipovic
B0529–6752	4.75	05 30 04.5 –67 52 06	05 29 55.5 –67 49 55	89	Filipovic
B0529–6752	4.85	05 30 02.4 –67 51 19	05 29 53.5 –67 49 08	90	Filipovic
B0529–6752	8.55	05 29 46.9 –67 52 01	05 29 37.9 –67 49 49	53	Filipovic
0532–675					
MOST #1	0.843		05 32 16.94 –67 33 09.3	270	
ATCA #1	4.79		05 32 16.40 –67 33 08.3	5	
B0532–6734	4.75	05 32 45.7 –67 34 55	05 32 38.7 –67 32 56	93	Filipovic
532.3–6742	X-ray	05 32 15.95 –67 42 14.0	05 32 08.04 –67 40 12.6	–	Wang
532.5–6734	X-ray	05 32 32.71 –67 33 30.9	05 32 25.93 –67 31 30.8	–	Wang
PSPC #540	X-ray		05 32 24.4 –67 31 10	–	Haberl
0533–725					
MOST #1	0.843		05 32 53.90 –72 31 54.7	534	
ATCA #1	4.79		05 32 54.18 –72 31 53.2	78	
B0533–7233	1.40	05 34 13.5 –72 33 13	05 33 16.2 –72 31 20	241	Filipovic
B0533–7233	2.30	05 33 43.4 –72 33 50	05 32 46.0 –72 31 53	164	Filipovic
B0533–7233	2.45	05 33 49.6 –72 33 36	05 32 52.2 –72 31 40	162	Filipovic
B0533–7233	4.75	05 33 48.7 –72 33 55	05 32 51.3 –72 31 59	101	Filipovic
B0533–7233	4.85	05 33 46.2 –72 33 49	05 32 48.8 –72 31 52	112	Filipovic
0534–720					
MOST #1	0.843		05 34 30.36 –72 01 54.9	200	Entire region
ATCA #1	4.79		05 34 30.10 –72 01 53.6	14	
B0534–7204	2.45	05 34 52.1 –72 04 06	05 34 00.8 –72 02 14	147	Filipovic
B0534–7204	4.75	05 34 50.8 –72 04 42	05 33 59.4 –72 02 50	103	Filipovic
B0534–7204	4.85	05 35 02.8 –72 04 57	05 34 11.3 –72 03 06	93	Filipovic

Table 5.1: (continued)

Source	Frequency (GHz)	Source Position (B1950.0)	Source Position (J2000.0)	Integrated Flux Density (mJy)	Reference/ Notes
0535–676					
MOST #1	0.843		05 35 23.35 −67 34 56.5	1786	
ATCA #1	4.79		05 35 25.44 −67 34 20.9	9	
B0535–6736	1.40	05 35 04.5 −67 35 39	05 34 57.2 −67 33 50	2532	Filipovic
B0535–6736	2.30	05 35 34.9 −67 35 53	05 35 27.5 −67 34 06	2307	Filipovic
B0535–6736	2.45	05 35 35.7 −67 35 55	05 35 28.3 −67 34 08	2340	Filipovic
B0535–6736	4.75	05 35 33.2 −67 36 22	05 35 25.8 −67 34 35	1454	Filipovic
B0535–6736	4.85	05 35 34.3 −67 36 12	05 35 26.9 −67 34 25	2267	Filipovic
B0535–6736	8.55	05 35 36.0 −67 36 22	05 35 28.6 −67 34 35	1264	Filipovic
PSPC #551	X-ray		05 36 01.7 −67 34 29	–	Haberl
0537–692					
MOST #1	0.843		05 36 56.19 −69 13 28.5	2132	Entire region
ATCA #1	4.79		05 36 57.11 −69 13 28.4	51	
ATCA #1	1.419		05 36 57.45 −69 13 28.7	125	Dickey
MDM 65	1.380		05 36 57.17 −69 13 29.0	174	Marx
MDM 65	2.378		05 36 57.23 −69 13 29.0	116	Marx
B0537–6914	8.55	05 37 22.2 −69 14 13	05 37 00.7 −69 12 33	1504	Filipovic
536.4–6914	X-ray	05 36 50.24 −69 13 36.8	05 36 28.83 −69 11 54.8	–	Wang
PSPC #866	X-ray		05 35 45.8 −69 18 10	–	Haberl
0540–696					
MOST #1	0.843		05 39 44.04 −69 38 41.2	1522	
ATCA #1	4.79		05 39 46.02 −69 38 38.8	179	
ATCA #1	1.419		05 39 45.85 −69 38 39.3	84	Dickey
MDM 75	1.380		05 39 45.82 −69 38 38.8	33	Marx
MDM 75	2.378		05 39 45.85 −69 38 39.0	61	Marx
B0540–6940	1.40	05 40 20.7 −69 40 39	05 39 54.8 −69 38 48	2164	Filipovic
B0540–6940	2.30	05 40 16.4 −69 40 53	05 39 50.6 −69 38 39	2592	Filipovic
B0540–6940	4.75	05 40 11.2 −69 39 22	05 39 45.4 −69 38 01	1939	Filipovic
B0540–6940	4.85	05 40 17.0 −69 40 12	05 39 51.1 −69 38 40	1875	Filipovic
B0540–6940	8.55	05 40 13.2 −69 40 22	05 39 47.4 −69 38 34	1713	Filipovic
0541–670					
MOST	0.843		05 41 37.44 −66 58 47.1	51	
ATCA #1	4.79		05 41 39.15 −66 58 46.3	2	
ATCA #2	4.79		05 41 38.55 −66 58 43.3	1	
ATCA #3	4.79		05 41 38.04 −66 58 48.3	3	
PSPC #456	X-ray		05 41 41.2 −66 58 26	–	Haberl
0543–681					
MOST #1	0.843		05 43 14.58 −68 06 52.0	387	
ATCA #1	4.79		05 43 15.94 −68 06 48.3	15	
ATCA #2	4.79		05 43 14.60 −68 06 52.3	13	
ATCA #1	1.419		05 43 14.81 −68 06 53.5	98	Dickey
MDM 90	1.380		05 43 15.29 −68 06 53.9	128	Marx
MDM 90	2.378		05 43 15.21 −68 06 53.7	76	Marx
B0543–6808	1.40	05 43 04.3 −68 08 12	05 42 52.0 −68 06 58	535	Filipovic
B0543–6808	2.45	05 43 16.8 −68 09 35	05 43 04.3 −68 08 21	219	Filipovic
B0543–6808	4.75	05 43 20.3 −68 08 37	05 43 08.0 −68 07 24	58	Filipovic
B0543–6808	4.85	05 43 20.5 −68 09 19	05 43 08.0 −68 08 06	47	Filipovic

Table 5.1: (continued)

Source	Frequency (GHz)	Source Position (B1950.0)	Source Position (J2000.0)	Integrated Flux Density (mJy)	Reference/ Notes
0543–710					
MOST #1	0.843		05 43 07.78 −71 04 09.4	255	
ATCA #1	4.79		05 43 06.14 −71 03 59.4	15	
ATCA #2	4.79		05 43 09.85 −71 04 26.3	9	
MDM 88	1.380		05 43 06.72 −71 04 05.7	58	Marx
B0543–7105	4.75	05 43 39.2 −71 05 01	05 42 58.5 −71 03 48	131	Filipovic
B0543–7105	4.85	05 43 42.8 −71 05 01	05 43 02.1 −71 03 48	131	Filipovic
B0543–7105	8.55	05 43 42.0 −71 05 09	05 43 01.3 −71 03 56	115	Filipovic
PSPC #1235	X-ray		05 42 40.3 −71 04 37	–	Haberl
0545–649					
MOST #1	0.843		05 45 53.78 −64 53 36.2	715	
ATCA #1	4.79		05 45 54.04 −64 53 34.5	204	
ATCA #1	1.419		05 45 54.08 −64 53 34.8	419	
B0545–6454	1.40	05 46 01.2 −64 55 25	05 46 12.4 −64 54 24	517	Filipovic
B0545–6454	2.30	05 45 38.5 −64 53 43	05 45 49.9 −64 52 41	395	Filipovic
B0545–6454	2.45	05 45 30.8 −64 54 47	05 45 42.1 −64 53 44	378	Filipovic
B0545–6454	4.75	05 45 44.1 −64 54 30	05 45 55.4 −64 53 28	295	Filipovic
B0545–6454	4.85	05 45 44.6 −64 54 51	05 45 55.9 −64 53 49	289	Filipovic
0545–719					
MOST #1	0.843		05 44 26.70 −71 55 26.5	410	
ATCA #1	4.79		05 44 27.12 −71 55 27.1	49	
ATCA #1	1.419		05 44 27.17 −71 55 27.5	205	Dickey
B0545–7156	2.30	05 45 11.8 −71 55 10	05 44 21.4 −71 54 03	302	Filipovic
B0545–7156	2.45	05 45 29.1 −71 55 47	05 44 38.5 −71 54 42	306	Filipovic
B0545–7156	4.75	05 45 26.3 −71 56 02	05 44 35.7 −71 54 56	101	Filipovic
B0545–7156	8.55	05 45 14.1 −71 56 06	05 44 23.5 −71 54 00	68	Filipovic
0547–677					
MOST #1	0.843		05 47 44.94 −67 45 04.5	185	
ATCA #1	4.79		05 47 45.17 −67 45 05.7	40	
ATCA #1	1.419		05 47 45.40 −67 45 07.2	81	Dickey
MDM 100	1.380		05 47 45.37 −67 45 07.1	90	Marx
MDM 100	2.378		05 47 43.35 −67 45 07.0	69	Marx
B0547–6746	2.45	05 47 43.0 −67 46 43	05 47 33.0 −67 45 49	126	Filipovic
B0547–6746	4.75	05 47 55.6 −67 46 05	05 47 46.1 −67 45 12	63	Filipovic
B0547–6746	4.85	05 47 52.6 −67 46 25	05 47 43.1 −67 45 32	69	Filipovic
B0547–6746	8.55	05 48 02.6 −67 46 27	05 47 53.1 −67 45 34	48	Filipovic
547.9–6746	X-ray	05 47 53.56 −67 46 13.9	05 47 44.06 −67 45 20.5	–	Wang
0547–704					
MOST	0.843		05 46 28.89 −70 26 38.2	218	
ATCA #1	4.79		05 46 29.29 −70 26 42.4	9	
ATCA #2	4.79		05 46 28.39 −70 26 30.9	6	
MDM 98	1.380		05 46 29.15 −70 26 40.7	83	Marx
MDM 98	2.378		05 46 29.34 −70 26 44.3	30	Marx
PSPC #1146	X-ray		05 43 40.7 −70 27 11	–	Haberl

Table 5.1: (continued)

Source	Frequency (GHz)	Source Position (B1950.0)	Source Position (J2000.0)	Integrated Flux Density (mJy)	Reference/ Notes
0550–684					
MOST #1	0.843		05 50 32.56 –68 20 55.4	651	Entire region
ATCA #1	4.79		05 50 33.14 –68 20 53.1	8	
ATCA #2	4.79		05 50 30.79 –68 20 47.6	4	
MDM 108	1.380		05 50 32.90 –68 20 55.5	48	Marx
B0550–6823	1.40	05 50 42.5 –68 23 42	05 50 27.6 –68 23 01	899	Filipovic
B0550–6823	2.30	05 50 29.0 –68 22 38	05 50 14.3 –68 21 56	552	Filipovic
B0550–6823	2.45	05 50 46.5 –68 23 29	05 50 31.7 –68 22 48	596	Filipovic
B0550–6823	4.75	05 50 44.3 –68 23 20	05 50 29.5 –68 22 39	388	Filipovic
B0550–6823	4.85	05 50 45.3 –68 23 36	05 50 30.5 –68 22 55	562	Filipovic
B0550–6823	8.55	05 50 49.6 –68 23 31	05 50 34.8 –68 22 50	320	Filipovic
0552–682					
MOST #1	0.843		05 52 05.84 –68 14 43.6	360	
ATCA #1	4.79		05 52 05.87 –68 14 39.0	51	
ATCA #1	1.419		05 52 05.90 –68 14 39.8	182	Dickey
MDM 112	1.380		05 52 05.81 –68 14 41.9	178	Marx
B0552–6815	2.45	05 52 21.7 –68 16 05	05 52 07.9 –68 15 31	116	Filipovic
B0552–6815	4.75	05 52 20.3 –68 15 14	05 52 06.6 –68 14 40	93	Filipovic
B0552–6815	4.85	05 52 18.7 –68 15 13	05 52 05.0 –68 14 39	118	Filipovic
B0552–6815	8.55	05 52 24.5 –68 15 29	05 52 10.8 –68 14 55	72	Filipovic
0552–703					
MOST #1	0.843		05 52 26.66 –70 21 38.0	852	
ATCA #1	4.79		05 52 29.05 –70 21 33.8	92	
ATCA #2	4.79		05 52 19.13 –70 21 54.3	77	
MDM 114	1.380		05 52 28.46 –70 21 37.0	56	Marx
B0552–7022	1.40	05 52 53.7 –70 21 56	05 52 20.2 –70 21 24	741	Filipovic
B0552–7022	2.30	05 52 55.7 –70 22 32	05 52 22.1 –70 22 00	401	Filipovic
B0552–7022	2.45	05 52 58.0 –70 22 23	05 52 24.5 –70 21 51	355	Filipovic
B0552–7022	4.75	05 52 55.6 –70 22 07	05 52 22.1 –70 21 35	268	Filipovic
B0552–7022	4.85	05 52 56.5 –70 22 27	05 52 23.0 –70 21 55	254	Filipovic
B0552–7022	8.55	05 52 59.7 –70 22 26	05 52 26.2 –70 21 54	180	Filipovic
0600–706					
MOST #1	0.843		06 00 04.72 –70 38 33.5	871	
ATCA #1	4.79		06 00 05.14 –70 38 32.0	133	
ATCA #1	1.419		06 00 05.12 –70 38 33.1	370	Dickey
B0600–7038	4.75	06 00 31.6 –70 38 47	05 59 55.0 –70 38 48	132	Filipovic
B0600–7038	4.85	06 00 28.0 –70 38 59	05 59 51.4 –70 39 00	127	Filipovic
PSPC #1175	X-ray		05 59 59.6 –70 38 55	–	Haberl

5.4 Classification of the LMC Sources

Integrated flux densities from the catalogued data and observations discussed here over a range of frequencies are given in Table 5.2. This table also contains spectral indices obtained from the fit to the data presented for each source. The discussion on each source explains which data were used to determine these spectral indices and the quoted uncertainty is from the formal least-squares fitting procedure. Uncalibrated 2290 MHz PTI flux densities are also given in this table.

The sources presented here have been classified using the decision-tree methodology developed earlier in this chapter and the results are also presented in Table 5.2. Although the introduction of a more formal classification methodology has significantly aided source categorization, there remain a number of sources which require follow-up observations over a range of wavelengths and baselines to be able to classify the source with some certainty.

The 41 sources observed can be classified as follows:

- undetermined: 1,
- background objects: 26,
- possible background objects: 8,
- H II regions: 5, and
- possible SNR: 1.

Three sources have a "hybrid" classification. Two of these, 0502–696 and 0510–689 appear to be background objects coincident with H II regions, and were included in the count of of H II regions. The extended emission associated with the source 0550–684 has been classified as a possible SNR with the compact component likely to be an extragalactic background source. A number of the background sources are located near to known H II regions or supernova remnants. Some nine sources have been classified with some uncertainty and flagged as requiring further observations in order to determine more definitely their identification. One source was not classified and additional observations are required in this case.

The follow-up observations could consist of ATCA continuum observations. A range of interferometer baseline configurations would be required to isolate and image the compact component(s) and to adequately sample the larger-scale extended emission. In many cases the extended emission has been resolved out in the observations presented in this chapter. Observations over a range of observing frequencies would be undertaken so that spectrum both the compact and extended components could be better determined.

5.5 Source Statistics

Some details on radio source counts applied to MOST data have been given in Chapter 3 in which the derivation of the $\log N / \log S$ curve is discussed.

The MOST 843 MHz survey of the Large Magellanic Cloud covers an area of approximately 50 square degrees. The source selection criteria used an arbitrary flux density cutoff of around 200 mJy with a further criterion that the sources chosen appeared compact at 843 MHz. The expected background source count for this flux density limit is approximately 1.1 sources/sq. deg, suggesting around 55 "background" objects should be detected with the MOST over this area.

Table 5.2: A comparison of the integrated flux densities across a range of frequencies for the sources observed in the Large Magellanic Cloud. The 408 MHz data are taken from either the Molonglo Reference Catalogue or from the MC4 Catalogue (the latter being denoted by *). The MOST 843 MHz values are from the data presented in this chapter as are ATCA 4790 MHz values (both repeated from Table 5.1). The 1419 MHz data is taken from Dickey et al. (1994). The 2290 MHz values are from Parkes-Tidbinbilla Interferometer observations. For sources which have a complex morphology a single integrated flux density has been determined and these values are indicated by (region). ND indicates that the appropriate field was observed but the source was not detected. Some PTI detections showed complex structure and this is indicated by (s); a marginal detection is denoted by (m). The classification of each source is denoted by "bg" for a background object, "H II" for an H II region and "SNR" for a supernova remnant; a "?" indicates that there is doubt over the classification. (obs) denotes that follow-up observations are suggested.

Source	S_{408} (mJy)	S_{843} (mJy)	S_{1419} (mJy)	S_{4790} (mJy)	α	S_{2290} (pseudo Jy)	Classification
0440–665	1520	889	360	152	$-(0.87 \pm 0.07)$	ND	bg
0449–709	980	632		71 & 66	$-(0.73 \pm 0.10)$		bg
0451–696	770	363		13, 6 & 4	$-(1.46 \pm 0.13)$		bg? (obs)
0454–649	2430	1402		35	$-(0.63 \pm 0.06)$		bg
0456–703	240*	201	101	76	$-(0.32 \pm 0.05)$	0.23	bg
0458–720	710	546		10	$-(0.60 \pm 0.02)$	0.04	bg? (obs)
0502–696	2760	1389		109	$-(1.27 \pm 0.07)$		H II + bg
0503–680	440*	325		17 & 28	$-(0.66 \pm 0.05)$		bg
0504–668	630*	370		20 & 14	$-(1.10 \pm 0.15)$		bg
0505–681	–	129		3	$-(0.31 \pm 0.19)$		H II
0510–689	790	969		19 & 32	$-(0.0. \pm 0.02)$		H II + bg
0513–692	1180*	287		9	–	ND	? (obs)
0514–676	740	279		16, 14 & 4	$-(1.24 \pm 0.03)$		bg
0515–660	1070	539	235	71	$-(1.09 \pm 0.05)$		bg
0515–674	3770	2576		417	$-(0.80 \pm 0.08)$	2.20	bg
0517–718	580*	535	353	200	$-(0.40 \pm 0.07)$	0.59 (s)	bg
0518–679	350*	332		2, 7 & 4	$-(0.08 \pm 0.13)$		bg?
0518–696	1040	588	330	102	$-(0.92 \pm 0.06)$		bg
0524–708	2350	1774	195 & 207	80 & 81	$-(0.88 \pm 0.07)$		bg
0526–658	640*	408	121	54	$-(1.03 \pm 0.15)$	0.06	bg
0526–659	530*	401		47 & 11	$-(0.63 \pm 0.07)$		bg (obs)
0527–651	1080	654	431	187	$-(0.69 \pm 0.03)$	0.20	bg
0528–692	–	83		3	$-(0.09 \pm 0.02)$		bg? (obs)
0530–678	500*	375	155	62	$-(0.76 \pm 0.05)$	0.05 & 0.04	bg
0532–675	370	270		5	$-(0.57 \pm 0.04)$		bg? (obs)
0533–725	900	534		78	$-(0.92 \pm 0.06)$		bg
0534–720	220	200 (region)		14	$-(0.34 \pm 0.05)$	0.03 (m)	bg? (obs)
0535–676	1150	1786		9	$-(0.05 \pm 0.10)$		H II
0537–692	–	2132 (region)	125	51	$-(0.84 \pm 0.13)$	0.02 & 0.02	bg? (obs)
0540–696	1480	1522	84	179	$-(0.18 \pm 0.08)$		H II
0541–670	300*	51		2, 1 & 3	$-(1.52 \pm 0.27)$		bg
0543–681	700*	387	98	15 & 13	$-(1.08 \pm 0.06)$		bg
0543–710	370*	255		15 & 9	$-(1.39 \pm 0.02)$		bg (obs)
0545–649	1330	715	419	204	$-(0.60 \pm 0.04)$	0.23	bg
0545–719	610*	410	205	49	$-(1.74 \pm 0.03)$	0.13	bg
0547–677	270*	185	81	40	$-(0.57 \pm 0.05)$	0.04	bg
0547–704	300*	218		9 & 6	$-(1.55 \pm 0.08)$		bg?
0550–684	980*	651 (region)		8 & 4	$-(0.33 \pm 0.07)$	ND	bg + SNR? (obs)
0552–682	720*	360	182	51	$-(0.82 \pm 0.04)$		bg
0552–703	1270	852		92 & 77	$-(0.67 \pm 0.04)$		bg
0600–706	1720	871	370	133	$-(1.04 \pm 0.05)$	0.09	bg

A total of 41 sources were observed and an initial comparison with the predicted number of 55 background sources suggests that even if all 41 sources presented in this sample were classified as background objects, the number is still well below that predicted. There are a number of possible reasons for this apparent discrepancy.

- *Uncertainty in the flux density limit.* The 200 mJy cutoff at 843 MHz is somewhat arbitrary and a change of 10% in this value will significantly change the expected number of background sources. For example, if the limit was 220 mJy, then the predicted number of background sources would decrease to 49.

- *Statistical uncertainty.* The calculation of the predicted number of background sources is a statistical determination based on observational data thus an uncertainty of $\sqrt{N}$ would be expected.

- *Selection of sources from the MOST images.* This was biased in that preference was given to those compact sources located in relatively isolated regions rather than those which appeared to be adjacent to, or superimposed on, regions of extended emission. Davies, Elliott & Meaburn (1976) compare the angular extent of the H II region complexes observed in the SMC and LMC. One of their findings is that the optical nebular complexes in the LMC are significantly larger than those observed in the SMC and have a similar angular scale to the largest complexes visible in other external galaxies. For example. some of the largest complexes in the LMC are the 30-Doradus region with a diameter of 80 arcmin, DEM 43 with a diameter of 35 arcmin and DEM 34 and DEM 221 each with an angular diameter of 25 arcmin. These regions may be associated with relatively large diffuse areas of radio emission at 843 MHz, leading to potentially significant positional and flux density uncertainties, making the detection of compact sources difficult. From the area covered by these regions, a small number of background sources are likely to be co-located with these H II regions.

From the classification determined here, there are 37 sources which are either background sources, possible background sources or have an apparent compact background component as part of a hybrid morphology (coincident with, for example, an H II region or SNR).

It is interesting to compare the list of sources studied in this chapter with the source catalogue from Dickey et al. (1994). The catalogue presented here was used as the basis of the Dickey et al. (1994) observations which was then expanded by the addition of further compact sources after a quick continuum survey at 1.4 GHz. A total of 18 sources observed here were observed by Dickey et al. (1994) with the lowest 1419 MHz integrated flux density being 79 mJy. From their catalogue, there are 7 additional sources with 1419 MHz integrated flux densities of 79 mJy or greater which may reasonably be expected to have 843 MHz integrated flux densities of around 200 mJy. This would take the total number of background sources to 44.

While the statistical uncertainties discussed suggest that most of the compact sources have been studied there may be a small number of compact background sources

that have not have been detected in this analysis of the MOST LMC survey presented here.

5.6 Summary

As discussed in Chapter 4, accurate source classification remains a challenging task. The development of a more formal approach to the classification of the Large Magellanic Cloud sources presented in this chapter has significantly improved the confidence with which sources can be categorized. This is particularly important for a region as rich as the LMC, in which the classification of sources is made more difficult due to the presence of often strong emission over a range of angular scales. In such environments, observations with instruments such as Parkes are often not able to distinguish between compact components and the broad scale extended emission. However, higher angular resolution synthesis instruments such as the ATCA, are often sensitive only to compact components and resolve out any extended emission, although this depends on the array configuration. For the observations reported here, for a source to be well imaged, the upper limit on the angular scale is around 30 arcsec. Thus observations over a range of angular scales are required to understand the nature of a particular object.

Further observations of the 10 "doubtful" sources listed in Table 5.2 should be undertaken to determine the relationship of the compact components to nearby extended regions. These observations would also have the benefit of imaging the extended emission over a range of frequencies potentially resulting in some of the highest fidelity images of sources which include known SNRs and H II regions.